

37
6-20-78

As. 179

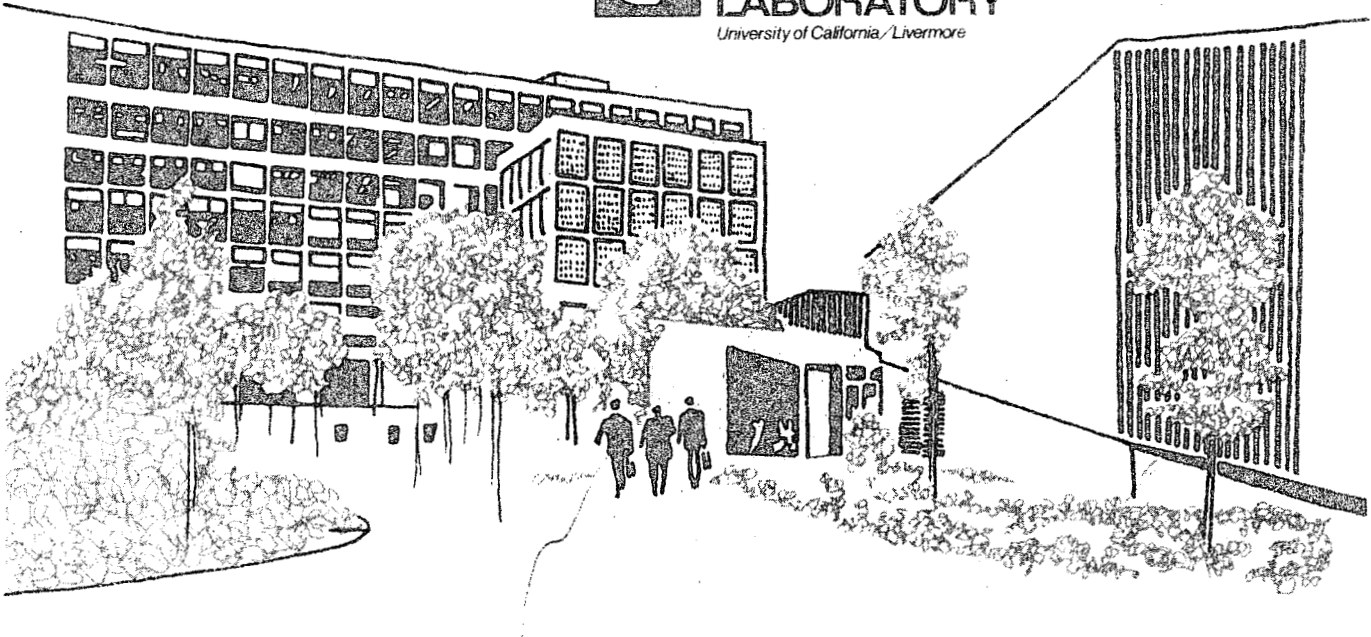
UCRL-52342

EFFECTIVE MASS AND DAMPING OF SUBMERGED STRUCTURES

R. G. Dong
April 1, 1978

MASTER

Work performed under the auspices of the U.S. Department of
Energy by the UCLLL under contract number W-7405-ENG-48.



DISTRIBUTION OF THIS DOCUMENT IS UNLIMITED

DISCLAIMER

This report was prepared as an account of work sponsored by an agency of the United States Government. Neither the United States Government nor any agency Thereof, nor any of their employees, makes any warranty, express or implied, or assumes any legal liability or responsibility for the accuracy, completeness, or usefulness of any information, apparatus, product, or process disclosed, or represents that its use would not infringe privately owned rights. Reference herein to any specific commercial product, process, or service by trade name, trademark, manufacturer, or otherwise does not necessarily constitute or imply its endorsement, recommendation, or favoring by the United States Government or any agency thereof. The views and opinions of authors expressed herein do not necessarily state or reflect those of the United States Government or any agency thereof.

DISCLAIMER

Portions of this document may be illegible in electronic image products. Images are produced from the best available original document.



LAWRENCE LIVERMORE LABORATORY

University of California, Livermore, California, 94550

NOTICE
This report was prepared as an account of work sponsored by the United States Government. Neither the United States nor the United States Department of Energy, nor any of their employees, nor any of their contractors, subcontractors, or their employees, makes any warranty, express or implied, or assumes any legal liability or responsibility for the accuracy, completeness or usefulness of any information, apparatus, product or process disclosed, or represents that its use would not infringe privately owned rights.

UCRL-52342

EFFECTIVE MASS AND DAMPING OF SUBMERGED STRUCTURES

R. G. Dong

MS. date: April 1, 1978

MASTER

EB



Contents

Abstract	1
1. Introduction	1
2. Structures and Excitations of Concern	3
3. Hydrodynamic Theories	3
4. Some Methods Used for Current Design Analysis	8
5. Single Isolated Members	10
5.1 Procedure Recommended by Newmark and Rosenblueth	10
5.2 Added Mass for Single Isolated Members	10
5.3 Effect of Finite Length on Added Mass for Single Isolated Members	19
5.4 Effect of Partial Submersion on Added Mass for Single Isolated Members	19
5.5 Added Damping for Single Isolated Members	19
5.6 Effect of Structural Size on Added Damping for Single Isolated Members	25
5.7 Range of Applicability of the Added Mass and Damping Concept for Single Isolated Members	29
6. Multiple Members	32
6.1 Complexities Associated With Multiple Members	32
6.2 Hydrodynamic Coupling for Groups of Cylinders	32
6.3 Hydrodynamic Coupling for Rigid Members Surrounded by a Rigid Circular Cylinder	40
6.4 Hydrodynamic Coupling for Coaxial Cylinders	47
6.5 Damping for Multiple Members	47
7. Conservative Choice for Added Mass	62
8. Computer Codes in Current Use	64
9. Conclusions and Recommendations	64
9.1 Idealized Single Isolated and Multiple Members	64
9.2 Spent Fuel Storage Racks	65
9.3 Main Steam-Relief Valve Line	66
9.4 Internals of the Reactor Vessel	66
9.5 Methods Used for Current Design Analysis	67
10. Acknowledgments	71
11. References	71

EFFECTIVE MASS AND DAMPING OF SUBMERGED STRUCTURES

ABSTRACT

Various structures important for safety in nuclear power plants must remain functioning in the event of an earthquake or other dynamic phenomenon. Some of these important structures, such as spent-fuel storage racks, main pressure-relief valve lines, and internal structures in the reactor vessel, are submerged in water. Dynamic analysis must include the force and damping effects of water. This report provides a technical basis for evaluating the wide variety of modeling assumptions currently used in design analysis. Current design analysis techniques and information in the literature form the basis of our conclusions and recommendations. We surveyed 32 industrial firms and reviewed 49 technical references. We compare various theories with published experimental results wherever possible. Our findings generally pertain to idealized structures, such as single isolated members, arrays of members, and coaxial cylinders. We relate these findings to the actual reactor structures through observations and recommendations. Whenever possible we recommend a definite way to evaluate the effect of hydrodynamic forces on these structures.

1. INTRODUCTION

To ensure that various structures important to the safety of nuclear power plants remain functioning during a severe earthquake or other dynamic phenomenon, detailed dynamic analyses must be performed. A number of structures, such as spent-fuel storage racks, main pressure-relief valve lines, and internals of the reactor vessel, are submerged in water. For these structures, the effect of the water in terms of forces and damping must be considered. A wide variety of modeling assumptions are being used in design analysis, and, at present, there are no uniform positions by which to judge the adequacy of the assumptions. The objective of this project is to provide a technical basis for evaluating the assumptions, and to recommend suitable methods to account for the effect of the water.

The methods investigated include the added mass and added damping concept, current design methods, and methods under development. Experimental results available in the literature form the basis of our evaluation whenever possible. Following a procedure agreed upon at the start of the project, we focus on two groups of idealized structures: single isolated members and multiple members. The second group includes two parallel cylinders, members near a boundary, an array of members, and coaxial cylinders. We relate our findings to spent-fuel

storage racks, main pressure-relief valve lines, and the internals of the reactor vessel through observations and recommendations. Development of new methods and performing rigorous analyses were not major endeavors for the project.

An extensive survey of the literature and industrial firms was carried out. Forty-nine references (1-49), listed in the order reviewed, covered single isolated members and multiple members. Thirty-two industrial firms were contacted (see Table I); this survey revealed that the design methods in current use are quite varied and that, in some instances, rather sophisticated developments are taking place.

Of special interest to the Nuclear Regulatory Committee (NRC) is a recommendation for added mass and damping values made by Newmark and Rosenblueth.⁵ This recommendation forms the baseline for NRC's current position on the subject. We compared this recommendation with the theoretical and experimental results we reviewed.

The fluid-structure interaction for multiple members is significantly more complex than for single isolated members and is less well understood. Consequently, we find it advantageous to separate single isolated members from multiple members in our presentation.

Table 1. Industrial firms surveyed.

Argonne National Lab. Argonne, Illinois James Kennedy Yao Chang S. S. Chen	Gilbert Reading, Pennsylvania Donald Croneberger Los Alamos Scientific Laboratories Los Alamos, New Mexico Tony Hirt	Program & Remote Systems St. Paul, Minnesota Donald F. Melton Carl Newmeyer
Babcock & Wilcox Lynchburg, Virginia Arthur F. J. Eckert	Lockheed Corp. Sunnyvale, California Robert L. Waid	Sargent & Lundy Chicago, Illinois Suren Singh Norman Webber
Bechtel San Francisco, California Sidney Ting Ching Wu	NASA Huntsville, Alabama Heinz Struck Denny Kross	Stone & Webster Boston, Massachusetts George Bushell
Civil Engineering Lab. Port Hueme, California William Armstrong Francis Liu Dallas Meggitt	Naval Post Graduate School Monterey, California Targut Sarpkaya	Southwest Research Institute San Antonio, Texas Frank Dodge
Combustion Engineering Windsor, Connecticut Bob Longo	Naval Research Laboratory Washington, D.C. Owen M. Griffin	Universal Analyties Los Angeles, California Dave Herting
EDAC Irvine, California Robert P. Kennedy	Nuclear Energy Services Incorp. Danbury, Connecticut Igbal Husain	University of California Berkeley, California Anil K. Chopra Ray Clough John Wehausen
EDS San Francisco, California Majoraj Kaul	Nuclear Services Corp. Campbell, California Henry Thailer	URS/John Blume San Francisco, California Roger Skjei Roger Scholl
EPRI Palo Alto, California Conway Chan	NUS Corporation Boston, Massachusetts Howard Eckert	Wachter Pittsburg, Pennsylvania Mr. Wachter Dave Secrist
Exxon Nuclear Co., Inc. Richland, Washington Denny Condotta Charles A. Brown	Offshore Power Systems Jacksonville, Florida Richard Orr Jeff Shulman	Westinghouse Pensacola, Florida John Gormley Tom C. Allen George J. Bohm
Frederick R. Harris, Inc. New York, New York Herman Bomze	Oregon State University Corvallis, Oregon Tokuo Yamamoto	
General Electric San Jose, California Lun-King Liu Bob Buckles	Physics International San Leandro, California Dennis Orphal	

2. STRUCTURES AND EXCITATIONS OF CONCERN

The nuclear power-plant structures and excitations of concern are shown in Table 2. Seismic loads are considered described by the response spectrum in the NRC's Regulatory Guide 1.60 (R.G. 1.60).⁵⁰ The horizontal spectrum is shown in Fig. 1. The time histories for the pressure-relief and blowdown loads were provided by NRC, and are shown in Figs. 2 and 3, respectively. The predominant frequencies are indicated. The structures of concern vary in dimension and arrangement depending on the design and the plant. A representative list of dimensions and/or natural frequencies are given in Table 3.

Table 2. Structures and excitations of concern.

Structures	Excitations
Spent-fuel storage racks	Seismic
Main steam-relief valve line	Pressure relief Blowdown-induced loads Seismic
Internals of reactor vessel	Blowdown-induced loads Seismic

Table 3. Representative sizes and natural frequencies of structures of concern.

Structure	Size	Natural frequency	Condition
Fuel elements	~ 0.5 in. D		
Fuel bundles, BWR	~ 5.5 x 5.5 in.	~ 3 Hz ^a	In water
Fuel bundles, PWR	~ 10 x 10 in.	~ 3 Hz ^a	In water
Fuel racks: firm (1) ^b		17 to 33 Hz	Full and in water
Fuel racks: firm (2)		10 to 20 Hz	Full and in water
Fuel racks: firm (3)		6 to 9 Hz	Full and in water
Fuel racks: firm (4)		~ 12 Hz	Full in air
Fuel racks: firm (4)		~ 10.5 Hz	Full in water
Fuel racks: firm (5)		~ 1.15 Hz	Full in water
Main steam-relief valve line ^c	8 in. D, 72 in. L	0.5 Hz	In air
	8 in. D, 72 in. L	1.2 Hz	In air
	8 in. D, 396 in. L	0.02 Hz	In air
	8 in. D, 396 in. L	0.04 Hz	In air
	12 in. D, 72 in. L	0.8 Hz	In air
	12 in. D, 72 in. L	1.8 Hz	In air
	12 in. D, 396 in. L	0.03 Hz	In air
	12 in. D, 396 in. L	0.06 Hz	In air
Reactor core barrel		40 Hz ^a	In air
		10 Hz ^a	In water

^a Approximate frequency values provided by NRC.

^b The industrial firms generally wished to remain anonymous.

^c Range of diameters and lengths provided by NRC.

3. HYDRODYNAMIC THEORIES

Five variations of hydrodynamic theory seen in the literature are listed in Table 4, approximately in the order of increasing complexity. For the dynamic effect on submerged structures, the two simplest theories are used most. The incompressible invicid

theory, sometimes referred to as potential theory, is used for nonflexible members; i.e., members that can be treated as translating rigid bodies. The compressible invicid theory is used for flexible members, such as flexible coaxial cylinders.

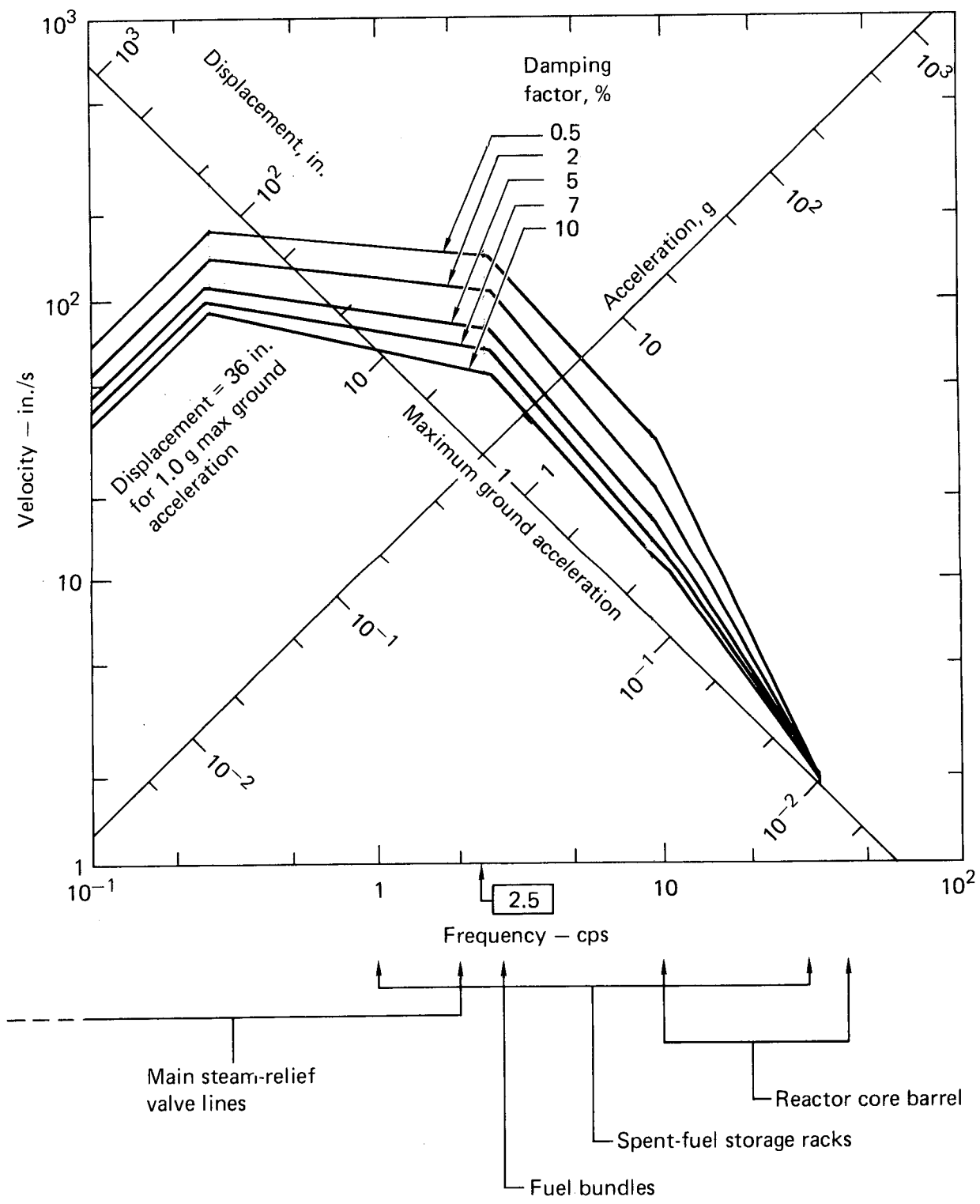


Fig. 1. Horizontal design response spectra, scaled to 1-g horizontal ground acceleration (from R. G. 1.60).⁵⁰

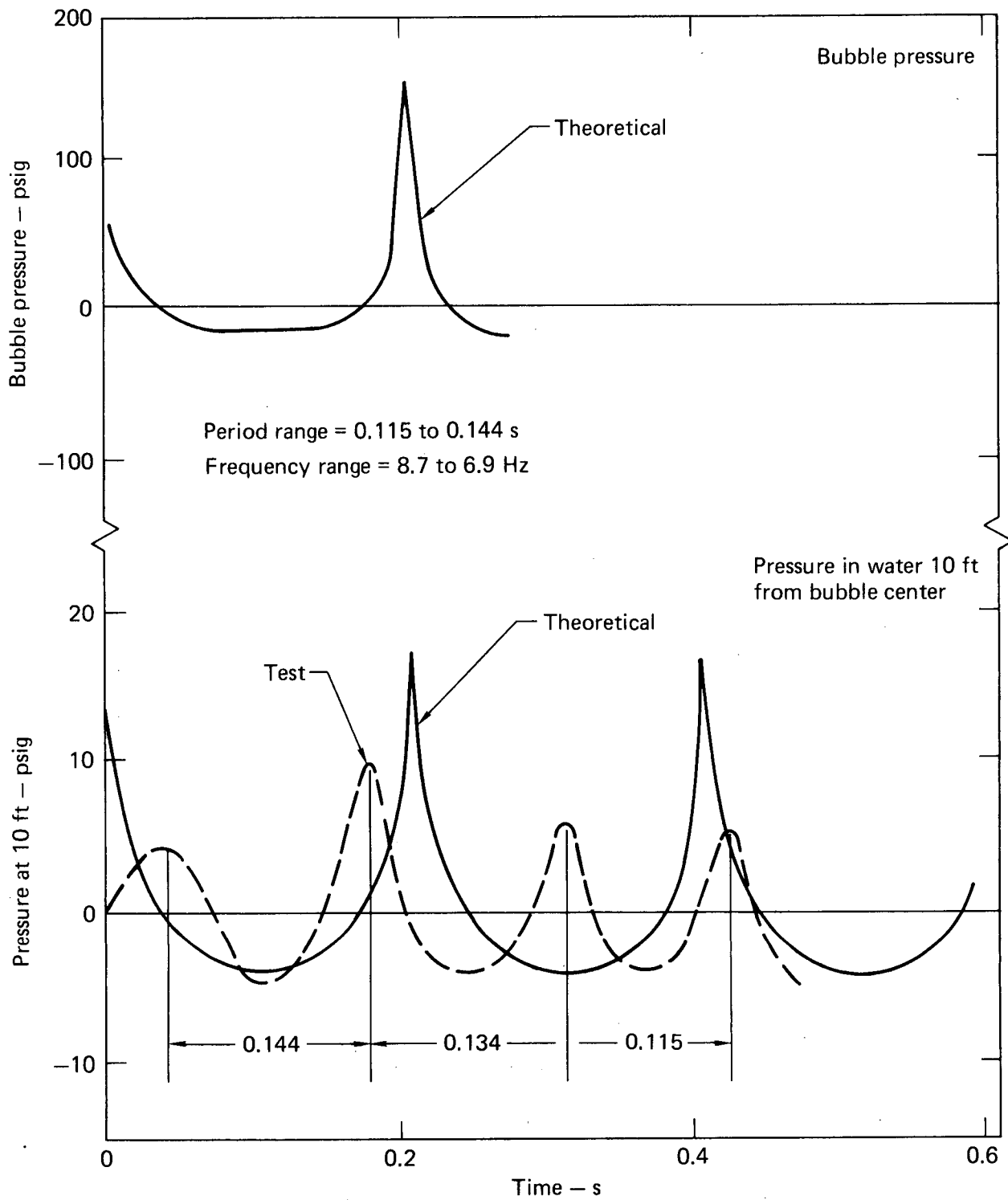


Fig. 2. Pressure in bubble and water, steam relief.

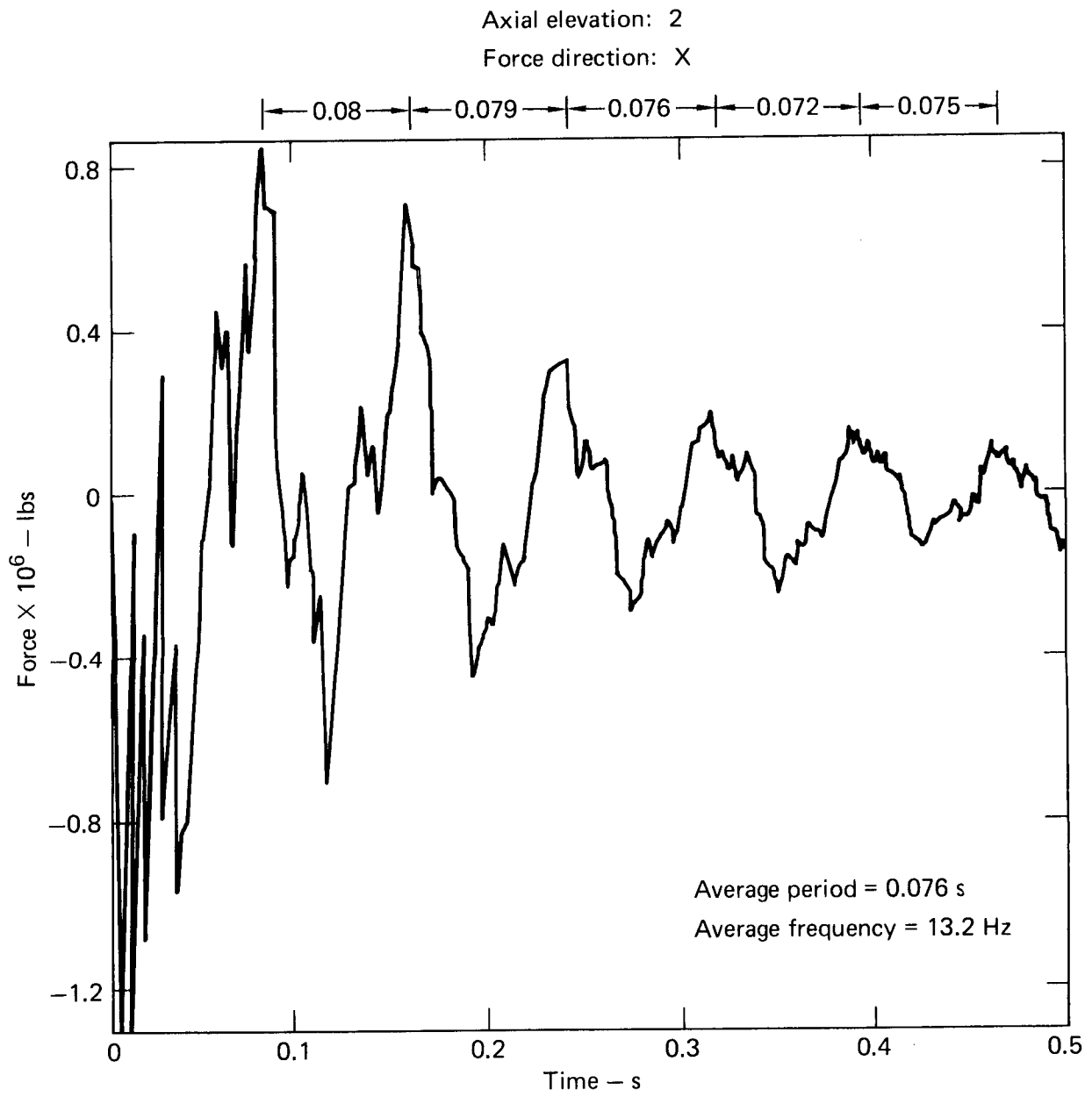
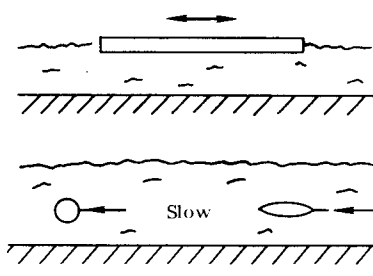
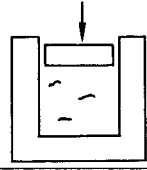
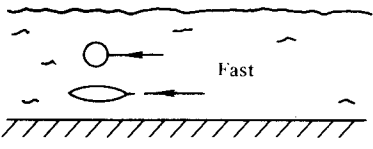
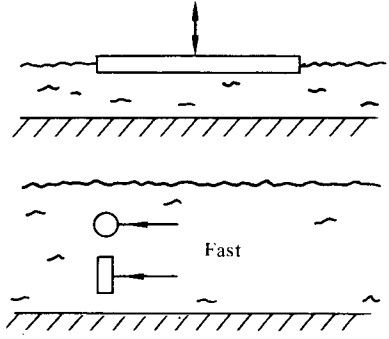
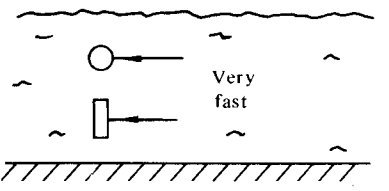


Fig. 3. Blowdown excitation; horizontal force on core barrel.

Table 4. Hydrodynamic theories.

Theories	Applicable conditions
Incompressible invicid (Potential theory)	<ul style="list-style-type: none"> • Virtually no boundary layer • Fluid escape is easy 
Compressible invicid	<ul style="list-style-type: none"> • Virtually no boundary layer • Fluid escape is not easy 
Incompressible viscous	<ul style="list-style-type: none"> • Appreciable boundary layer • Fluid escape is easy 
Compressible viscous (Navier-Stokes)	<ul style="list-style-type: none"> • Appreciable boundary layer • Fluid escape is not easy or velocity is high 
Nonlinear	<ul style="list-style-type: none"> • Appreciable boundary layer • Velocity is very high 

4. SOME METHODS USED FOR CURRENT DESIGN ANALYSIS

Our survey of industrial firms revealed a variety of methods (see, Table 5), for calculating added mass and damping. The firms' identifications are kept in confidence, as was desired by a majority of those providing information. Some overlap exists, so that each method shown may represent more than one firm. The philosophy behind each method is illustrated using a simplified representation of a fuel bundle with its can enclosure. For clarity, we show only four fuel elements per bundle, although in reality a typical fuel bundle has from 60 to 200 fuel elements. A single fuel bundle with its can is an example of a single isolated member in Table 5, and two or more fuel bundles are examples of multiple members. The volumes of water included in the calculations of virtual mass are shaded in crosshatch. In the case of fuel bundles, the mass of the water within the can is simply taken as part of the structural mass. The mass of a certain volume of water outside of the can is added to the structural mass, and this is commonly referred to as the added mass from submersion. The methods used for calculating this added mass is quite varied, as indicated in Table 5, and they are largely based on engineering judgment together with whatever analytical and/or experimental information was available at the time.

A detailed description of the basis for each method was not provided by the firms contacted; perhaps for most, the only basis was engineering judgement. In a few cases, references were cited; however, we found

no direct relation between the methods and the references.

Table 5 is self-explanatory for most of the cases shown. In method 5, the procedure presented by Fritz⁷ for coaxial cylinders was used to approximate the interaction between the central member and the eight peripheral members of a 3 x 3 array. In method 9, the cans are in contact with each other, so that virtually no water exists between adjacent cans.

The bases for the damping value used are likewise quite varied. Zero damping was chosen in some cases to ensure conservatism. In some instances, the structural plus added damping was taken as 2 to 2-1/2 times the structural damping. The basis for this appears to be various references, such as 3 and 17, which choose to present experimental results for total damping in terms of a factor, such as 2, times the structural damping. We disagree with this interpretation, for it implies that the submerging water somehow knows how much damping is in the structure, and it subsequently adds an equal amount. The experimental results given in Ref. 3 and 17 could just as well be expressed in terms of an added damping, which we feel is a more valid interpretation. It is our opinion that the use of a factor times the structural damping, as used in method 3 and considered for use in methods 7 and 8, should be discouraged.

Our assessment of the methods described in Table 5 is given in Section 9.5 of this report.

Table 5. Design methods for evaluating added mass in current use for seismic excitations.


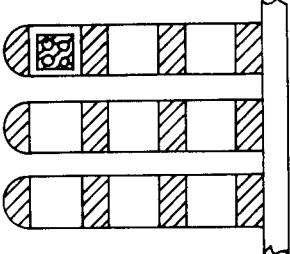

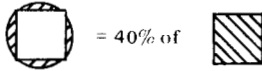
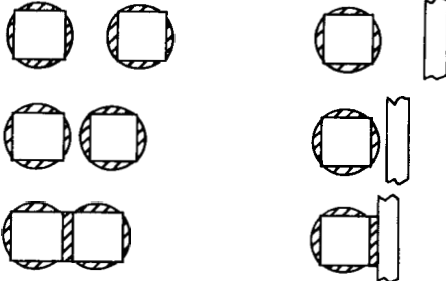
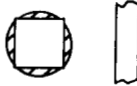
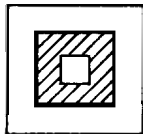
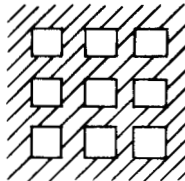




Method number	Single, isolated member	Multiple members	Damping
1	Potential theory (perfect fluid)	Potential theory	
2	Potential theory	Potential theory modified by experiments	
3			2 times structural damping

Table 5. (continued)

Method number	Single, isolated member	Multiple member	Damping
4	 <p>Where</p>  <p>= 40% of</p>		 <p>Added damping = 0%</p>
5	Potential theory	 <p>Fritz (Ref. 7)</p> <p>≈</p> 	Added damping = 0 to 3%
6	Added mass = displaced water	<p>For natural frequency evaluations</p>  <p>For inertial load evaluations</p> 	Added damping = 2%
7	Added mass = displaced water	<p>Use the smaller of:</p> <ul style="list-style-type: none"> Actual measured amount of water surrounding the racks Evaluate the added mass as if the cans were single and isolated 	Prefer to use 2 to 2-1/2 × structural damping, but are using added damping of 2% per NRC's request
8			Added damping = Usually 0%, but might consider using 2 times structural damping
9		 <p>Very thin film of water</p>	Added damping = 0%

An assessment of validity of these methods is given in Section 9.5 of this report. A method recommended by LLL, not shown in this table, is explained in Sections 9.1 and 9.2 of this report.

5. SINGLE ISOLATED MEMBERS

5.1 Procedure Recommended By Newmark and Rosenblueth

A procedure for evaluating the added mass and damping of single isolated members submerged in a fluid was suggested by Newmark and Rosenblueth.⁵ For added mass, they suggested:

"If the structure is a long, rigid prism on flexible supports, moving in a direction perpendicular to its axis, flow of liquid around the structure is essentially two-dimensional. Under these conditions, the added mass is that of a circular cylinder of liquid having the same length as the prism and a diameter equal to the width of the projection of the prism on a plane perpendicular to the direction of motion (Fig. 4)." For added damping they said:

"...damping due to liquid viscosity may be disregarded. Energy dissipation due to radiation into the liquid may be more important, but the model tests to which we have referred [1] indicate that it will not exceed about 2% of critical for submerged structures of ordinary dimensions." An evaluation was carried out and included in our presentation.

5.2 Added Mass for Single Isolated Members

If a single isolated member is accelerated in a stationary fluid, its acceleration induces the fluid in its immediate neighborhood to accelerate. The accelerating fluid in return induces an added mass effect onto the member. Under sufficiently small amplitudes of motion, cyclic or unidirectional, the

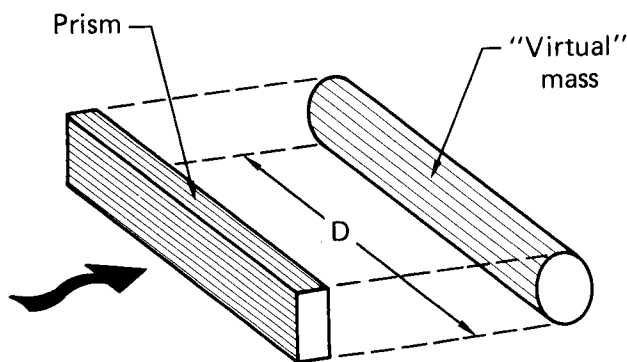


Fig. 4. Submerged body and its virtual mass.⁵

added mass phenomenon can be described in terms of an added mass coefficient C_m defined as

$$C_m = \frac{\text{added mass of fluid}}{\text{reference fluid mass}}$$

where the reference fluid mass is that of the cylinder of fluid of diameter equal to the dimension perpendicular to the direction of motion, or, in some cases, it is the mass of the displaced fluid. The added mass phenomenon for single isolated members has been rather extensively investigated experimentally and analytically. Theoretical treatment has been quite successful using the potential theory.

Experimental data for single isolated members are available in Refs. 1, 3, 4, 6, 12, 13, 17, 20, and 29. Potential theory results are given in Refs. 2 and 7, Table 6. The available experimental data, potential theory results, and Newmark and Rosenblueth's (N&R) recommendations are compared in Figs. 5a through 5i for a variety of specimen geometries. N&R's recommendation as worded in Ref. 5 applies only to the situations of Figs. 5a, 5c, and 5d; therefore, comparison with the recommendation is carried out only for these three cases. Notice that the added mass coefficient is independent of the cross-sectional geometry of the specimen for N&R's recommendation. This is a simplification embodied in the recommendation, which is important to keep in mind, for we will see later that it will give rise to some uncertainties about conservatism when using the recommendation.

A comparison between Figs. 5a and 5b and between Figs. 5e and 5f reveals that the value of C_m for a fluid moving around a stationary specimen is higher than the value for a specimen moving in a stationary fluid. This higher value of C_m is exhibited theoretically,^{6,11} as well as experimentally, and is important to account for in real applications. For a stationary circular cylinder in a moving fluid, $C_m = 2$, which means the hydrodynamic force acting on the stationary cylinder is *twice* the mass of fluid displaced times the acceleration of the fluid. By comparison, for a translating circular cylinder in a stationary fluid, $C_m = 1$, which means the total force required to accelerate the cylinder is the mass of the cylinder plus the mass of the displaced fluid multiplied by acceleration *of the cylinder*. For the case in which both the cylinder and fluid are in motion, these two force contributions should be calculated separately and superimposed.

Table 6. Two-dimensional bodies.²

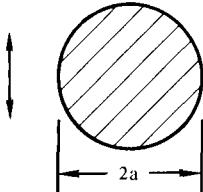
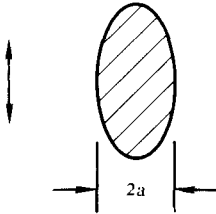
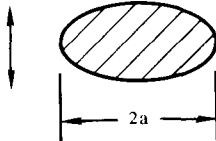
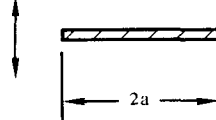
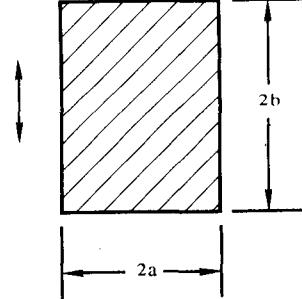
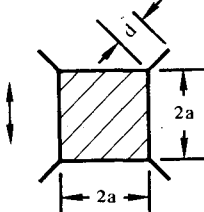
Section through body	Translational direction	Hydrodynamic mass per unit length																
	Vertical	$m_h = 1 \pi \rho a^2$																
	Vertical	$m_h = 1 \pi \rho a^2$																
	Vertical	$m_h = 1 \pi \rho a^2$																
	Vertical	$m_h = 1 \pi \rho a^2$																
	Vertical	<table border="0"> <tr><td>$a/b = \infty$</td><td>$m_h = 1 \pi \rho a^2$</td></tr> <tr><td>$a/b = 10$</td><td>$m_h = 1.14 \pi \rho a^2$</td></tr> <tr><td>$a/b = 5$</td><td>$m_h = 1.21 \pi \rho a^2$</td></tr> <tr><td>$a/b = 2$</td><td>$m_h = 1.36 \pi \rho a^2$</td></tr> <tr><td>$a/b = 1$</td><td>$m_h = 1.51 \pi \rho a^2$</td></tr> <tr><td>$a/b = 1/2$</td><td>$m_h = 1.70 \pi \rho a^2$</td></tr> <tr><td>$a/b = 1/5$</td><td>$m_h = 1.98 \pi \rho a^2$</td></tr> <tr><td>$a/b = 1/10$</td><td>$m_h = 2.23 \pi \rho a^2$</td></tr> </table>	$a/b = \infty$	$m_h = 1 \pi \rho a^2$	$a/b = 10$	$m_h = 1.14 \pi \rho a^2$	$a/b = 5$	$m_h = 1.21 \pi \rho a^2$	$a/b = 2$	$m_h = 1.36 \pi \rho a^2$	$a/b = 1$	$m_h = 1.51 \pi \rho a^2$	$a/b = 1/2$	$m_h = 1.70 \pi \rho a^2$	$a/b = 1/5$	$m_h = 1.98 \pi \rho a^2$	$a/b = 1/10$	$m_h = 2.23 \pi \rho a^2$
$a/b = \infty$	$m_h = 1 \pi \rho a^2$																	
$a/b = 10$	$m_h = 1.14 \pi \rho a^2$																	
$a/b = 5$	$m_h = 1.21 \pi \rho a^2$																	
$a/b = 2$	$m_h = 1.36 \pi \rho a^2$																	
$a/b = 1$	$m_h = 1.51 \pi \rho a^2$																	
$a/b = 1/2$	$m_h = 1.70 \pi \rho a^2$																	
$a/b = 1/5$	$m_h = 1.98 \pi \rho a^2$																	
$a/b = 1/10$	$m_h = 2.23 \pi \rho a^2$																	
	Vertical	<table border="0"> <tr><td>$d/a = 0.05$</td><td>$m_h = 1.61 \pi \rho a^2$</td></tr> <tr><td>$d/a = 0.10$</td><td>$m_h = 1.72 \pi \rho a^2$</td></tr> <tr><td>$d/a = 0.25$</td><td>$m_h = 2.19 \pi \rho a^2$</td></tr> </table>	$d/a = 0.05$	$m_h = 1.61 \pi \rho a^2$	$d/a = 0.10$	$m_h = 1.72 \pi \rho a^2$	$d/a = 0.25$	$m_h = 2.19 \pi \rho a^2$										
$d/a = 0.05$	$m_h = 1.61 \pi \rho a^2$																	
$d/a = 0.10$	$m_h = 1.72 \pi \rho a^2$																	
$d/a = 0.25$	$m_h = 2.19 \pi \rho a^2$																	

Table 6. (continued)

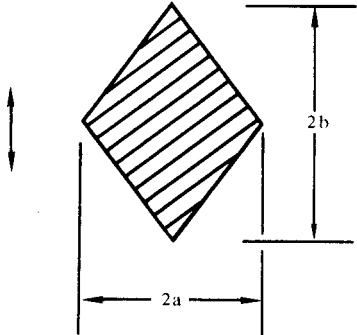
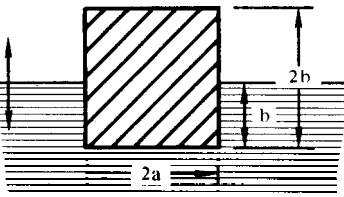
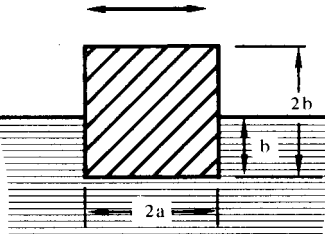
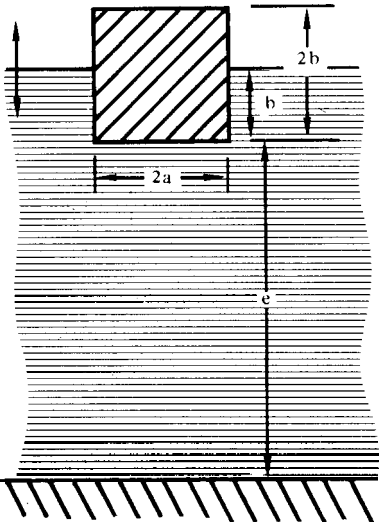
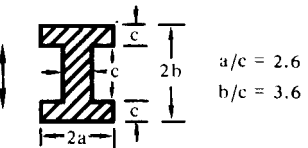
Section through body	Translational direction	Hydrodynamic mass per unit length
	Vertical	$m_h = 0.85 \pi \rho a^2$
	$a/b = 2$	$m_h = 0.76 \pi \rho a^2$
	$a/b = 1$	$m_h = 0.67 \pi \rho a^2$
	$a/b = 1/2$	$m_h = 0.61 \pi \rho a^2$
	$a/b = 1/5$	
	Vertical (normal to free surface)	$m_h = 0.75 \pi \rho a^2$
	$a/b = 1$	
	Horizontal (parallel to free surface)	$m_h = 0.25 \pi \rho a^2$
	$a/b = 1$	
	Vertical (normal to free surface)	$m_h = 0.75 \pi \rho a^2$
	$a/b = 1$; $e/b = \infty$	$m_h = 0.83 \pi \rho a^2$
	$e/b = 2.6$	$m_h = 0.89 \pi \rho a^2$
	$e/b = 1.8$	$m_h = 1.00 \pi \rho a^2$
	$e/b = 1.5$	$m_h = 1.35 \pi \rho a^2$
	$e/b = 0.5$	$m_h = 2.00 \pi \rho a^2$
	$e/b = 0.25$	
	Vertical	$m_h = 2.11 \pi \rho a^2$
	$a/c = 2.6$	
	$b/c = 3.6$	
	$a/c = 2.6$	
	$b/c = 3.6$	

Table 6. (continued)

Three-dimensional bodies


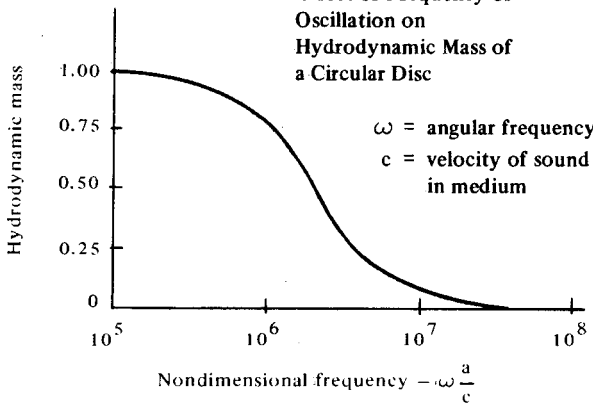
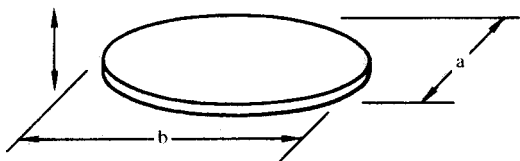
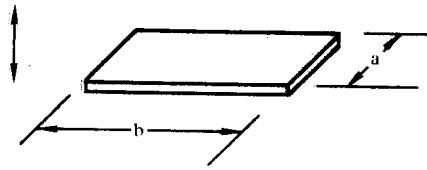
Body shape	Translational direction	Hydrodynamic mass																														
1. FLAT PLATES																																
<p>Circular disk</p> 	Vertical	$m_h = \frac{8}{3} \rho a^3$ <p>Effect of Frequency of Oscillation on Hydrodynamic Mass of a Circular Disc</p>  <p>ω = angular frequency c = velocity of sound in medium</p>																														
<p>Elliptical disk</p> 	As shown	$m_h = Kba^2 \frac{\pi}{6} \rho$ <table border="1"> <thead> <tr> <th>b/a</th> <th>K</th> </tr> </thead> <tbody> <tr> <td>∞</td> <td>1.00</td> </tr> <tr> <td>14.3</td> <td>0.991</td> </tr> <tr> <td>12.75</td> <td>0.987</td> </tr> <tr> <td>10.43</td> <td>0.985</td> </tr> <tr> <td>9.57</td> <td>0.983</td> </tr> <tr> <td>8.19</td> <td>0.978</td> </tr> <tr> <td>7.00</td> <td>0.972</td> </tr> <tr> <td>6.00</td> <td>0.964</td> </tr> <tr> <td>5.02</td> <td>0.952</td> </tr> <tr> <td>4.00</td> <td>0.933</td> </tr> <tr> <td>3.00</td> <td>0.900</td> </tr> <tr> <td>2.00</td> <td>0.826</td> </tr> <tr> <td>1.50</td> <td>0.748</td> </tr> <tr> <td>1.00</td> <td>0.637</td> </tr> </tbody> </table>	b/a	K	∞	1.00	14.3	0.991	12.75	0.987	10.43	0.985	9.57	0.983	8.19	0.978	7.00	0.972	6.00	0.964	5.02	0.952	4.00	0.933	3.00	0.900	2.00	0.826	1.50	0.748	1.00	0.637
b/a	K																															
∞	1.00																															
14.3	0.991																															
12.75	0.987																															
10.43	0.985																															
9.57	0.983																															
8.19	0.978																															
7.00	0.972																															
6.00	0.964																															
5.02	0.952																															
4.00	0.933																															
3.00	0.900																															
2.00	0.826																															
1.50	0.748																															
1.00	0.637																															
<p>Rectangular plates</p> 	Vertical	$m_h = K \pi \rho \frac{a^2}{4} b$ <table border="1"> <thead> <tr> <th>b/a</th> <th>K</th> </tr> </thead> <tbody> <tr> <td>1.0</td> <td>0.478</td> </tr> <tr> <td>1.5</td> <td>0.680</td> </tr> <tr> <td>2.0</td> <td>0.840</td> </tr> <tr> <td>2.5</td> <td>0.953</td> </tr> <tr> <td>3.0</td> <td>1.00</td> </tr> <tr> <td>3.5</td> <td>1.00</td> </tr> <tr> <td>4.0</td> <td>1.00</td> </tr> <tr> <td>-</td> <td>1.00</td> </tr> </tbody> </table>	b/a	K	1.0	0.478	1.5	0.680	2.0	0.840	2.5	0.953	3.0	1.00	3.5	1.00	4.0	1.00	-	1.00												
b/a	K																															
1.0	0.478																															
1.5	0.680																															
2.0	0.840																															
2.5	0.953																															
3.0	1.00																															
3.5	1.00																															
4.0	1.00																															
-	1.00																															

Table 6. (continued)

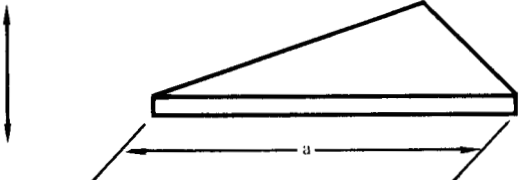
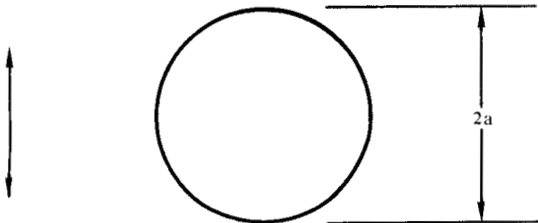
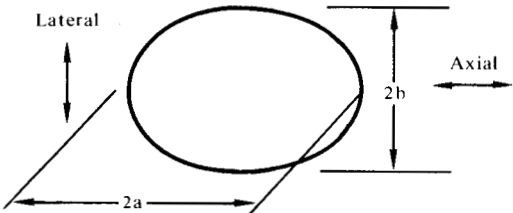
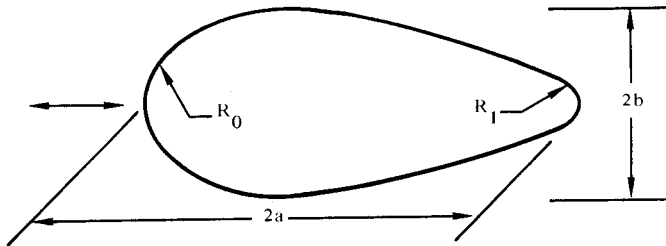
Body shape	Translational direction	Hydrodynamic mass																														
Triangular plates	Vertical	$m_h = \frac{\rho}{3} a^3 \frac{(\text{TAN } \theta)^{3/2}}{(\pi)}$																														
																																
2. BODIES OF REVOLUTION																																
Spheres	Vertical	$m_h = \frac{2}{3} \pi \rho a^3$																														
																																
Ellipsoids	Vertical	$m_h = K \cdot \frac{4}{3} \pi \rho a b^2$																														
	a/b	<table border="1"> <thead> <tr> <th data-bbox="1153 1149 1226 1223">K for axial motion</th> <th data-bbox="1339 1149 1412 1223">K for lateral motion</th> </tr> </thead> <tbody> <tr><td>1.00</td><td>0.500</td></tr> <tr><td>1.50</td><td>0.305</td></tr> <tr><td>2.00</td><td>0.209</td></tr> <tr><td>2.51</td><td>0.156</td></tr> <tr><td>2.99</td><td>0.122</td></tr> <tr><td>3.99</td><td>0.082</td></tr> <tr><td>4.99</td><td>0.059</td></tr> <tr><td>6.01</td><td>0.045</td></tr> <tr><td>6.97</td><td>0.036</td></tr> <tr><td>8.01</td><td>0.029</td></tr> <tr><td>9.02</td><td>0.024</td></tr> <tr><td>9.97</td><td>0.021</td></tr> <tr><td></td><td>0</td></tr> <tr><td></td><td>1.000</td></tr> </tbody> </table>	K for axial motion	K for lateral motion	1.00	0.500	1.50	0.305	2.00	0.209	2.51	0.156	2.99	0.122	3.99	0.082	4.99	0.059	6.01	0.045	6.97	0.036	8.01	0.029	9.02	0.024	9.97	0.021		0		1.000
K for axial motion	K for lateral motion																															
1.00	0.500																															
1.50	0.305																															
2.00	0.209																															
2.51	0.156																															
2.99	0.122																															
3.99	0.082																															
4.99	0.059																															
6.01	0.045																															
6.97	0.036																															
8.01	0.029																															
9.02	0.024																															
9.97	0.021																															
	0																															
	1.000																															

Table 6. (continued)

Body shape	Translational direction	Hydrodynamic mass
------------	-------------------------	-------------------

Approximate method for elongated bodies of revolution.



$$m_h = K_1 \rho V = K_e \left[1 + 17.0 \left(C_p - \frac{2}{3} \right)^2 + 2.49 \left(M - \frac{1}{2} \right)^2 + 0.283 \left[\left(r_0 - \frac{1}{2} \right)^2 + \left(r_1 - \frac{1}{2} \right)^2 \right] \right]$$

where; K_1 – Hydrodynamic mass coefficient for axial motion

K_e – Hydrodynamic mass coefficient for axial motion of an ellipsoid of the same ratio of a/b

V · Volume of body

$$C_p - \text{Prismatic coefficient} = \frac{4V}{b^2 (2a)}$$

M – Nondimensional abscissa $\frac{X_m}{l}$ corresponding to maximum ordinate

r_0, r_1 – Dimensionless radii of curvature at nose and tail

$$r_0 = \frac{R_0 (2a)}{b^2}$$

$$r_1 = \frac{R_1 (2a)}{b^2}$$

Lateral motion

Munk has shown that the hydrodynamic mass of an elongated body of revolution can be reasonably approximated by the product of the density of the fluid, the volume of the body, and the k factor for an ellipsoid of the same a/b ratio.

Table 6. (continued)

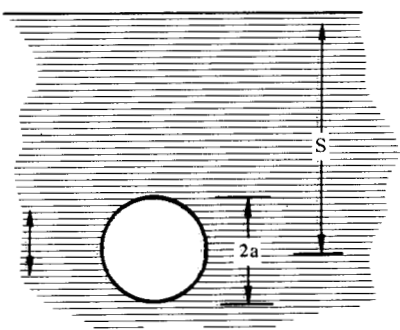
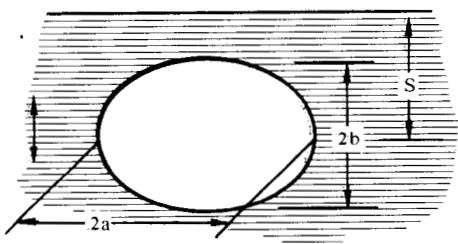
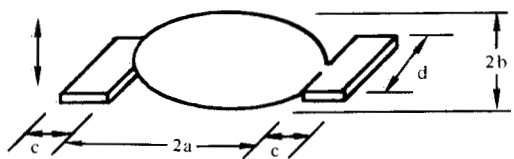
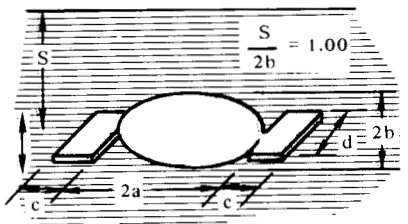
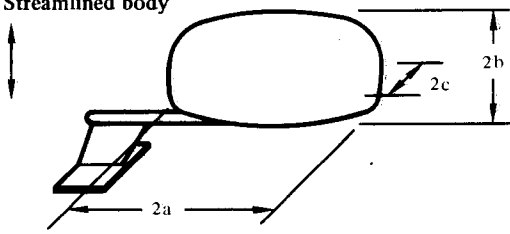
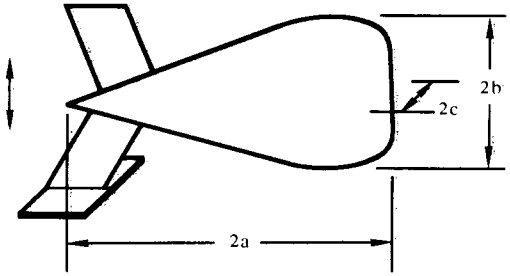
Body shape	Translational direction	Hydrodynamic mass																						
<p>Sphere near a free surface</p> 	Vertical	$m_h = K \frac{2}{3} \pi \rho a^3$ <table border="1"> <thead> <tr> <th>$s/2a$</th> <th>K</th> </tr> </thead> <tbody> <tr><td>0</td><td>0.50</td></tr> <tr><td>0.5</td><td>0.88</td></tr> <tr><td>1.0</td><td>1.08</td></tr> <tr><td>1.5</td><td>1.16</td></tr> <tr><td>2.0</td><td>1.18</td></tr> <tr><td>2.5</td><td>1.18</td></tr> <tr><td>3.0</td><td>1.16</td></tr> <tr><td>3.5</td><td>1.12</td></tr> <tr><td>4.0</td><td>1.04</td></tr> <tr><td>4.5</td><td>1.00</td></tr> </tbody> </table>	$s/2a$	K	0	0.50	0.5	0.88	1.0	1.08	1.5	1.16	2.0	1.18	2.5	1.18	3.0	1.16	3.5	1.12	4.0	1.04	4.5	1.00
$s/2a$	K																							
0	0.50																							
0.5	0.88																							
1.0	1.08																							
1.5	1.16																							
2.0	1.18																							
2.5	1.18																							
3.0	1.16																							
3.5	1.12																							
4.0	1.04																							
4.5	1.00																							
<p>Ellipsoid near a free surface</p> 	Vertical	$m_h = K \cdot \frac{4}{3} \pi \rho ab^2$ <p>$a/b = 2.00$</p> <table border="1"> <thead> <tr> <th>$s/2b$</th> <th>K</th> </tr> </thead> <tbody> <tr><td>1.00</td><td>0.913</td></tr> <tr><td>2.00</td><td>0.905</td></tr> </tbody> </table>	$s/2b$	K	1.00	0.913	2.00	0.905																
$s/2b$	K																							
1.00	0.913																							
2.00	0.905																							
3. BODIES OF ARBITRARY SHAPE																								
<p>Ellipsoid with attached rectangular flat plates</p> 	Vertical	$m_h = K \cdot \frac{4}{3} \pi \rho ab^2$ <p>$a/b = 2.00; c = b$</p> <p>$c \cdot d = N \pi ab$</p> <table border="1"> <thead> <tr> <th>N</th> <th>K</th> </tr> </thead> <tbody> <tr><td>0</td><td>0.7024</td></tr> <tr><td>0.20</td><td>0.8150</td></tr> <tr><td>0.30</td><td>1.0240</td></tr> <tr><td>0.40</td><td>1.1500</td></tr> <tr><td>0.50</td><td>1.2370</td></tr> </tbody> </table>	N	K	0	0.7024	0.20	0.8150	0.30	1.0240	0.40	1.1500	0.50	1.2370										
N	K																							
0	0.7024																							
0.20	0.8150																							
0.30	1.0240																							
0.40	1.1500																							
0.50	1.2370																							
<p>Ellipsoid with attached rectangular flat plates near a free surface</p> 	Vertical	$m_h = K \cdot \frac{4}{3} \pi \rho ab^2$ <p>$a/b = 2.00; c = b$</p> <p>$c \cdot d = N \pi ab$</p> <table border="1"> <thead> <tr> <th>N</th> <th>K</th> </tr> </thead> <tbody> <tr><td>0</td><td>0.9130</td></tr> <tr><td>0.20</td><td>1.0354</td></tr> <tr><td>0.30</td><td>1.3010</td></tr> <tr><td>0.40</td><td>1.4610</td></tr> <tr><td>0.50</td><td>1.5706</td></tr> </tbody> </table>	N	K	0	0.9130	0.20	1.0354	0.30	1.3010	0.40	1.4610	0.50	1.5706										
N	K																							
0	0.9130																							
0.20	1.0354																							
0.30	1.3010																							
0.40	1.4610																							
0.50	1.5706																							

Table 6. (continued)

Body shape	Translational direction	Hydrodynamic mass
<p>Streamlined body</p>  <p>$\frac{a}{b} = 2.38$ $\frac{a}{c} = 2.11$</p> <p>Area of horizontal "tail" = 25% of area of body maximum horizontal section.</p>	Vertical	$m_h = 1.124 \rho \left[\frac{4}{3} \pi a d^2 \right]$ $d = \frac{c + b}{2}$

<p>Streamlined body</p>  <p>$\frac{a}{b} = 2.4$ $\frac{a}{c} = 3.0$</p> <p>Area of horizontal "tail" = 20% of area of body maximum horizontal section.</p>	Vertical	$m_h = 0.672 \rho \left[\frac{4}{3} \pi a d^2 \right]$ $d = \frac{c + b}{2}$
---	----------	---

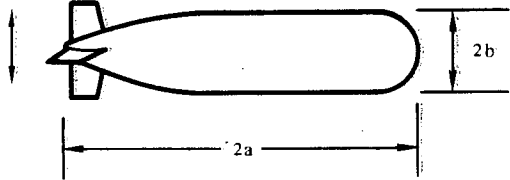
<p>"Torpedo" type body</p>  <p>$\frac{a}{b} = 5.0$</p> <p>Area of horizontal "tail" = 10% of area of body maximum horizontal section.</p>	Vertical	$m_h = 0.818 \pi \rho b^2 (2a)$
---	----------	---------------------------------

Table 6. (continued)

Body shape	Translational direction	Hydrodynamic mass																		
V-Fin type body	Vertical	$m_h = .3975 \rho L^3$																		
$\frac{L}{b} = 1.0$	$\frac{L}{c} = 2.0$																			
Parallelepipeds	Vertical	$m_h = K \rho a^2 b$																		
		<table border="1"> <thead> <tr> <th data-bbox="1144 968 1182 995">b/a</th> <th data-bbox="1307 968 1344 995">K</th> </tr> </thead> <tbody> <tr><td>1</td><td>2.32</td></tr> <tr><td>2</td><td>0.86</td></tr> <tr><td>3</td><td>0.62</td></tr> <tr><td>4</td><td>0.47</td></tr> <tr><td>5</td><td>0.37</td></tr> <tr><td>6</td><td>0.29</td></tr> <tr><td>7</td><td>0.22</td></tr> <tr><td>10</td><td>0.10</td></tr> </tbody> </table>	b/a	K	1	2.32	2	0.86	3	0.62	4	0.47	5	0.37	6	0.29	7	0.22	10	0.10
b/a	K																			
1	2.32																			
2	0.86																			
3	0.62																			
4	0.47																			
5	0.37																			
6	0.29																			
7	0.22																			
10	0.10																			

Some scatter is seen in the experimental data. Various possible effects contributing to the scatter includes specimen flexibility, frequency dependency, amplitude dependency, and normal experimental variability. Specimen flexibility appears to be an important factor that tends to lower the added mass.^{1,3} The cantilevered and the thin-walled specimens exhibited lower added masses than do spring-mounted rigid specimens. Taking into consideration this lowering effect from specimen flexibility, the agreement between experiments and potential theory can be considered quite good. The exception is Fig. 5i, where we suspect the theoretical results reported in Refs. 2 and 7 are incorrect. Our reasoning is that C_m for a cube and a sphere should be similar. Yet, Fig. 5i gives $C_m = 2.32$ for a cube ($b/a = 1$), while Fig. 5e gives $C_m = 0.5$ for a sphere. The experimental value for a cube shown in Fig. 5i is $C_m = 0.67$. This compares much more favorably with C_m for a sphere than with the theoretical value for a cube, which supports our contention that the theoretical results of Fig. 5i are incorrect. To our knowledge, the case of Fig. 5i is the only error contained in Refs. 2 and 7; however, some caution might be exercised in using these references for cases in which no experimental data is available for comparison.

The good agreement between potential theory and experimental data lead us to conclude that potential theory satisfactorily describes the added mass phenomenon. This confirms the opinion, as expressed in Refs. 15, and 16, that for single isolated members the compressibility and viscous effects of the water are negligible compared with inertial effects. Potential theory, while unable to model compressibility and viscosity, can model inertial effects quite well. Taking the position that the added mass given by potential theory is valid, a basis for evaluating the adequacy of N&R's recommendation becomes possible. In the case of a circular cylinder moving in a stationary fluid, N&R's recommendation coincides with potential theory, Fig. 5a. In the case of a rectangular cylinder moving in a stationary fluid, N&R's C_m value can be less than (Fig. 5c) or greater than (Fig. 5d) that given by potential theory, depending on the direction of motion of the specimen as illustrated by Figs. 5c and 5d. The difference between N&R's C_m values and those given by potential theory can be quite significant. For example, consider a cylinder of square geometry; i.e., $a/b = 1.0$. In Fig. 5e, the theoretical C_m value is 1.5 compared with N&R's C_m value of again 1.0. We will show later that to help assure conservatism we would want to maximize C_m under some conditions and to minimize C_m under

others. Because using N&R's recommendation can result in C_m values either greater than or less than the theoretical C_m values, conservatism is not necessarily ensured by following this recommendation. The use of potential theory to evaluate added mass is preferred in terms of greater control over the conservatism as well as providing greater general accuracy.

5.3 Effect of Finite Length on Added Mass for Single Isolated Members

In the case of a finite length member, the fluid flows around the end(s) as well as around the length. Therefore, the inertial resistance to motion is less than that for an infinitely long member. Figures 6 and 7, from Ref. 4, illustrate the effect experimentally and theoretically for specimens with both ends free for fluid to flow around. These curves could apply in an approximate sense to cross sections other than those of the figures.

5.4 Effect of Partial Submersion on Added Mass for Single Isolated Members

The added mass effect decreases near the water surface for a partially submerged member. The added mass distribution based on potential theory is shown in Fig. 8 for a vertical circular pier for three levels of partial submersion.^{5,9} The decrease in total added mass as a function of depth of submersion is given in terms of a correction factor in Fig. 9. Experimental results for vertical cylinders are shown in Fig. 10 with the partial submersion given as a fraction of the total length.³ Unfortunately, the specimen length was not given, so that no comparison can be made with Fig. 9. The general trend, however, agrees with that of Fig. 9. The correction factors of Fig. 9 could apply in an approximate sense to vertical cylinders of cross sections other than circular.

5.5 Added Damping for Single Isolated Members

The damping force acting on a submerged member is usually relatively small and not included in analysis as an acting force. Instead, the effect is usually

$$C_m = \frac{\text{Added mass of water}}{\text{Reference water mass}}$$

Ref. water mass = Cylinder of water of diameter equal to dimension perpendicular to direction of motion unless otherwise noted

Curves:

————— Potential theory (Refs. 2 and 7)

----- Newmark and Rosenblueth's recommendation (Ref. 5)

Experimental results:







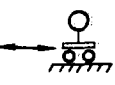



○	Solid on springs		Ref. 1
□	Cantilevered beams		Ref. 1
△	Cantilevered beams		Ref. 3
◁	Solid on springs		Ref. 4
▷	Fixed solid in flow		Ref. 13
◇	Fixed solid in oscillating fluid		Ref. 6
⊖	Solid oscillating in fluid		Ref. 12
⊗	Thin-walled hollow beams		Ref. 17
⊙	Solid oscillating in fluid		Ref. 20
⊚	Fixed solid in oscillating fluid		Ref. 29

Fig. 5. Comparisons of the potential theory, Newmark and Rosenblueth's recommendations, and experimental data.

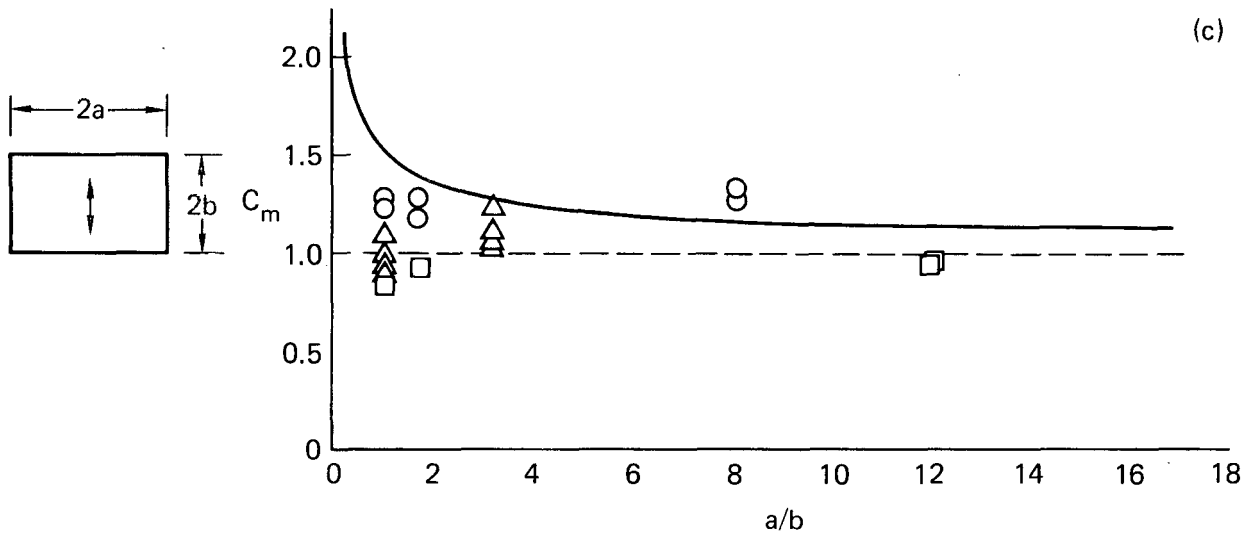


Fig. 5c. Comparisons for an oscillating rectangular cylinder in still fluid.

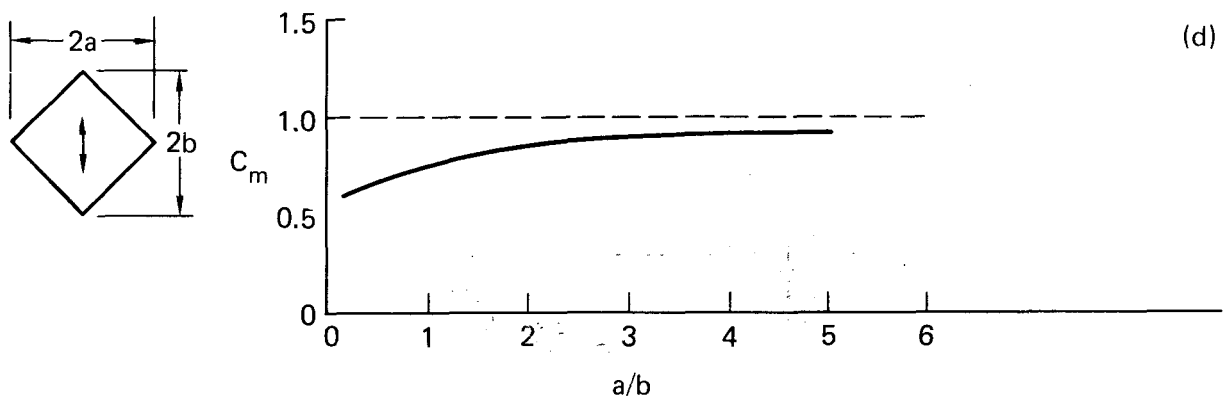


Fig. 5d. Comparisons for an oscillating rhombic cylinder in still fluid.

(e)

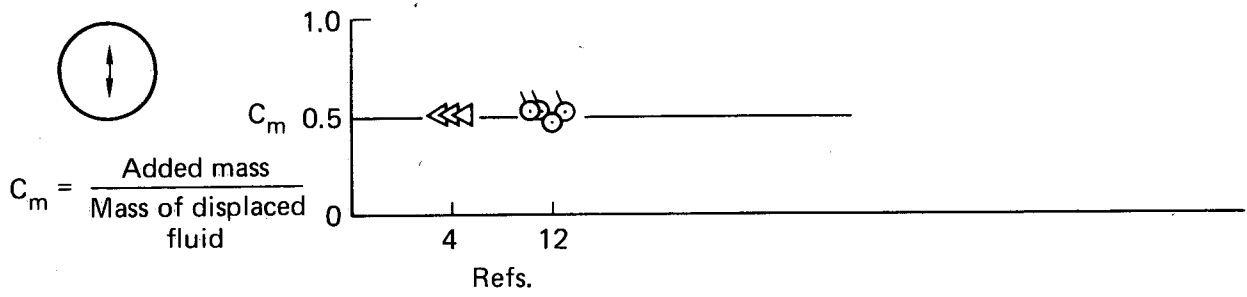


Fig. 5e. Comparisons for an oscillating sphere in still fluid.

(f)

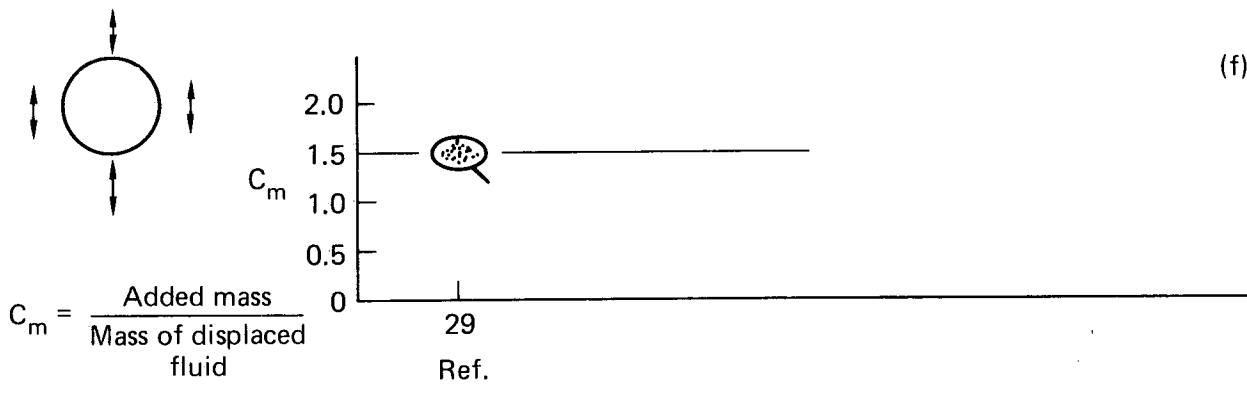


Fig. 5f. Comparisons for a fixed sphere in an oscillating fluid.

(g)

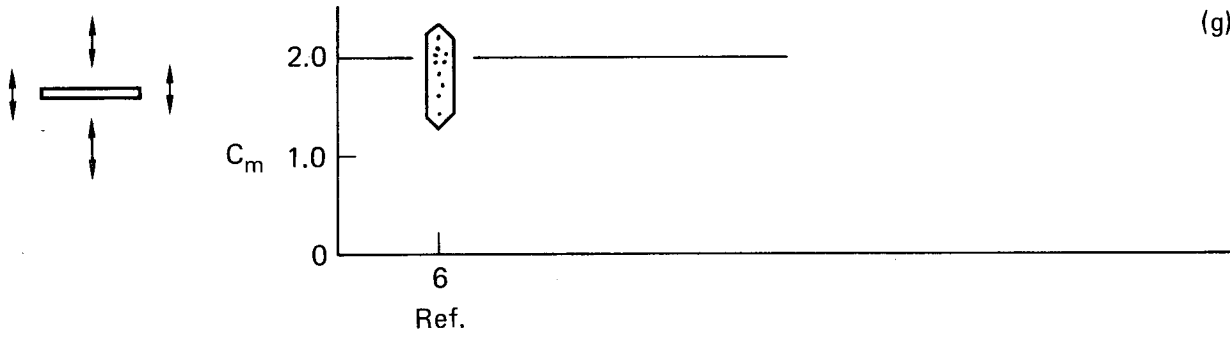


Fig. 5g. Comparisons for a fixed infinitely long plate in oscillating fluid.

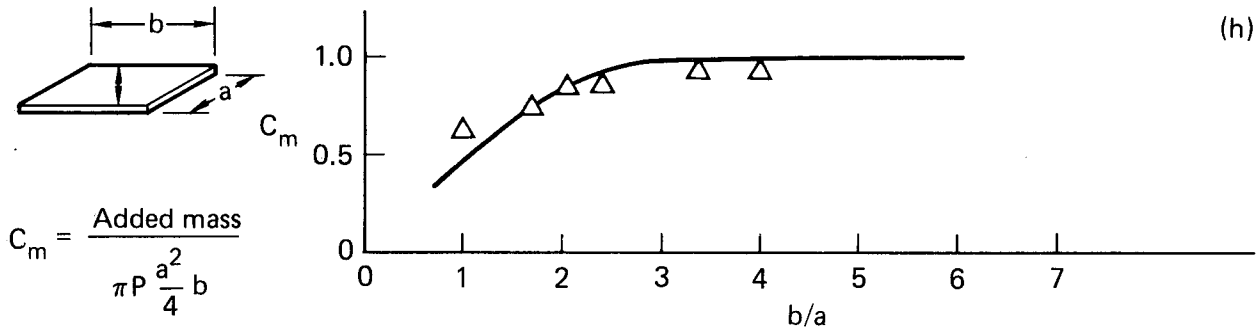


Fig. 5h. Comparisons for an oscillating, finite plate in still fluid.

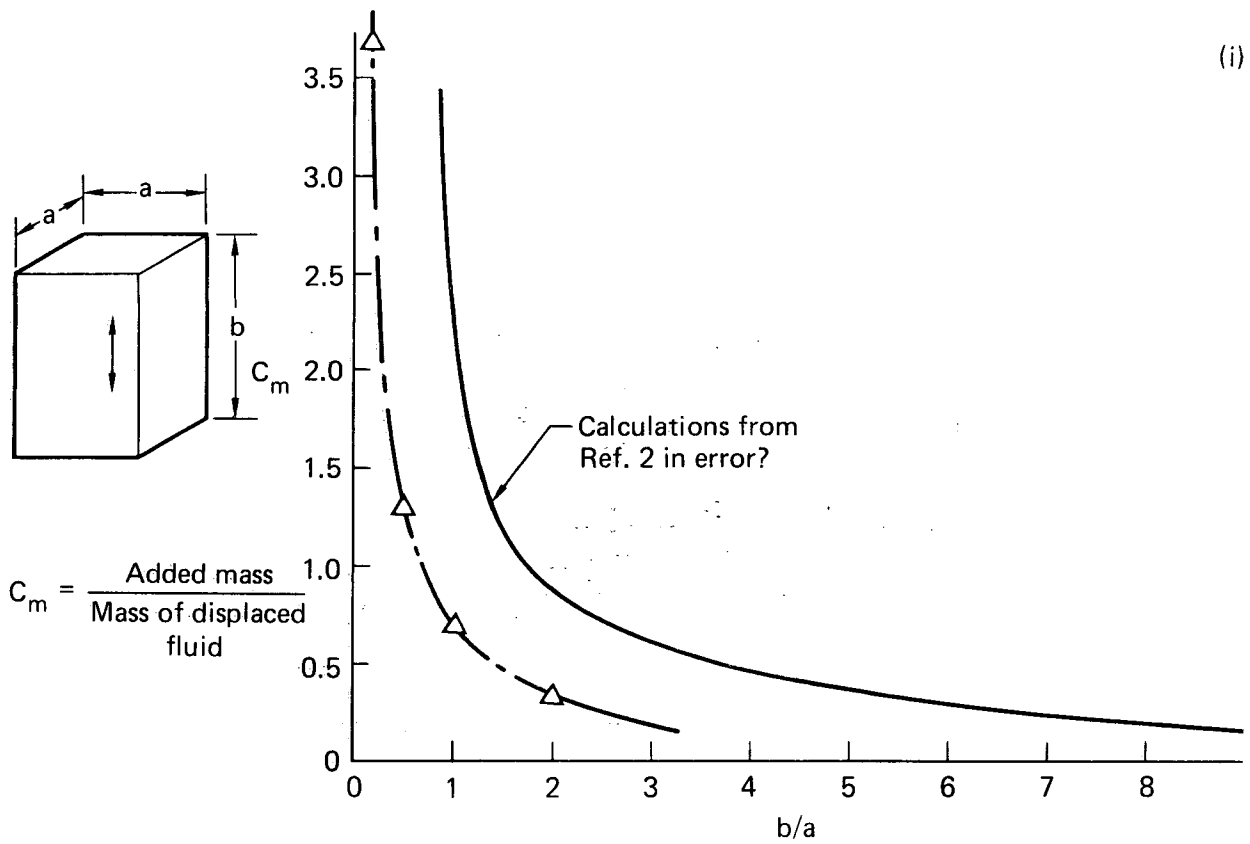


Fig. 5i. Comparisons for an oscillating solid in still fluid.

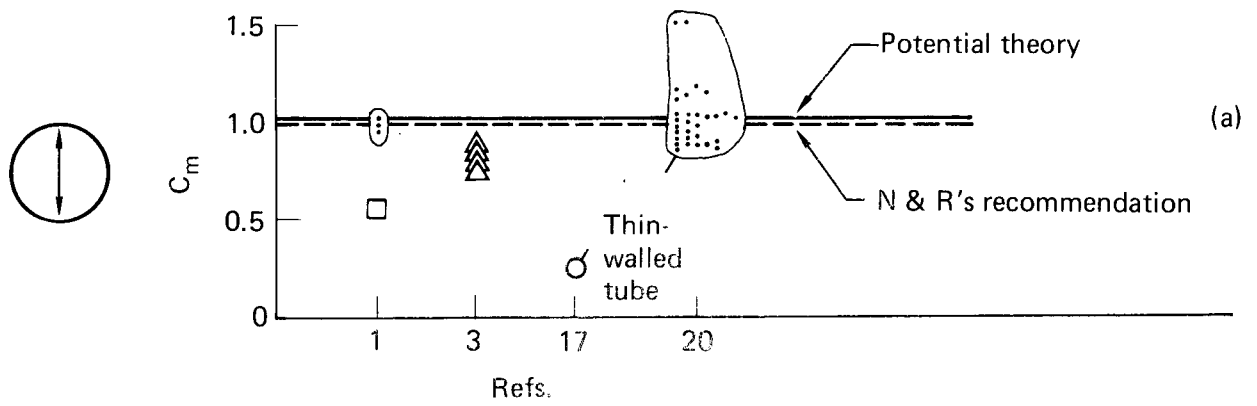


Fig. 5a. Comparisons for an oscillation circular cylinder in still fluid.

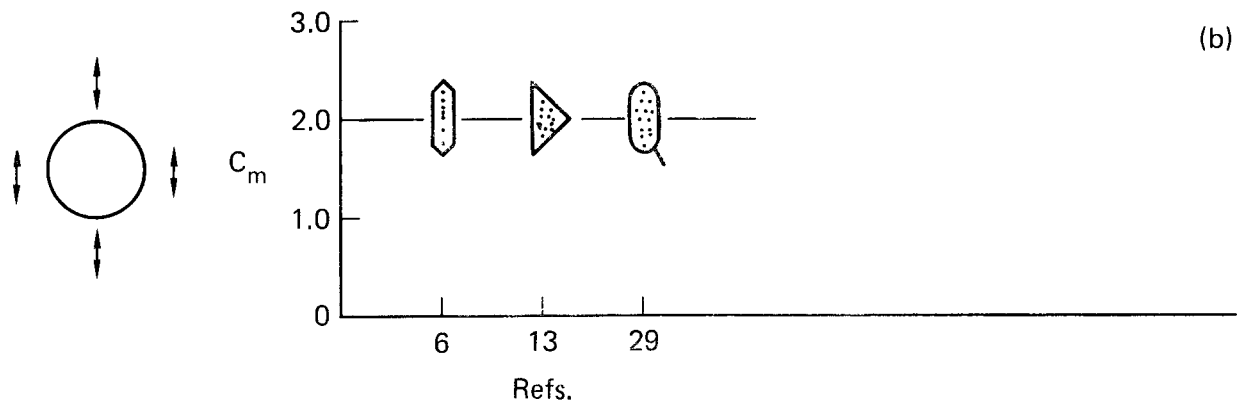


Fig. 5b. Comparisons for a fixed circular cylinder in oscillating fluid.

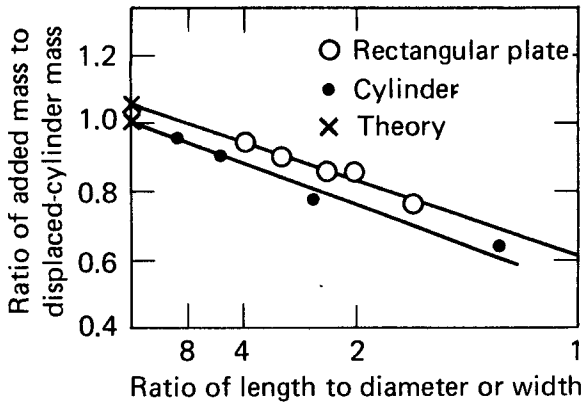


Fig. 6. Circular cylinders and rectangular plates.⁴

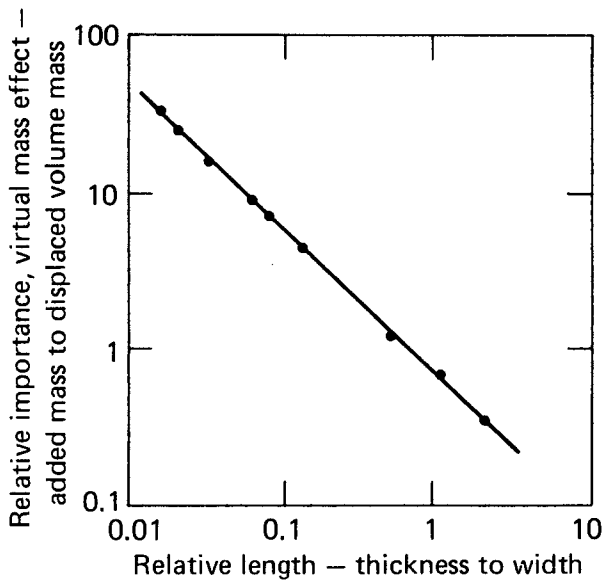


Fig. 7. Relative effect of virtual mass in parallelepipeds — square side moving broadside on.⁴

described as an equivalent viscous damping. The contributions to added damping are:

- Fluid viscosity.
- Component impact.
- Wave generation.
- Acoustic generation.

The last two are forms of radiation-damping; i.e., wave or acoustic energy generated radiate away from the submerged member. We do not expect a significant amount of acoustic energy generation for the structures and excitations of concern. Wave generation is generally not important for fully submerged structures under seismic excitation,^{1,5} and it seems reasonable to extend this to other types of excitations, such as vibrations induced in the main

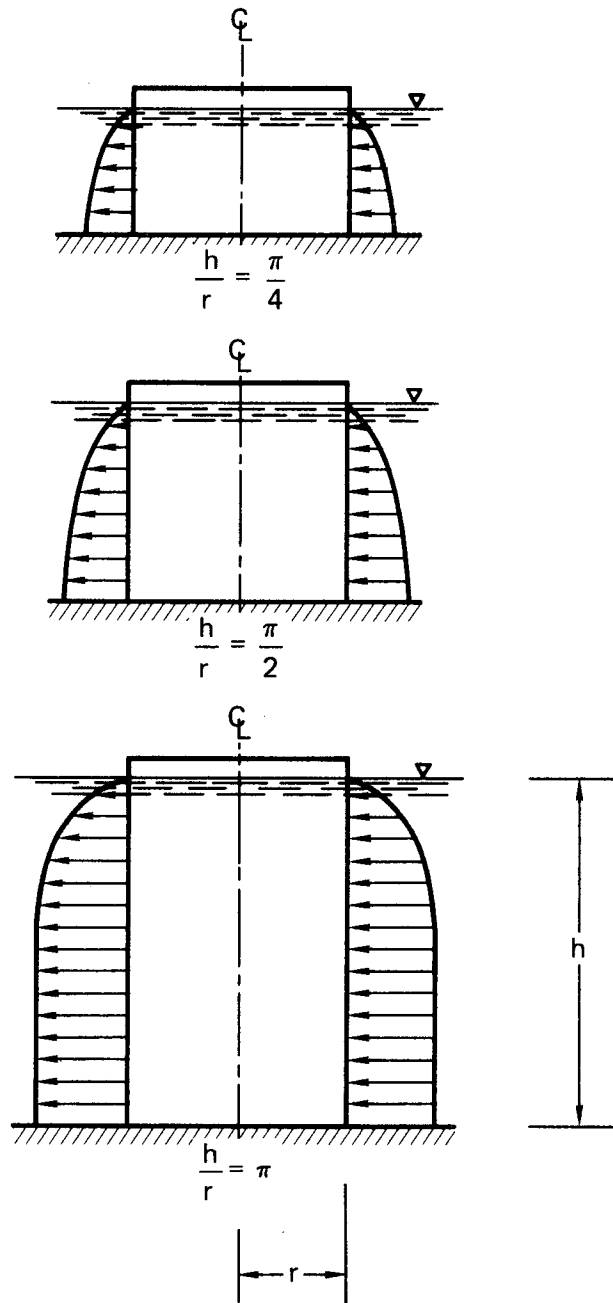


Fig. 8. Added mass distribution for a partially submerged member.^{5,9}

steam-relief valve line by normal pressure relief. For partially or fully submerged members in a finite-size water enclosure, radiation damping is again, usually not taken into consideration, because the radiation energy may bounce off the enclosure walls back to the submerged member. Therefore, in the actual structures of concern, we choose to ignore wave generation as a source of damping. Component impact may be a significant source of damping for

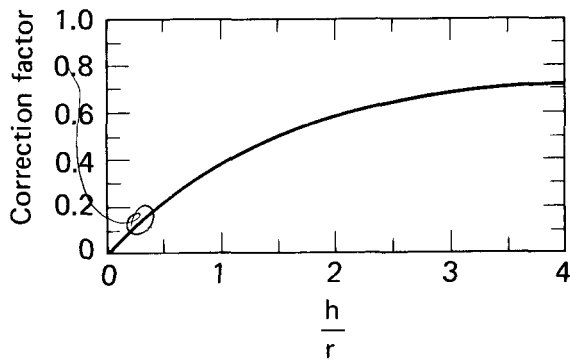


Fig. 9. Liquid mass correction factor in circular pier.^{5,9}

multiple members, and this will be discussed further when we address multiple members later in this report; however, it is not a source of damping for single isolated members. Therefore, for single isolated members, fluid viscosity is the only source of damping in need of consideration.

Added damping is not as thoroughly investigated in the literature as was added mass. Theoretical predictions of damping are seldom attempted because experimental values are usually more reliable. Therefore, our conclusions on added damping are based whenever possible on published experimental data.

Experimental data on added damping are represented in Refs. 1, 3, 20, and 27 covering a variety of specimen shapes and experimental conditions. The most extensive set of data is found in Ref. 20 where circular cylinders of 0.31-, 0.5-, 0.75-, and 1.0-in. diameters are investigated over the frequencies 2.5 to 18.6 Hz and amplitude-to-diameter (A/D) ratios of up to 2.0. The data of Ref. 20 indicate that viscous damping applies up to an A/D value of 0.32 for the smallest specimen (0.31 in. diam) and 0.5 for the largest (1.0 in. diam). Beyond the viscous damping range is the nonlinear range where the damping force becomes proportional to the square of the velocity. The change from linear to nonlinear behavior with increasing A/D value was quite distinct as indicated in Fig. 11 for two examples from Ref. 20. Nonlinear damping is seen to be greater than linear damping, so that using the linear damping value as an approximation in the nonlinear range will be conservative. The A/D values where the change from linear to nonlinear damping occurs are plotted vs. specimen diameter in Fig. 12. A gradual increase with diameter is seen; however, without data for larger diameters we are uncertain if the trend would continue to increase for the sizes of actual structures of concern.

In structural analysis, damping is expressed as either a damping coefficient or a percent of critical

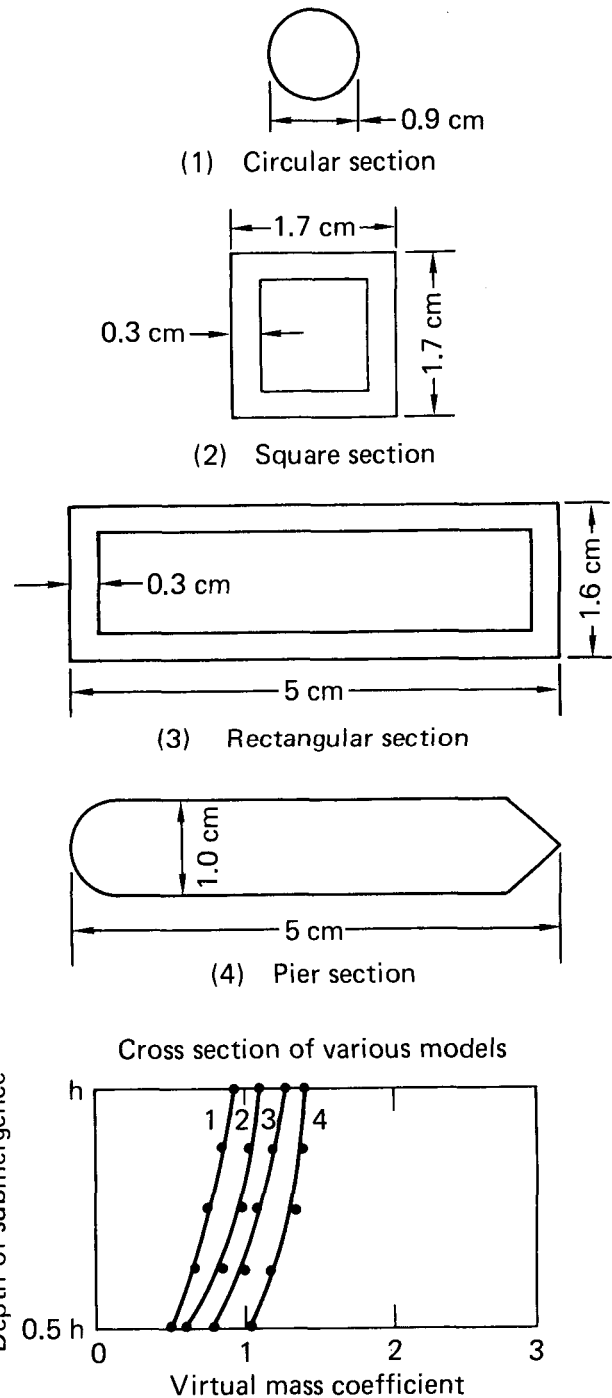


Fig. 10. Variation of virtual mass vs depth of submergence.³

damping. Damping coefficient describes the damping independent of the mass and stiffness of a structure, whereas, the percent of critical damping is a description associated with the mass and stiffness. To see which description best fits the added damping from water we converted the data in Ref. 20 to both an added coefficient and an added percent of critical

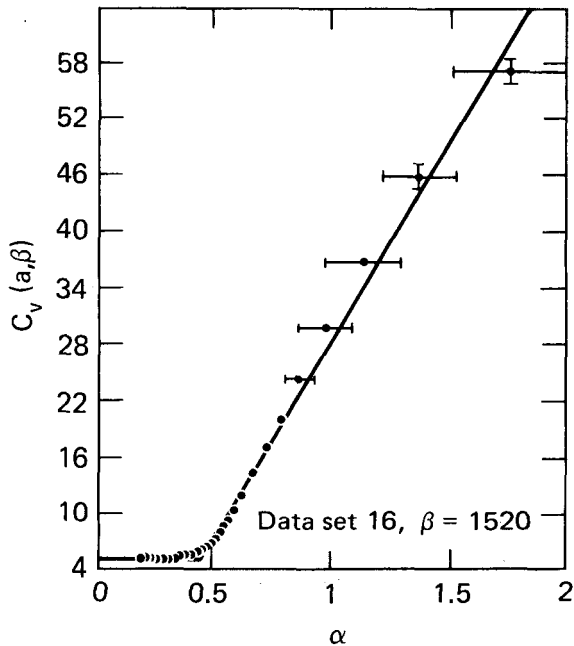
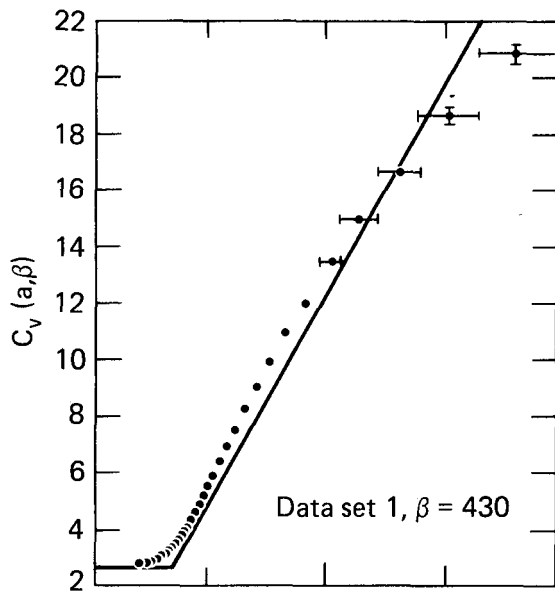


Fig. 11. The calculated viscous damping coefficient $C_v(\alpha, \beta)$ vs the dimensionless amplitude $\alpha = A/D$. The calculated points are denoted by the "+" symbol and the inherent error bounds on these points are enclosed by the "()" symbol. The solid curve is the two-segment straight line fit to the calculated points.²⁰

damping. These are plotted vs. frequency in Figs. 13a and 13b, respectively. The added coefficient varied significantly with frequency in an inconsistent manner; i.e., the 0.13-, 0.5-, and 0.75-in. specimen showed an increase with frequency, whereas the 1.0-in.-specimen showed a decrease. The added percent

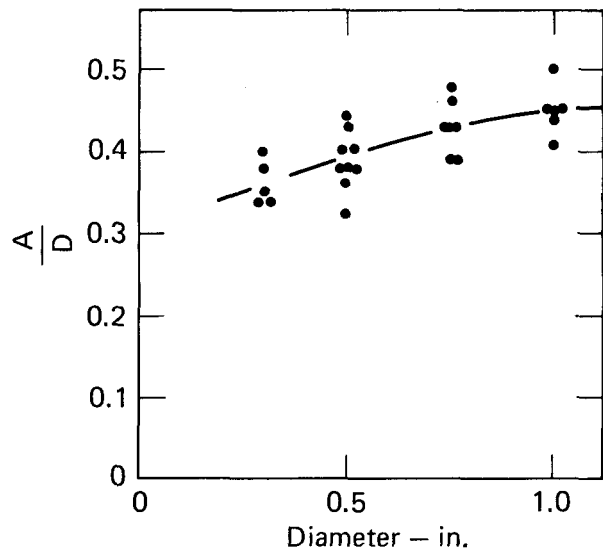
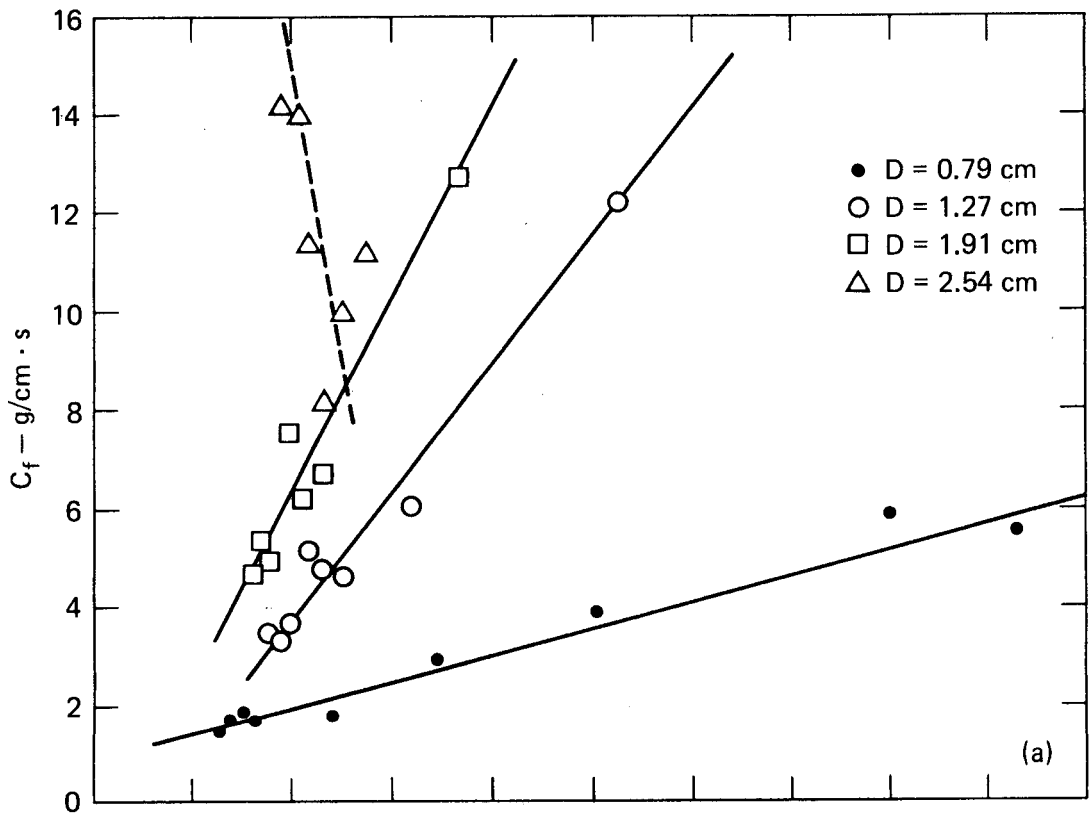


Fig. 12. Amplitude/diameter value for linear damping, oscillating submerged circular cylinders.²⁰

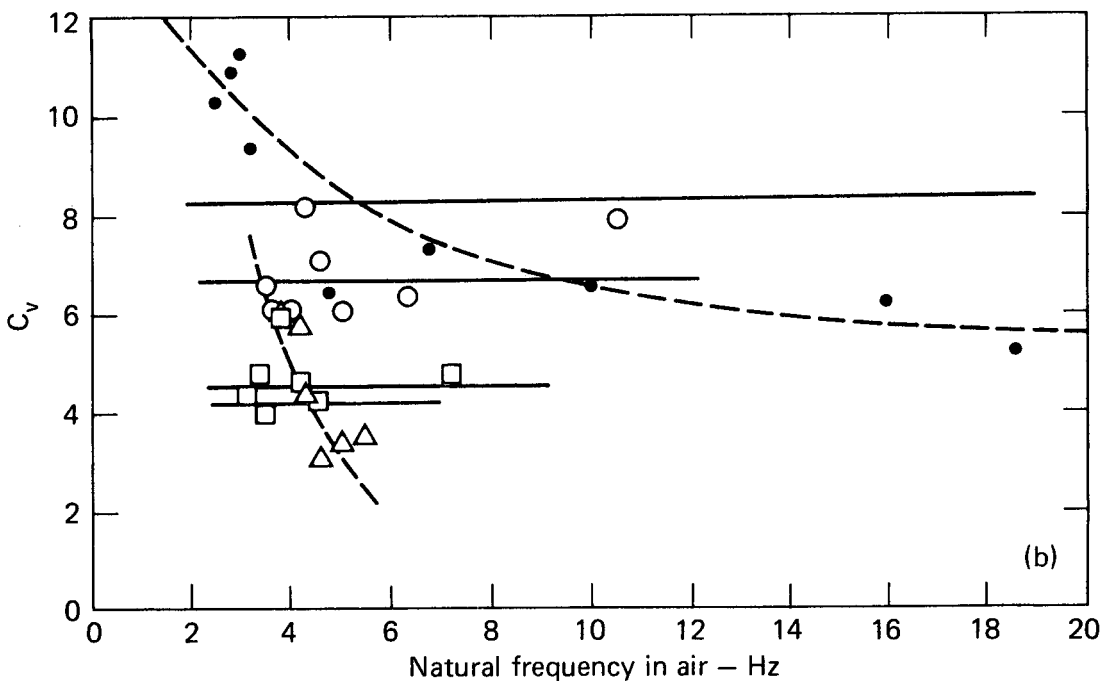
of critical damping varied less and was more consistent; i.e., all specimens showed either a constant value or decreasing value with frequency. Those showing decreasing values are the 0.31- and 1.0-in. specimens, as indicated by dashed curves in Fig. 13b. At this point, we chose to impose a simplification to proceed with forming a workable recommendation. Therefore, we chose to describe the percent of critical damping as a constant with respect to frequency. The constant values are indicated by the solid curves in Fig. 13b, and are plotted in Fig. 14 as a function of specimen size. Experimental data from Refs. 1, 3, and 27 are added, and these included specimens of circular, square, and plate cross-sections. The data points are few, and the scatter is moderate; yet a general trend is apparent in that added damping decreases with increasing specimen size. The trend was established by the data for circular specimens and was not contradicted by the data for square and plate specimens. Further discussion of this trend follows.

5.6 Effect of Structural Size on Added Damping for Single Isolated Members

The decrease in added damping with increasing structural size indicated in Fig. 14 is further confirmed by comparing with a similar trend established for damping of water sloshing in pools. The latter trend is well established, and expressions for the dependence of damping on pool size are given



Added damping in terms of damping coefficient.



Added damping in terms of the percent of critical damping.

Fig. 13. Damping data on oscillating circular cylinders in still water.²⁰

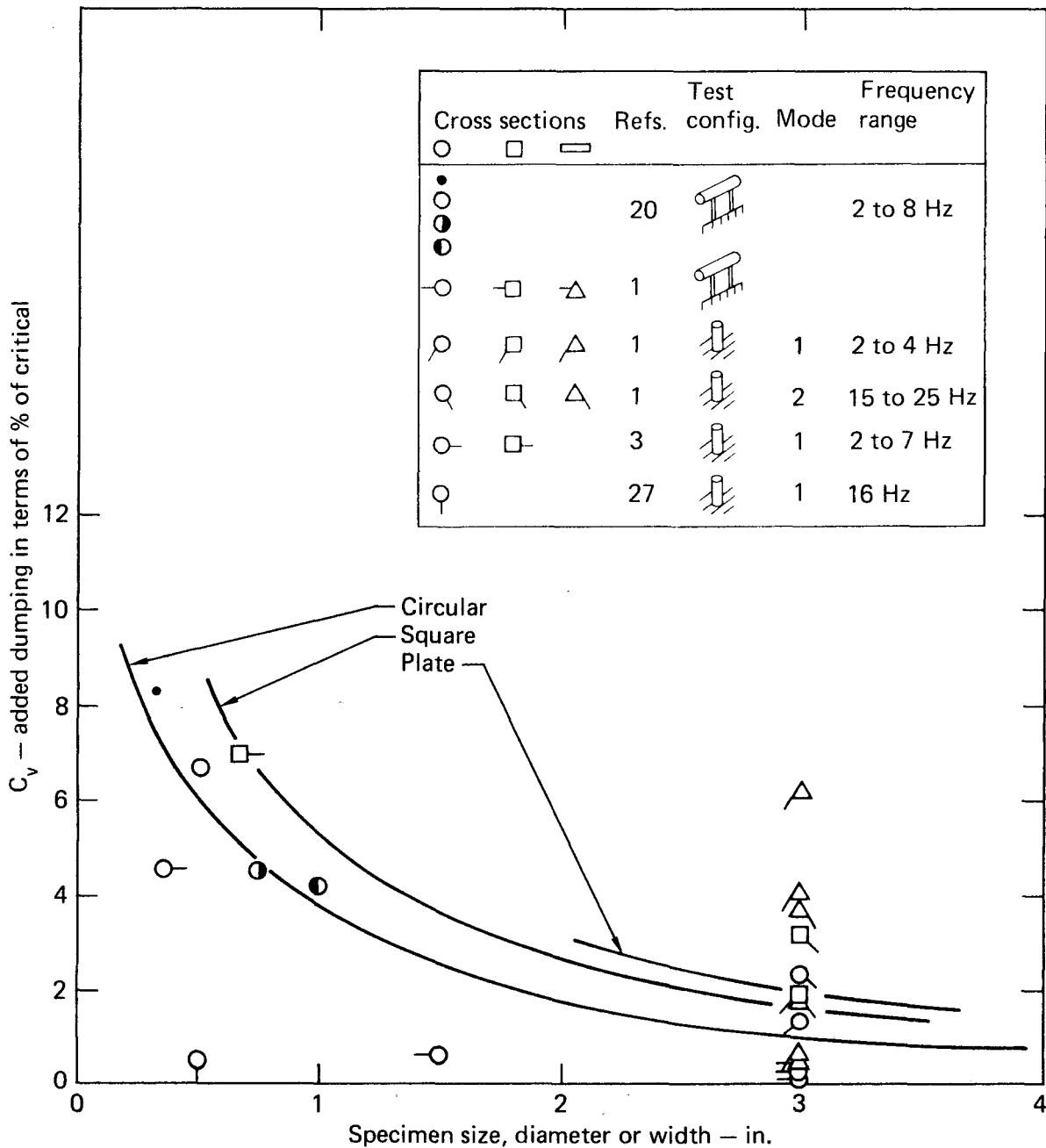


Fig. 14. Percent of added damping for various specimen cross sections and sizes.

in Refs. 51, 52, and 53. Several different expressions are seen in these references; however, they all have a common form of,

$$\log(\delta) = \log(A) - (q) \cdot \log(R)$$

where δ is the damping of the water sloshing in the pool, A is a constant, q is the constant defining the dependence on the pool size, and R is the length of the pool. Depending on the expression used, the value of q ranged from 0.75 to 1.0.

To see if the decrease in added damping for submerged single isolated members follows the trend established for water sloshing in pools, the data in Fig. 14 is replotted in Fig. 15 in terms of $\log(\text{damping})$ vs $\log(\text{specimen size})$. The scatter is rather wide; however, the decreasing trend is apparent. A straight line was least-square fitted to the data as shown. The slope of this line gave $q = 0.85$. Because the value of 0.85 fell between the values of 0.75 and 1.0 established for pools, we interpret this as good

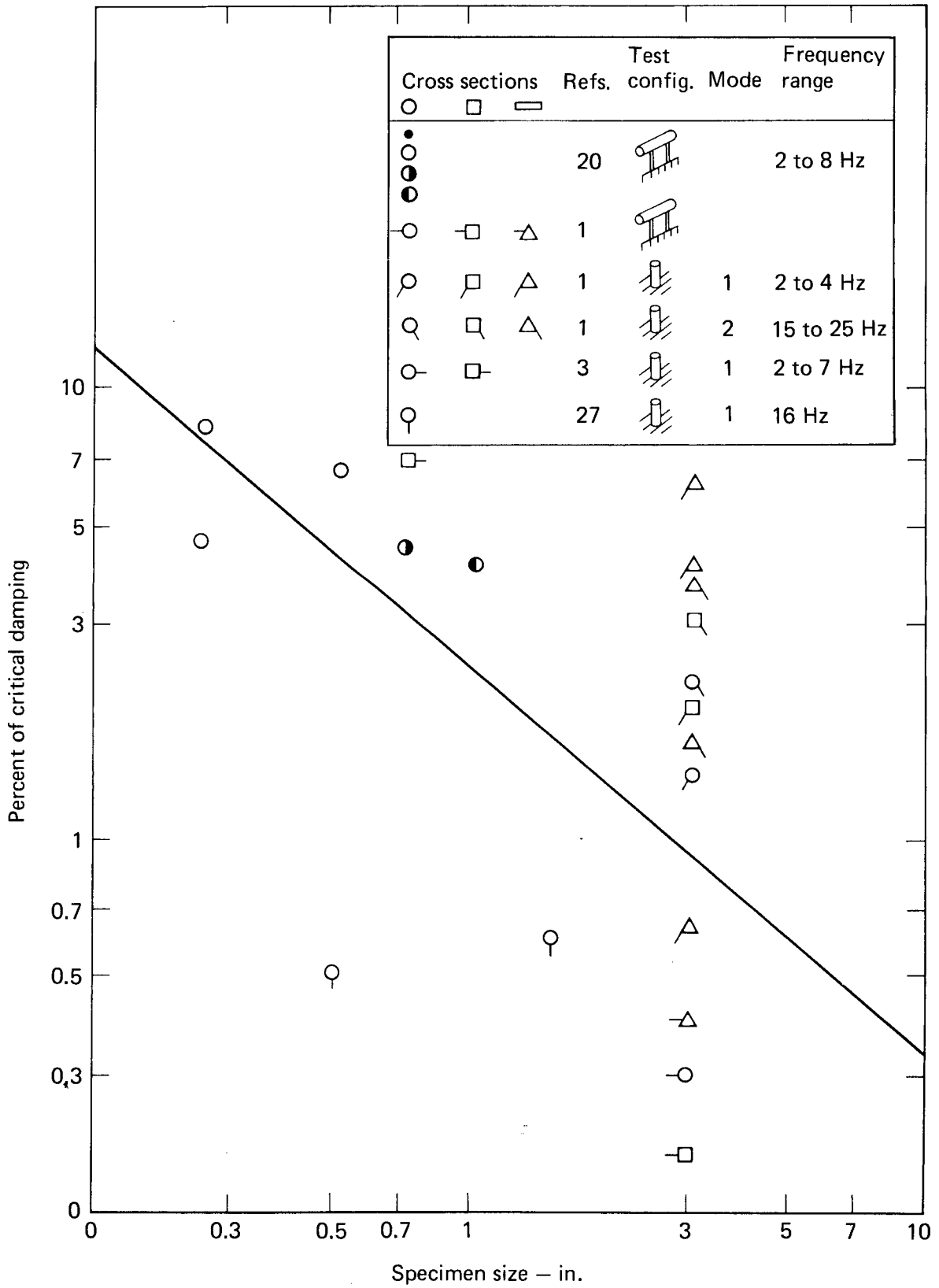


Fig. 15. A log vs log plot of the percent of added damping for various specimen cross sections and sizes.

confirmation that added damping for submerged single isolated members decreases with increasing structural size and that the dependence on structural size is reasonably characterized by Fig. 15. Our findings were shown to D. D. Kana of the Southwest Research Institute,⁵⁴ and he agreed that our treatment and interpretations are reasonable in view of the current state of understanding of the added damping phenomenon. We, then, used Fig. 15 to extrapolate the added damping values for the structural sizes of concern shown in Table 3. The results are given in Table 7. Except for single isolated fuel elements, the damping for all other single isolated members of the structures shown in Table 7 is quite low. These low values are in agreement with Newmark and Rosenblueth's suggestion⁵ (See Section 5.1 of this report) that "damping due to liquid viscosity may be disregarded" for single isolated members of common structural sizes.

5.7 Range of Applicability of the Added Mass and Added Damping Concept for Single Isolated Members

The range of applicability of the added mass and added damping concept for single isolated members can be considered as being defined by the smaller of either the range for added mass or the range for added damping. In Section 5.4 of this report, the range of applicability of added linear damping was found to vary from an amplitude to diameter (A/D) ratio of 0.32 for a 0.31-in. diameter specimen to an A/D value of 0.5 for a 1.0-in. diameter specimen. The applicable range increases with specimen size, so that we would expect the range to be greater than an A/D value of 0.5 for specimen diameters larger than 1.0 in. Also in Section 5.4, we observed that beyond the range of applicability for linear damping, the damping increases. Therefore, using linear damping beyond the linear range would be conservative. Consequently, depending on the degree of conservatism desired, linear added damping may be used to

some degree beyond its applicability range. Again in Section 5.4 of this report, the added damping values for single isolated members of structural sizes of actual concern are generally quite low. (See Table 7). Except for the single isolated fuel element, we may choose to ignore the added damping. In this case, the range of applicability for the added damping concept may be disregarded.

Turning now to the range of applicability of the added mass concept for single isolated members, experimental results for added mass coefficient C_m over a wide range of amplitudes for various specimen geometries are shown in Figs. 16 through 19. The abscissa in all four figures is $U_m T/D$ which is simply 2π times the A/D ratio; U_m is the velocity amplitude, and T is the period of oscillation in seconds per cycle. Comparing these curves with the theoretical value for C_m obtained using potential theory we defined the range of applicability as the range of $U_m T/D$ corresponding to experimental values of C_m within $\pm 10\%$ of the theoretical value. The resulting A/D values for the applicable range of added mass are tabulated in Table 8. The A/D values for the applicable range of linear damping are also indicated.

The four values of A/D in Table 8 for the applicable range of the added mass concept are in good agreement. The A/D value for a sphere is expected to be higher than that for a cylinder or plate because it is a finite length specimen (more streamlined), and, therefore, potential flow can be expected to apply over higher values of displacements. The A/D range of 0.32 to 0.5 for the applicability of linear damping is not drastically different from the 0.8 and 1.4 values for added mass. Therefore, we consider the ranges for both to be mutually supportive.

Because the smallest structure of concern shown in Table 7 is 0.5-in. diameter, the range of applicability for the added mass and added damping concept for these structures, as single isolated members, can be considered to be no less than an A/D value of 0.4 according to Table 8. If added damping should be ignored, then the range would be an A/D value of

Table 7. Added damping values projected in Fig. 15 for single, isolated structures

Structure	Size, in.	Added damping, % of critical
Fuel elements	$\sim 0.5 D$	≤ 4.2
BWR fuel bundle	$\sim 5.5 \times 5.5$	≤ 0.55
PWR fuel bundle	$\sim 10 \times 10$	≤ 0.33
Main steam-relief valve line	$\left\{ \begin{array}{l} 8 D \\ 12 D \end{array} \right.$	≤ 0.40
		≤ 0.29

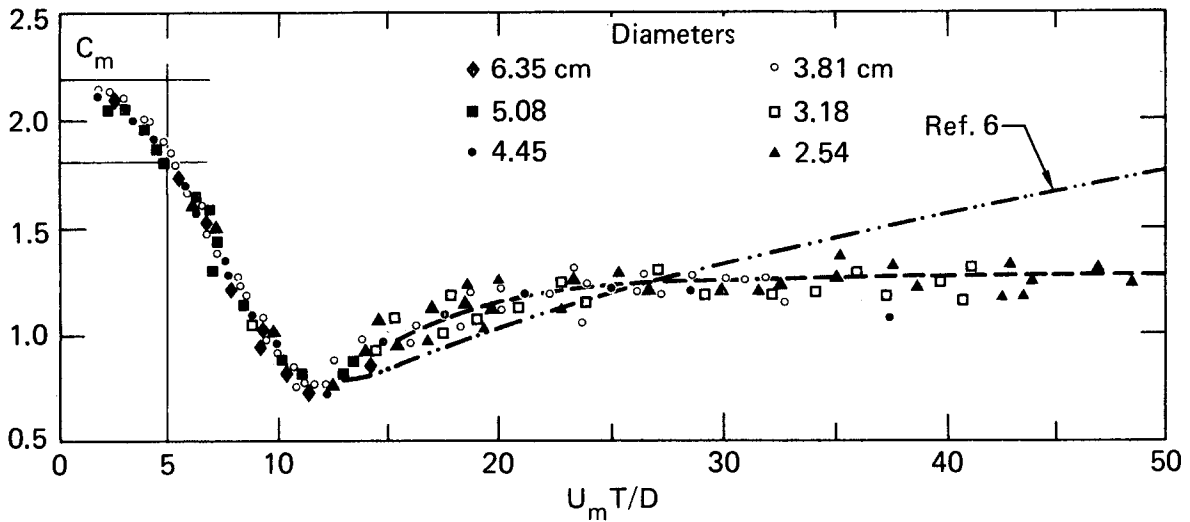


Fig. 16. Mass coefficient vs the period parameter for a cylinder.²⁹

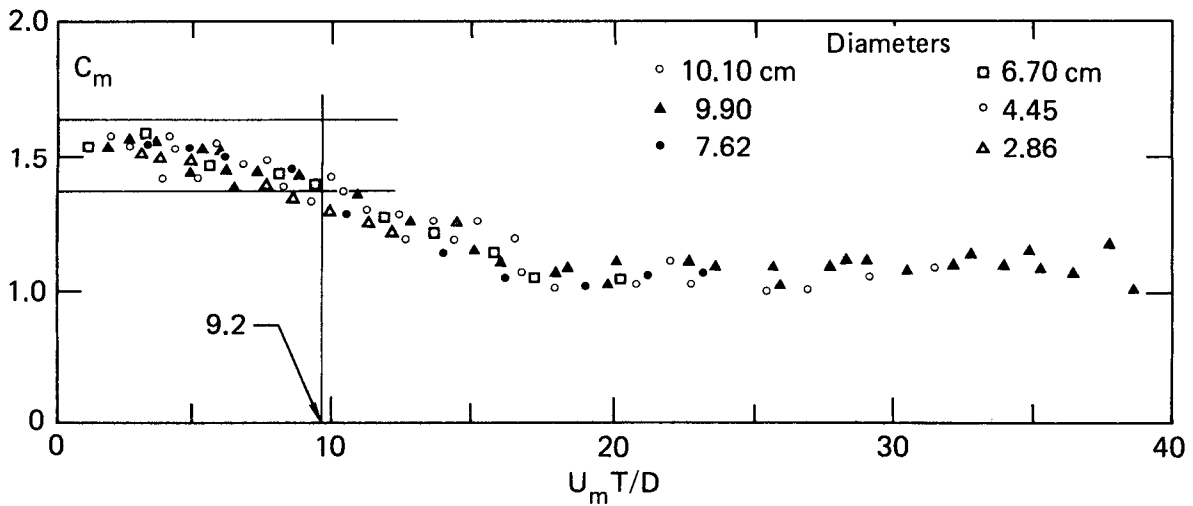


Fig. 17. Mass coefficient vs the period parameter for a sphere.²⁹

Table 8. Applicable range of motion amplitude determined from added mass and added damping experimental data

Type of data	Specimen geometry	$A/D = U_m T / 2\pi D^*$
Added mass	Circular cylinder ²⁹	0.8
	Sphere ²⁹	1.4
	Circular cylinder ⁶	0.8
	Plate ⁶	0.8
Added damping	Circular cylinder ²⁰	
	diameter:	
	0.31 in.	0.32
	0.5 in.	0.4
	0.75 in.	0.43
	1.0 in.	0.5

* U_m = maximum oscillating velocity
 T = period in seconds/cycle
 D = specimen diameter or width
 A = maximum oscillating displacement

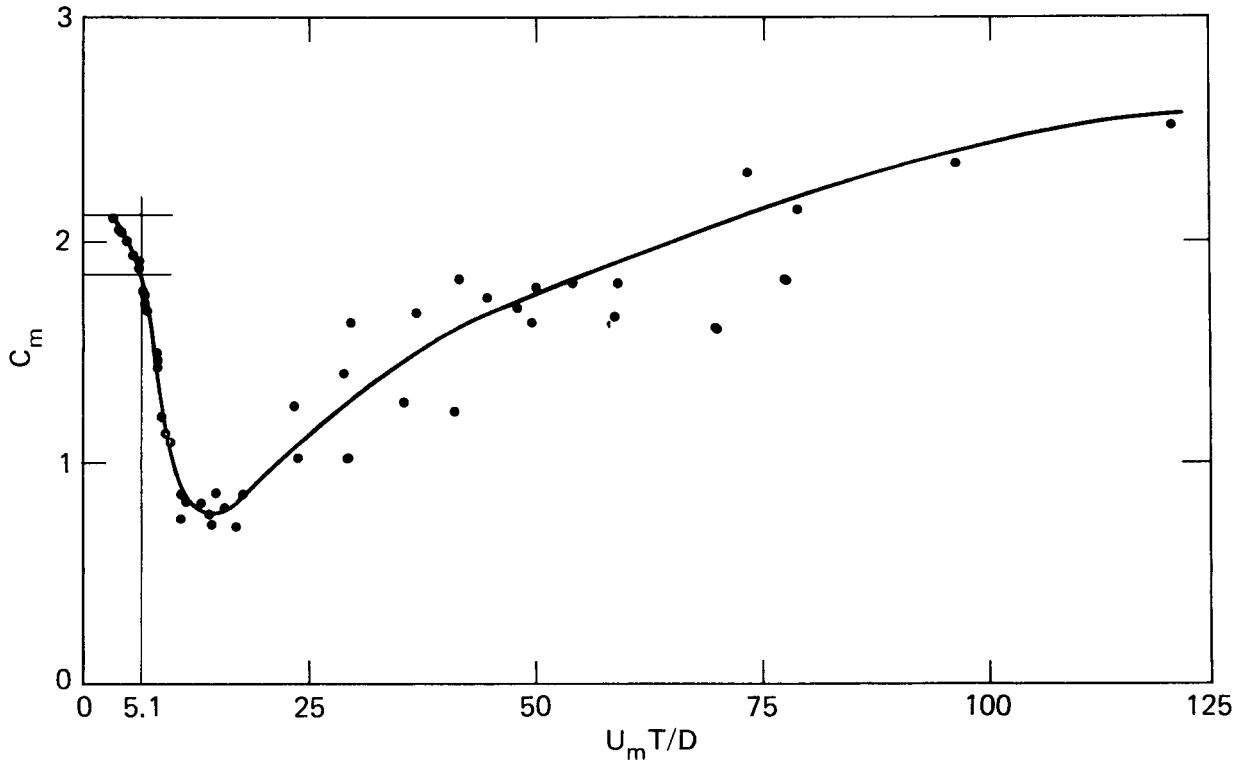


Fig. 18. Variations of the mass coefficient of cylinder.⁶

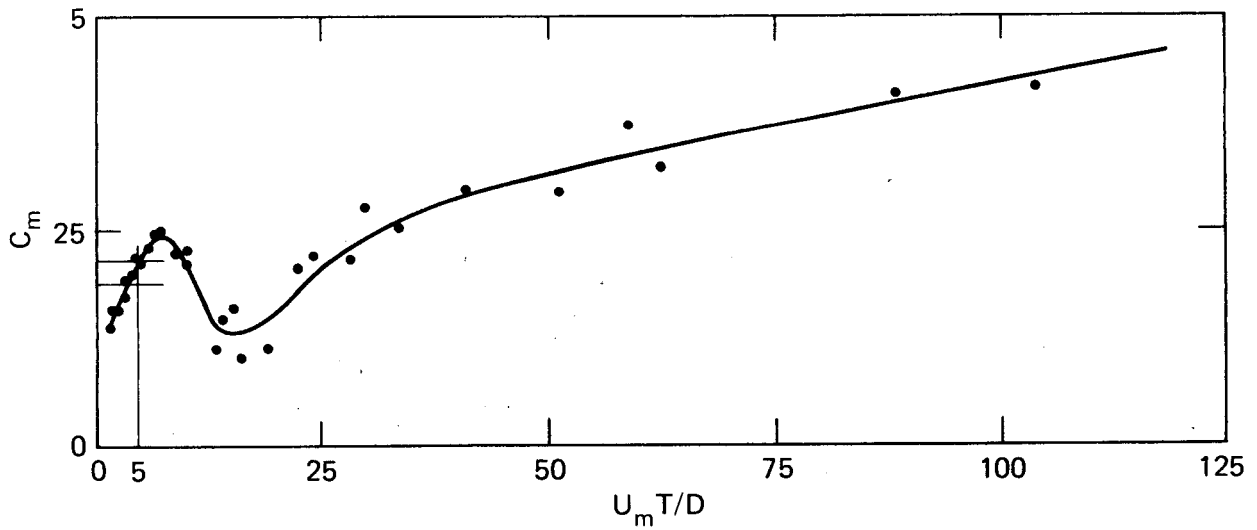


Fig. 19. Variations of the mass coefficients of plates.

0.8. In either case, however, the applicable range would probably adequately cover any response to seismic and normal steam-relief excitations. The response to an accident condition may or may not be within the applicability range depending on the structure involved and its location relative to the accident site.

Our conclusions are based on experimental data from rather small specimens, sizes up to 3.0 in. in diameter, and on rather low frequencies (0.35 Hz for

Ref. 29, 0.48 Hz for Ref. 6, and from 2.5 to 18.6 Hz for Ref. 20). Theoretical considerations indicated in the added mass coefficients should be size and frequency independent. We made a simplifying assumption that added damping is frequency independent, and we developed a technique to describe added damping as a function of structural size. Although we feel comfortable with our assumptions and developments, some additional experimental verification at higher frequencies and with larger specimens would be highly desirable.

6. MULTIPLE MEMBERS

6.1 Complexities Associated with Multiple Members

The fluid dynamic effects on multiple members are more complex than for a single isolated member. The arrangement of the members, space between members, motion of one member relative to another, and the generation of lift forces are all additional important considerations. Added mass forces are no longer necessarily in line with the direction of motion, and lift forces may be generated which tend to act perpendicularly to the direction of motion.^{10,26,36} Damping tends to be higher than for single isolated members, and tight spaces between members, in particular, can increase the damping measurably.^{27,47,49} Multiple-member response, in general, is not too well understood. Current interest appears high as evidenced in recent publications, particularly relating to nuclear reactors. Many highly theoretical works are presented; some are rather complicated in terms of practical, everyday use in design analyses. Some experimental data are available to validate certain, often limited, aspects of the theoretical solutions. In general, additional experimental validation is needed, and the range of applicability of the various analytical techniques needs to be established.

Although many of the investigations are motivated by reactor internal concerns, the results published so far apply at best only to normal reactor operations and not to conditions associated with a blowdown accident. The flow rates and/or component motions are assumed small. Conditions associated with a blowdown accident are very likely beyond the range of applicability of the various techniques presented.

For our presentation, we separate our findings with respect to three types of structural arrangements:

- (1) groups of cylinder, such as arrays,
- (2) groups of cylinders, or a single cylinder, surrounded by a large circular cylinder, and
- (3) coaxial flexible cylinders.

The first category can apply to the main steam-relief valve line next to the pressure suppression pool wall, an array of fuel elements in a fuel bundle, an array of fuel bundles in a spent-fuel storage rack, and an array of storage racks in a spent-fuel storage pool. The second and third categories can apply to the reactor-vessel internals.

6.2 Hydrodynamic Coupling for Groups of Cylinders

Closed form solutions using potential theory are presented in Refs. 10, 18, 19, 32, 33, 34, 35, 36, 42, 43, and 48 for added mass and lift forces for a group of cylinders. The solutions are given in terms of multiple summations and infinite series. The analyses are rather complicated but quite general; a group of different sized cylinders arranged arbitrarily can be handled, at least theoretically. A clear physical interpretation of the complex solutions is not immediately apparent. Some insight is provided in Refs. 32, 34, 35, and 36, where the solution is expressed in terms of "self-added" and "added" mass coefficients. The self-added mass coefficients characterize the hydrodynamic forces on a member from its own motion with all other members held stationary. The added mass coefficients characterize

the hydrodynamic forces in a stationary member with other members in motion. Because potential theory is linear, reciprocity applies; i.e., the force induced onto member i from the motion of member j is the same as the force induced onto member j from the motion of member i .

Experimental comparisons with theory are given in Refs. 30, 32, and 36 for a seven-member hexagonal array (Fig. 20) and a 3 x 3 square array (Fig. 21). In both configurations, the central member is in motion while the rest are stationary. The self-added mass coefficients for the central member are determined for four sizes of space between members. The agreement between theory and experiment is good. Comparisons between theory and experiment are made for a row of five cantilevered cylinders, a group of three cantilevered cylinders, and a group of four cantilevered cylinders⁴⁸ in terms of natural frequencies and mode shapes. The group arrangements are shown in Figs. 22, 23, 24, and 25, respectively, and the comparisons in Figs. 26, 27, and 28, respectively. The agreement between theory and experiment is good. Further comparisons were made in terms of acceleration response under steady-state sinusoidal excitation for the row of five cylinders and the group of three cylinders. The frequency of excitation was swept from 50 Hz to 80 Hz. The comparisons are shown in Figs. 29 and 30 for the two cases, respectively. The agreement is good in Fig. 29 and fair in Fig. 30.

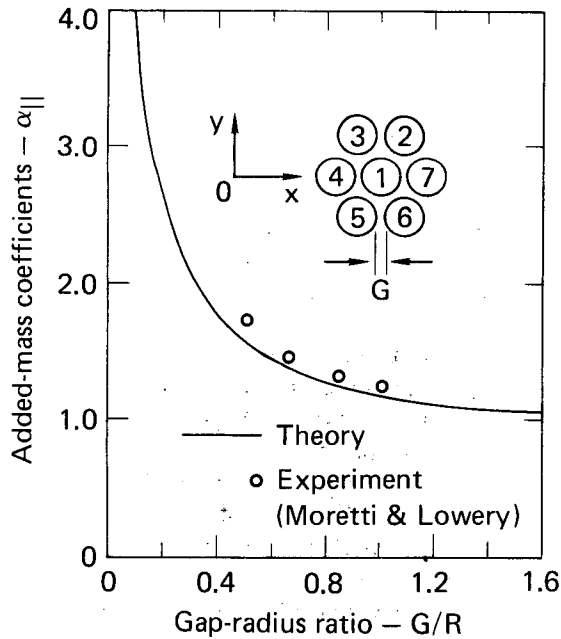


Fig. 20. Theoretical and experimental values of added mass coefficients for a seven-rod bundle.²³

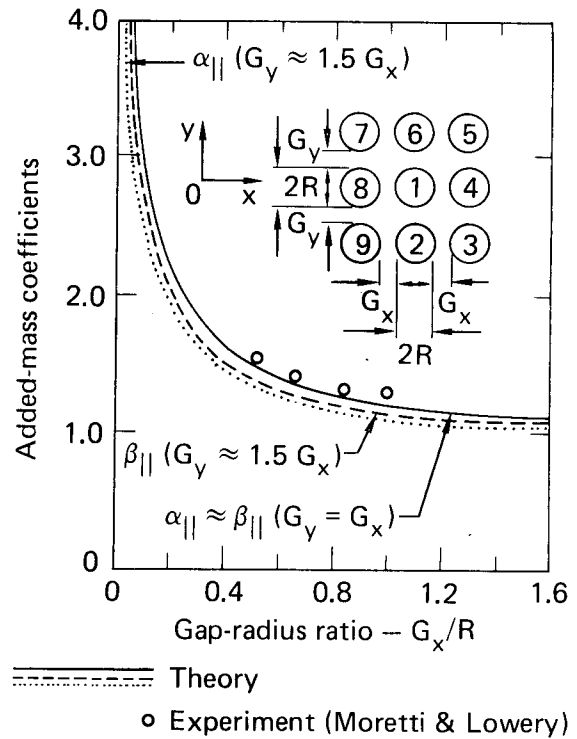


Fig. 21. Theoretical and experimental values of added mass coefficients for a nine-rod bundle.³²

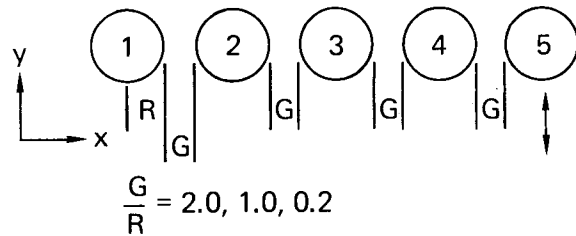


Fig. 22. Row of five cantilevered cylinders.⁴⁸

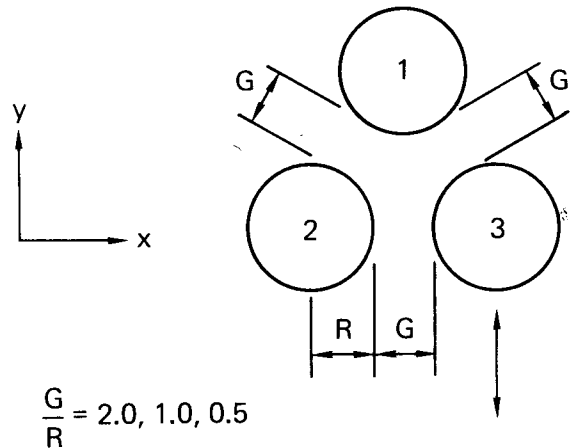


Fig. 23. Group of three cantilevered cylinders.⁴⁸

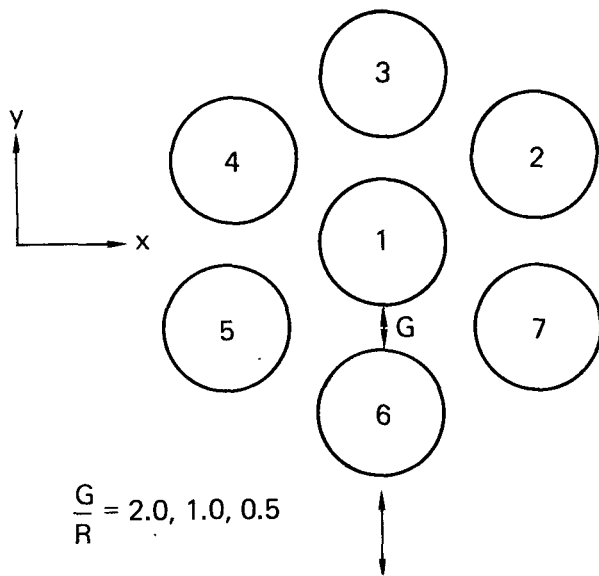


Fig. 24. Array of seven cantilevered cylinders.⁴⁸

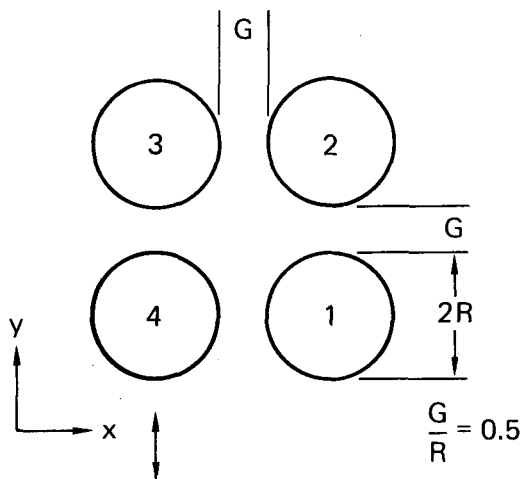


Fig. 25. A 2 x 2 array of cantilevered cylinders.⁴⁸

Although experimental confirmations are few, they are generally good for arrays of cylinders. Combining this with the excellent confirmation established for single isolated members that was discussed earlier in this report, we feel rather confident that the potential theory will adequately describe the added mass and lift forces for groups of cylinders. We would expect the range of applicability with respect to motion amplitude to be less than that for single isolated members because of the close proximity of the members. Whether or not the potential theory will be adequate under excitations of normally expected earthquakes is unknown. However, for the time being, we believe the potential theory can be assumed adequate based on the rather

high range of displacement amplitudes applicable for single isolated members; see Section 5.7.

The added mass and lift forces for a 4 x 4 array of cylinders moving in unison, as shown in Fig. 31, are calculated using potential theory.¹⁰ This illustrates an important effect resulting from hydrodynamic coupling among groups of members. The added mass forces are not necessarily in line with the direction of the motion, and lift forces tending to act perpendicular to the direction of motion are generated. In addition, the distribution of forces is not uniform among the members. The total load on each member, the vector sum of the added mass and lift forces, accentuates this nonuniformity. In terms of the total load, cylinders 4 and 6 in Fig. 31 carry the highest, while cylinders 1 and 13 carry the lowest. Non-uniformity in the load for arrays are not accounted for among the design methods in current use outlined in Section 4 of this report. It may, or may not, be important, depending on the purpose of the analysis and on the configuration of the array; however, its existence and possible effects should be kept in mind.

For the 4 x 4 array shown in Fig. 31, the net lift force for the entire array is zero because of symmetry. The total added mass force, however, depends on the space between members. For the case where the X and Y center-to-center, distance-to-diameter (X/D and Y/D) ratios are both 1.5, the total added mass force is equal to 16 times that of a single isolated cylinder.¹⁰ However, for X/D = 1.5 Y/D = 3.0, the total is 20 times that of a single isolated cylinder.¹⁰ In the latter case, the total force carried by the array is greater than that carried by 16 individual isolated cylinders. The direction of the motion or flow, as well as the spacing, affect the force magnitudes as shown in Figs. 32 through 35 taken from Ref. 10. These effects, as well as the nonuniform load distribution, underscore the importance of considering hydrodynamic coupling for groups of cylinders.

If the spacing between members is increased, when will the members respond as if isolated? For a single isolated circular cylinder the added mass coefficient is unity, and the lift force is zero. Using these values as the criteria for defining when members of a group become essentially isolated, Figs. 33a and 34a indicate that the members of the 4 x 4 array of Fig. 31 become essentially isolated at X/D and Y/D ratios of 2.5.¹⁰ Similarly, an X/D ratio of 2.5 was obtained for the case of two parallel cylinders as reported in Refs. 18, 19, and 26. Other arrangements also gave ratio values of 2.5; these include in-line and staggered arrangements of three cylinders and arrays other than 4 x 4 square arrangements (Refs. 18, 19, 26, 30, 31, 32, 34, 35, 36, and 42). Thus, a ratio value of 2.5 seems to be more or less universally applicable.

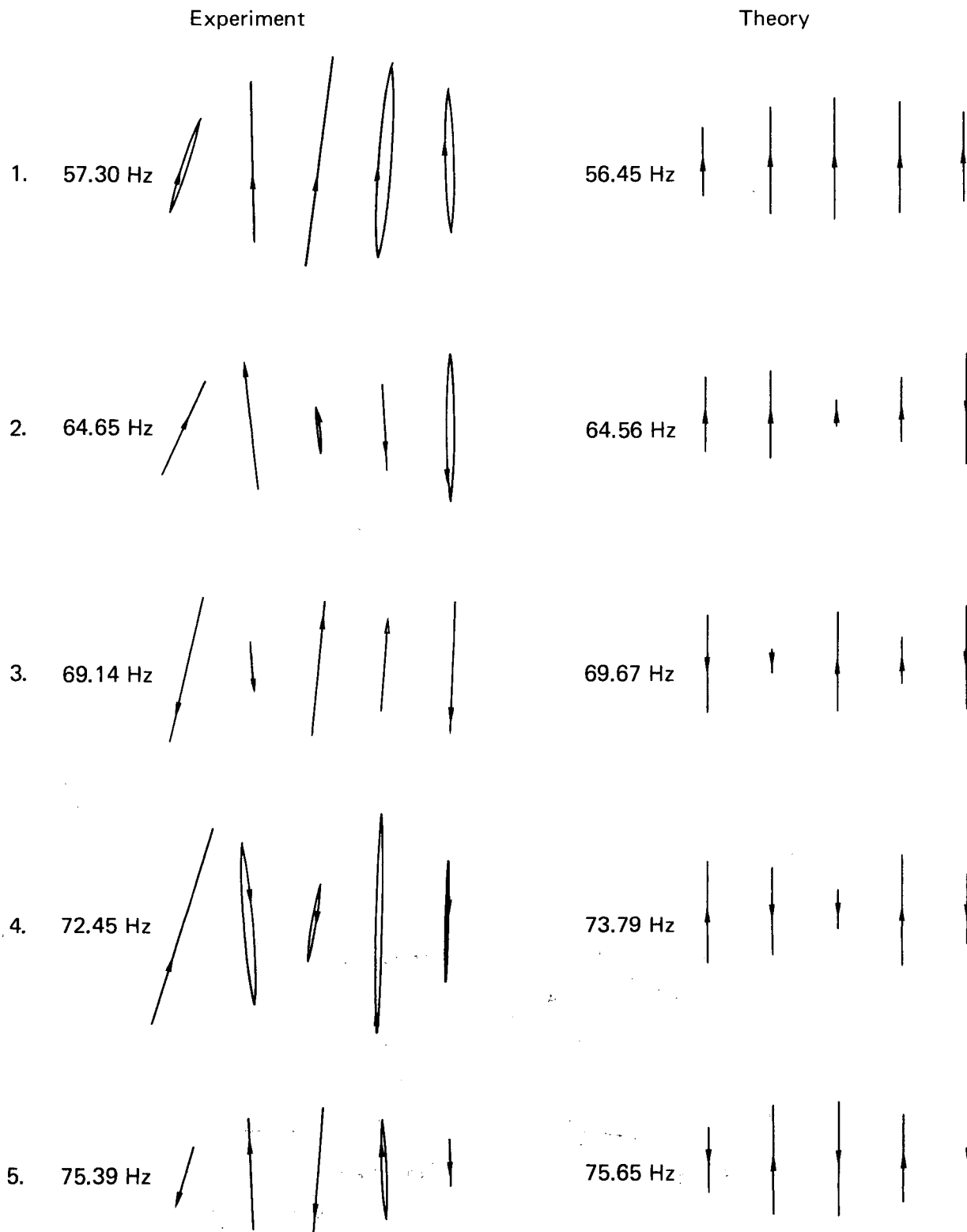


Fig. 26. Mode shapes of a row of five tubes with a $G/R \approx 0.25$.⁴⁸

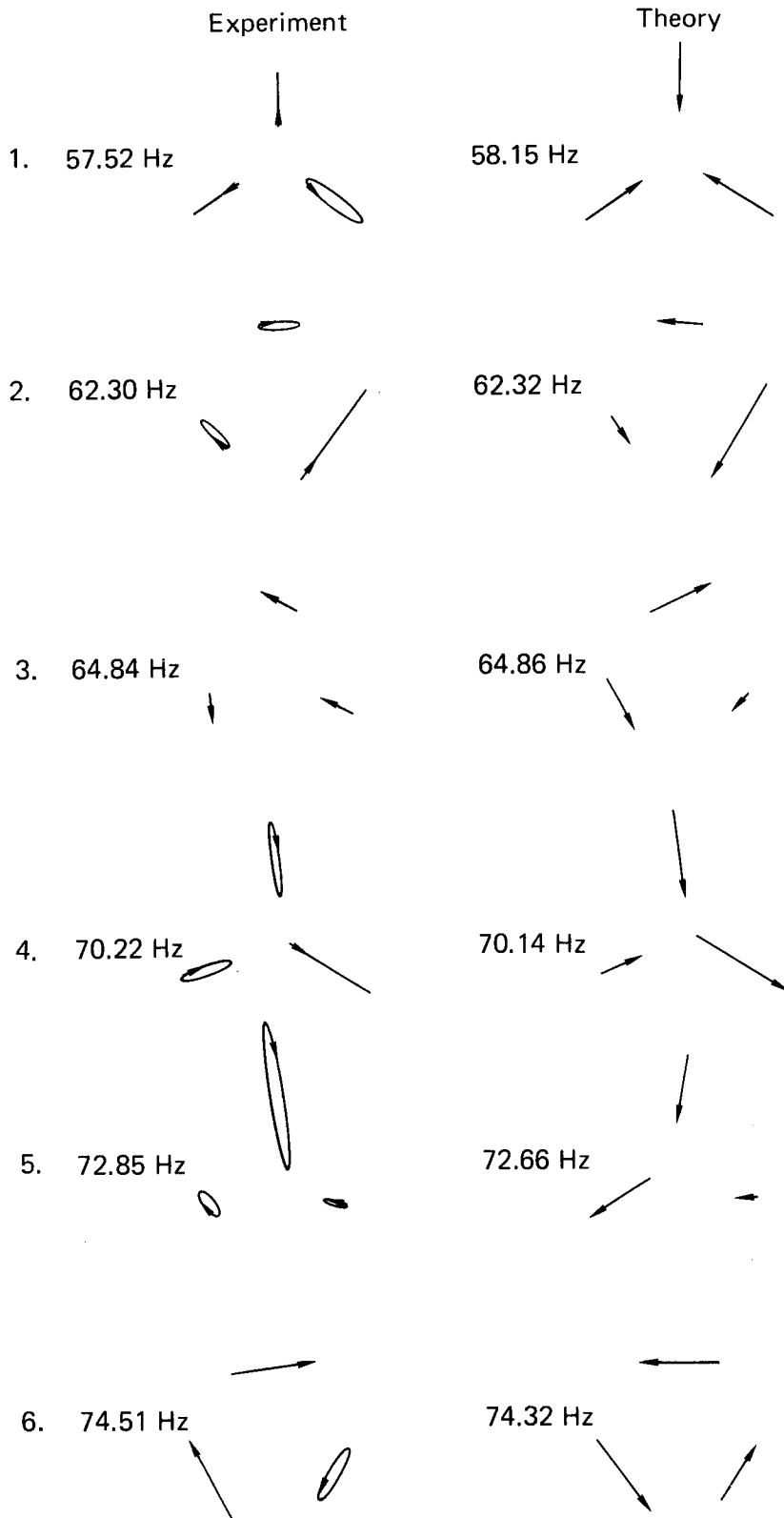


Fig. 27. Mode shapes of a group of three tubes with a $G/R = 0.5^{48}$

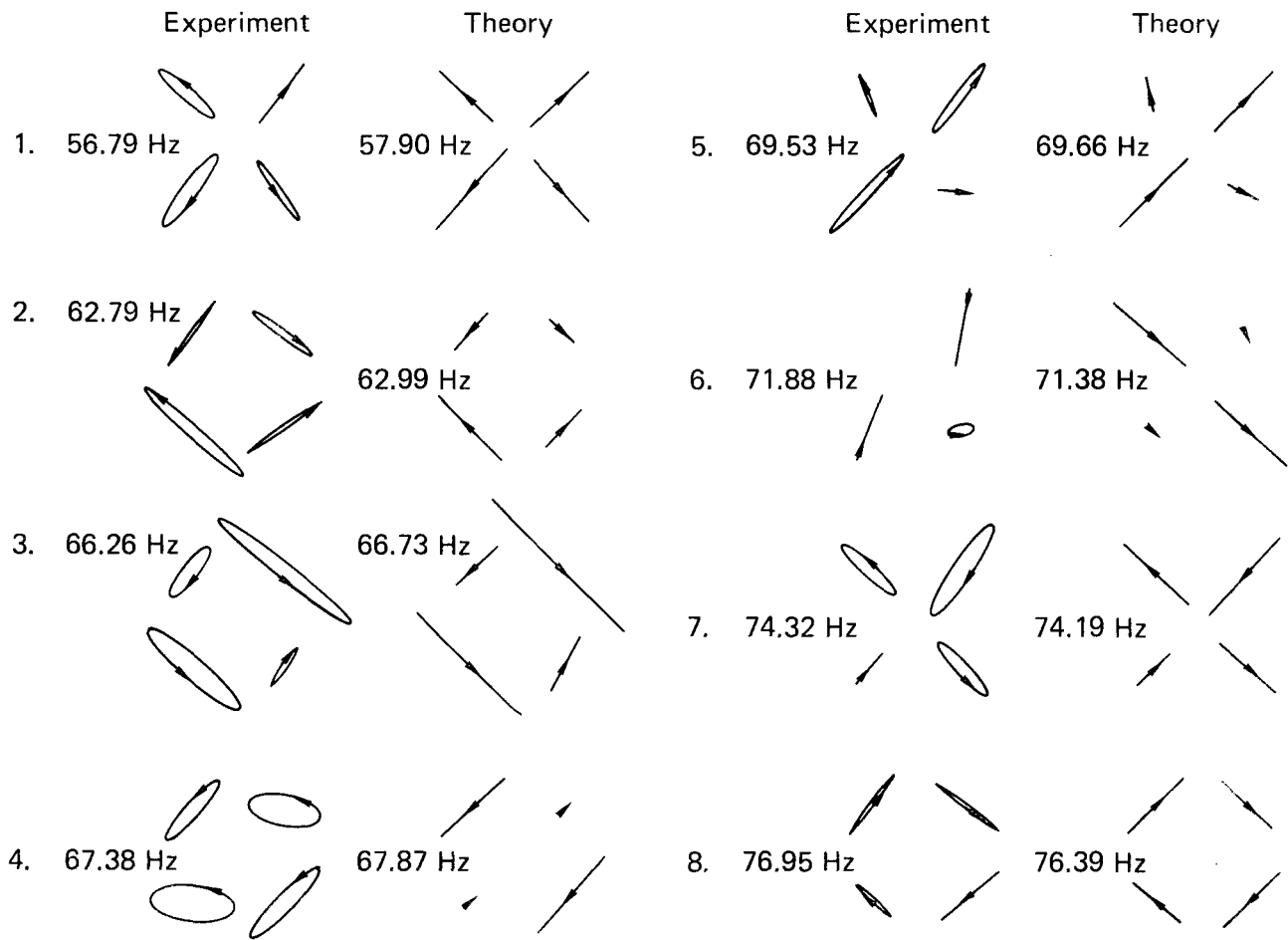


Fig. 28. Mode shapes of a group of four tubes in unconfined water.⁴⁸

For applications practical to large arrays, a simplification was suggested in Ref. 35. In a regular array of cylinders the most significant hydrodynamic coupling for a given member is with its immediate neighbors, and coupling with members further removed can be neglected. This means that, regardless of the size of the array, it can be analyzed in subparts consisting of each member and its immediate neighbors. The author of Ref. 35 reached this conclusion upon theoretically analyzing regular hexagonal arrays of 7, 19, and 37 cylinders. For each case, the added mass coefficients of the central cylinder was calculated and compared from case to case. The coefficients for the 19- and 37-cylinder arrays matched almost identically, and those for the 7-cylinder array were close. Thus, the simplification suggested seemed reasonable. We can make a further confirmation of this simplification by examining the 4 x 4 array shown in Fig. 31. Considering the high

degree of similarity in the magnitudes and directions of the forces on cylinders 6, 7, 10, and 11, each of these four centrally located cylinders must be influenced to approximately the same degree by the hydrodynamic coupling. Each is surrounded in the same manner by eight immediate neighbors so, had the simplification been applied, the forces on each would have been the same. This comparison may not provide strong additional confirmation, but it is supportive. A precaution needs to be mentioned; the highest loads are carried by the corner members, cylinders 14 and 16. The simplification was developed based on results for centrally located members, so that it may, or may not, apply to peripheral and corner members. In the case of the 4 x 4 array, the corner members are the most important to analyze. We suspect the corner members might also be the most important to analyze in other size arrays.

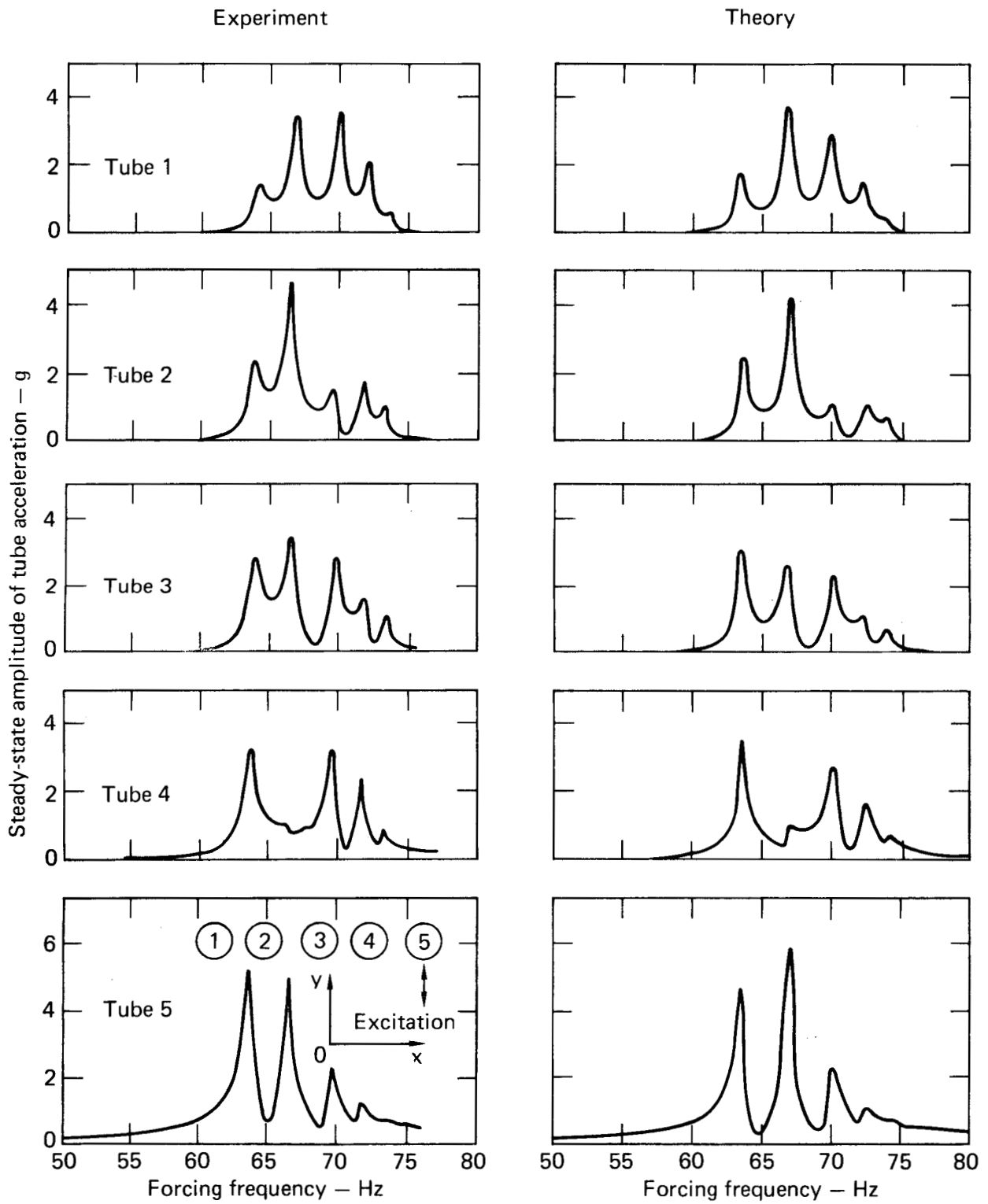


Fig. 29. Steady-state responses of a row of five tubes to an excitation on tube 5 with a $G/R \approx 1.0$.⁴⁸

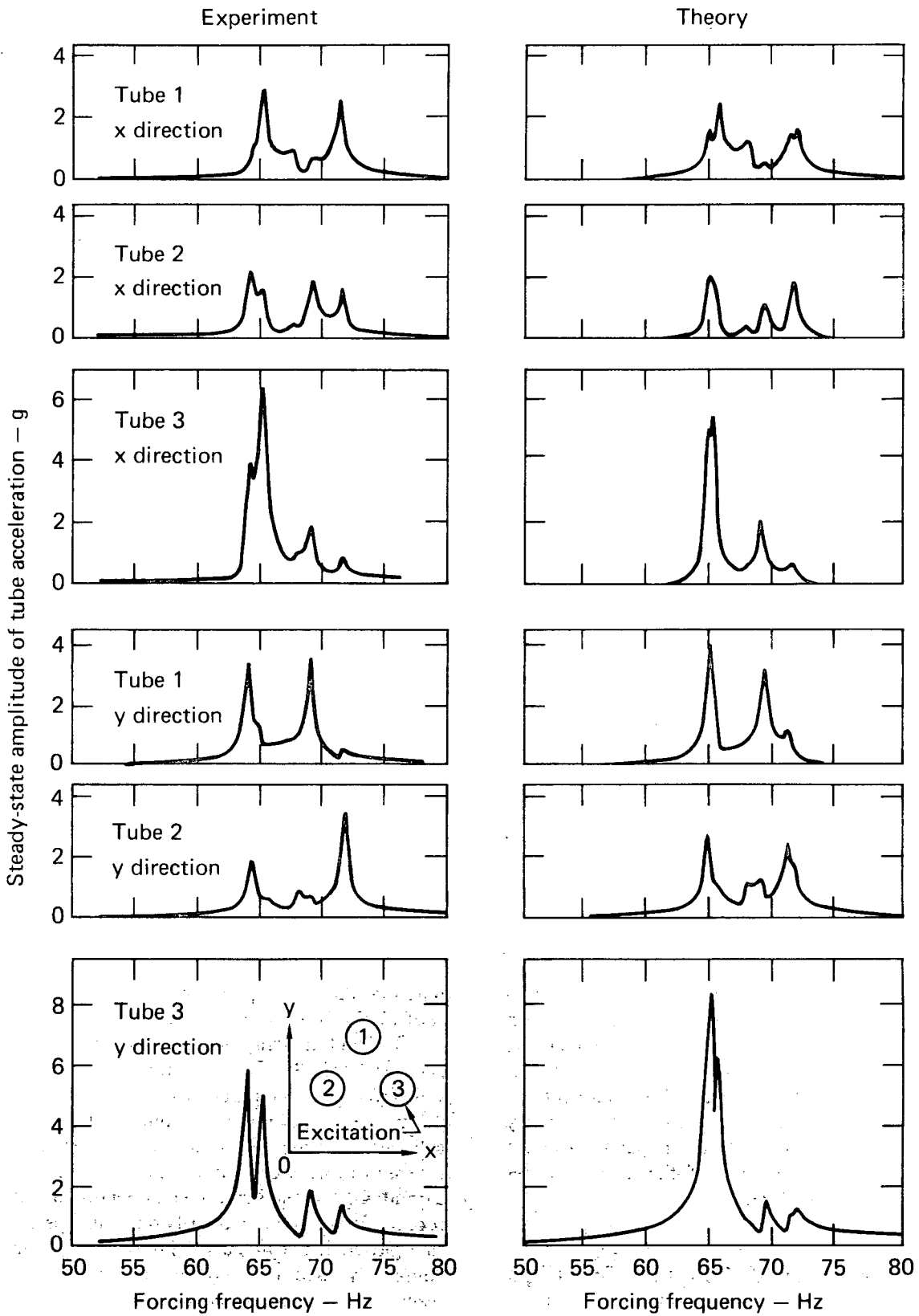


Fig. 30. Steady-state responses of a group of three tubes to an excitation on tube 3 with a $G/R = 2.0$.⁴⁸

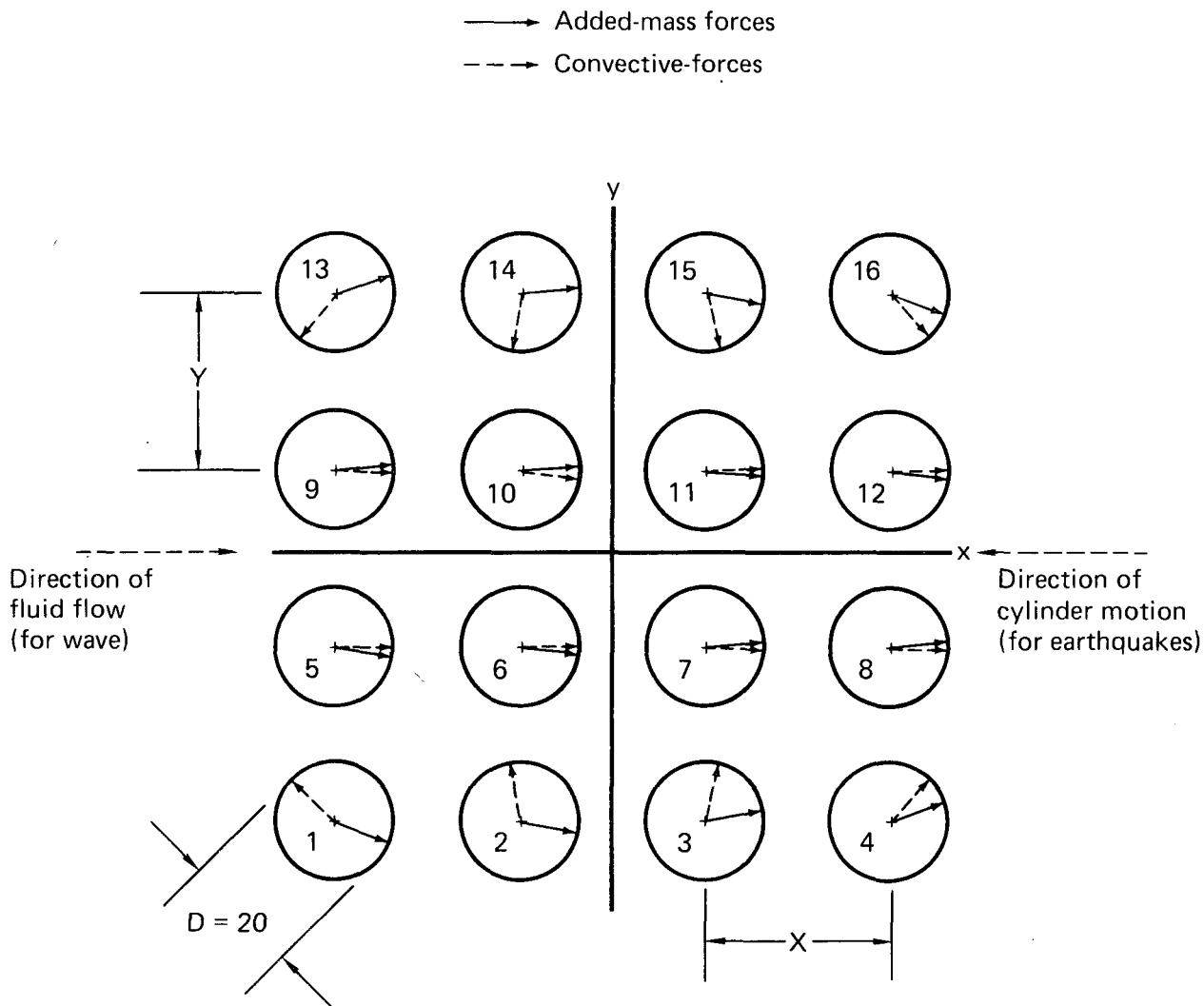


Fig. 31. Added-mass and convective forces on a 4×4 array with $X = Y = 1.5 D$.¹⁰

An approximation that is even simpler was suggested in Ref. 10. The total interaction is considered to be the sum of interactions between each two adjacent members. Therefore, the members of the array are analyzed two at a time and the results superimposed. The approximation was shown to be accurate to within 2 to 25% for a 4×4 array compared to a rigorous analysis. The accuracy varied depending on the member of the array. Corner members can be analyzed.

6.3 Hydrodynamic Coupling for Rigid Members Surrounded by a Rigid Circular Cylinder

A number of different member arrangements surrounded by a rigid circular cylinder have been

investigated. Closed-form solutions based on potential theory are presented for coaxial cylinders (Refs. 7, 30, 26, and 34), eccentric cylinders (Refs. 26 and 34), and an array of cylinders surrounded by a cylinder (Refs. 26 and 34). A finite element method was developed and applied to coaxial cylinders and to an array of cylinders surrounded by a circular cylinder.^{21,42} Analyses of coaxial cylinders using an incompressible viscous fluid theory are given in Refs. 27 and 45. For the remainder of Section 6.3 of this report, we will focus primarily on results pertaining to rigid coaxial cylinders. This is a simple model commonly used to simulate the internals of the reactor vessel under seismic excitation.

For two rigid coaxial cylinders in motion, as shown in Fig. 36, with the annular space filled with fluid, the potential theory solution is expressible in a form quite convenient for design applications. The

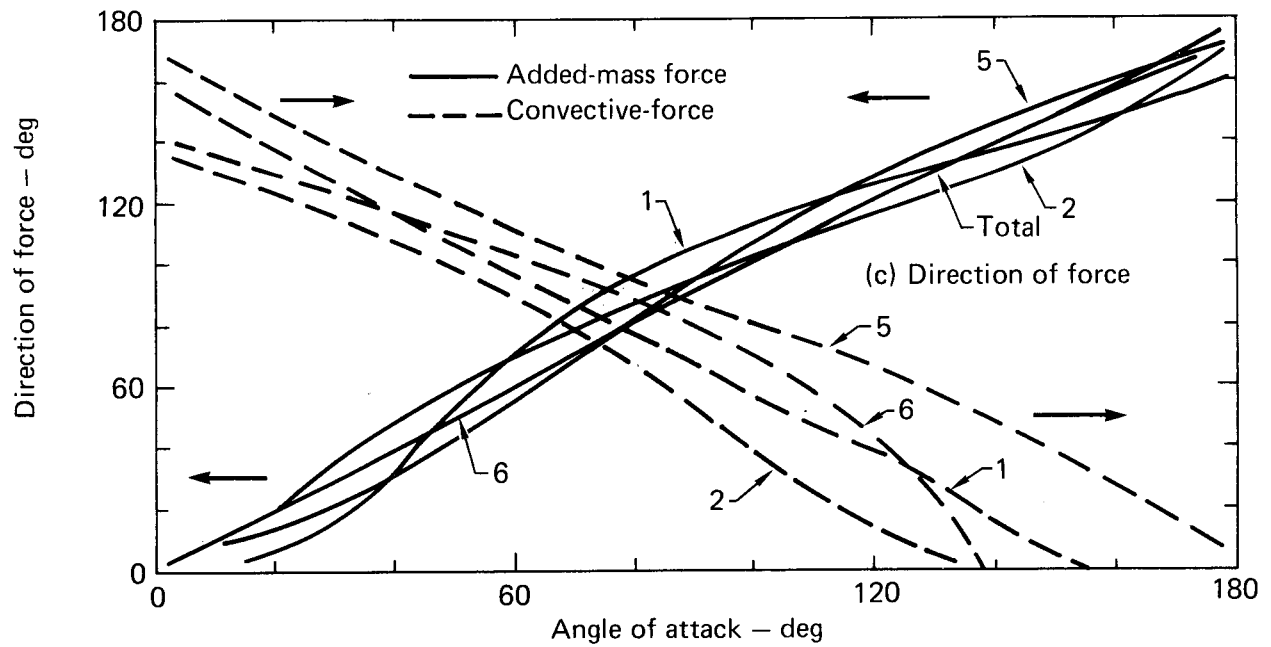
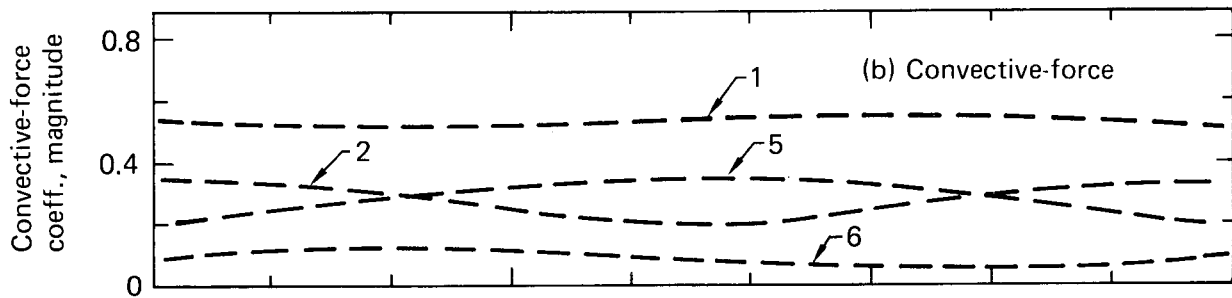
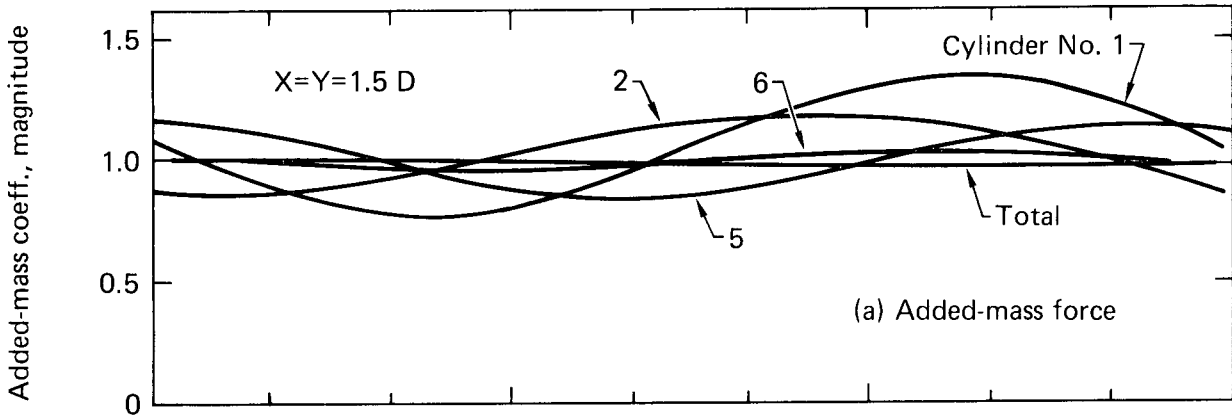


Fig. 32. Hydrodynamic forces vs angle of attack for a 4 x 4 array with X = Y = 1.5 D.¹⁰

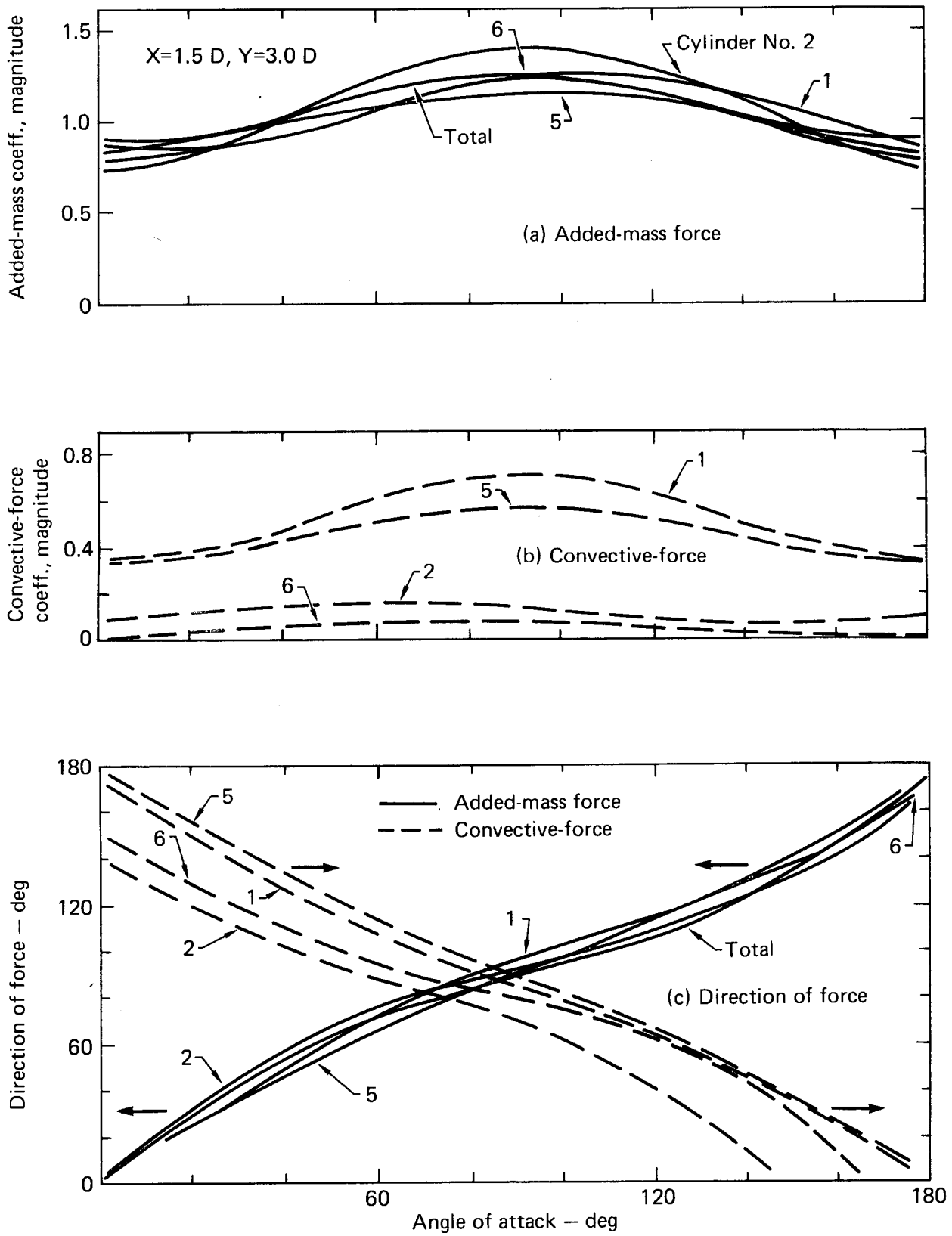


Fig. 33. Hydrodynamic forces vs angle of attack for a 4×4 array with $X = 1.5 D$ and $Y = 3 D$.¹⁰

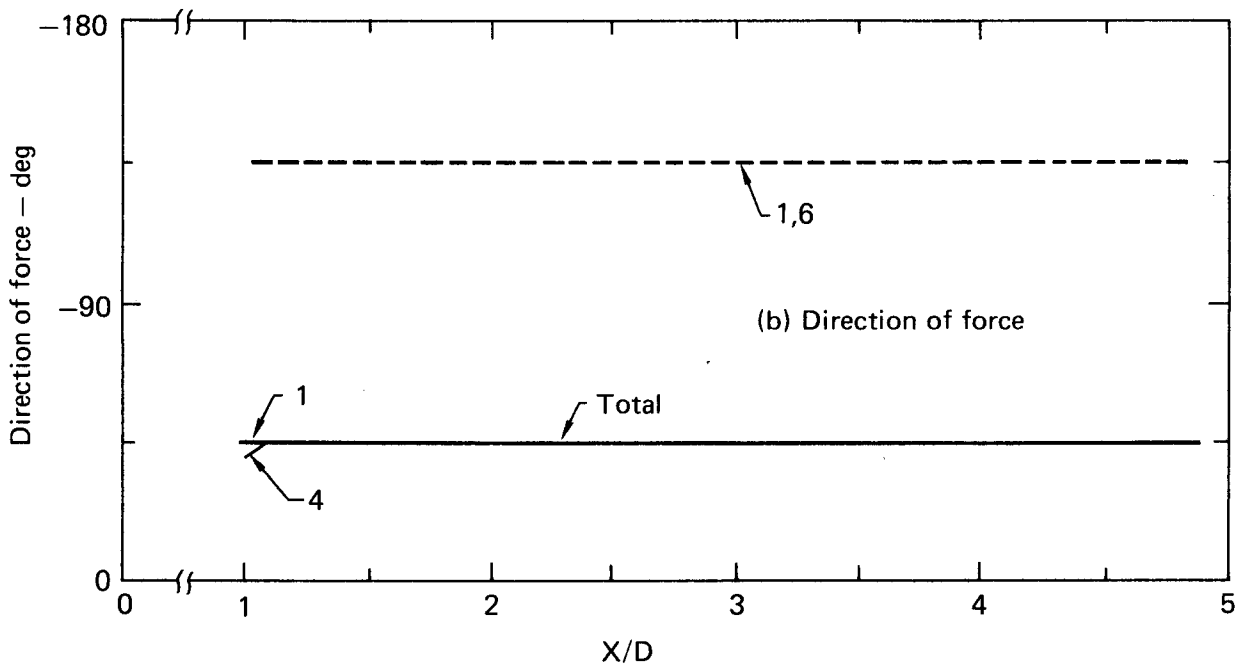
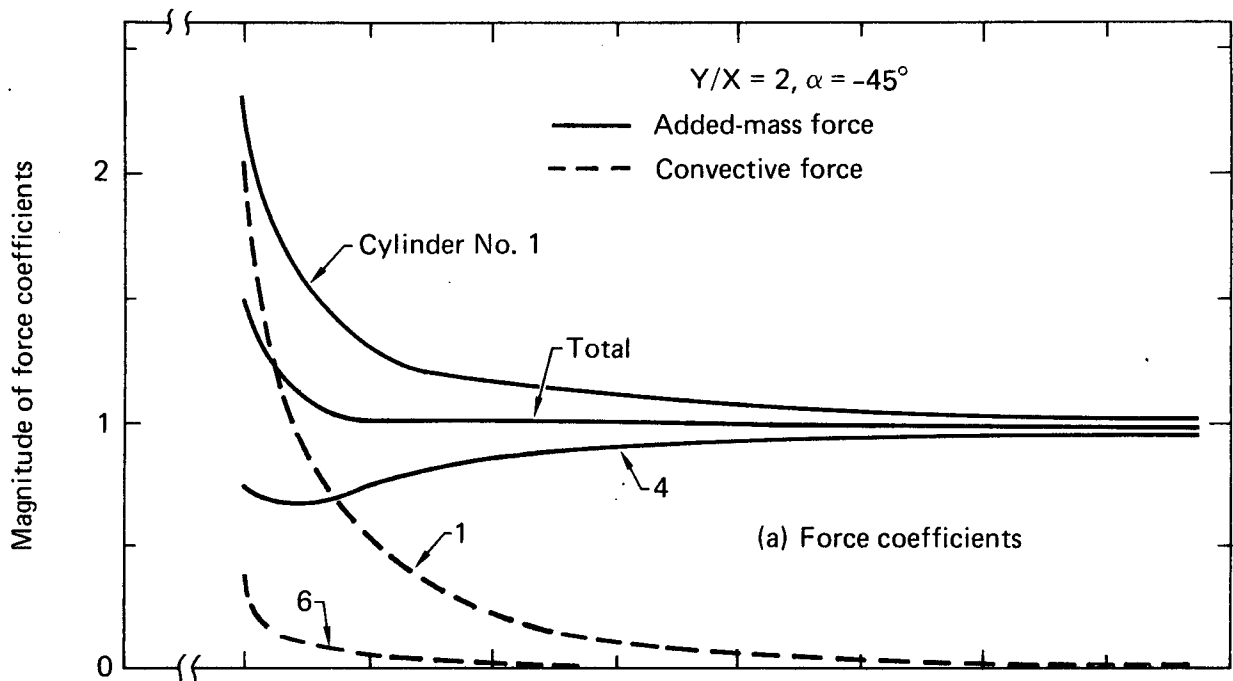


Fig. 34. Hydrodynamic forces vs spacing for a 4×4 array with $Y/X = 1.0$ and $\alpha = 45 \text{ deg.}^{10}$

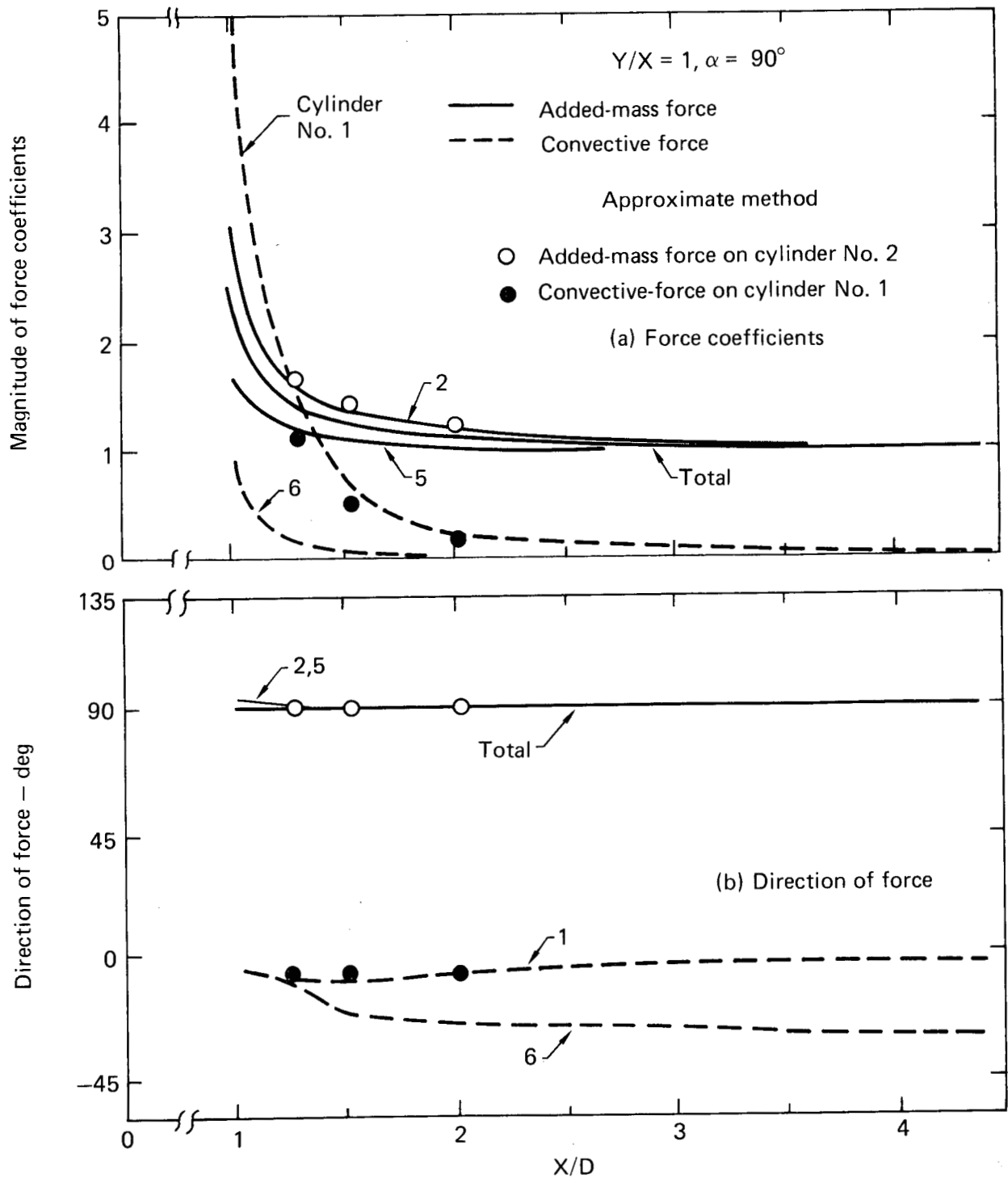


Fig. 35. Hydrodynamic forces vs spacing for a 4×4 array with $Y/X = 2.0$ and $\alpha = 90 \text{ deg.}^{10}$

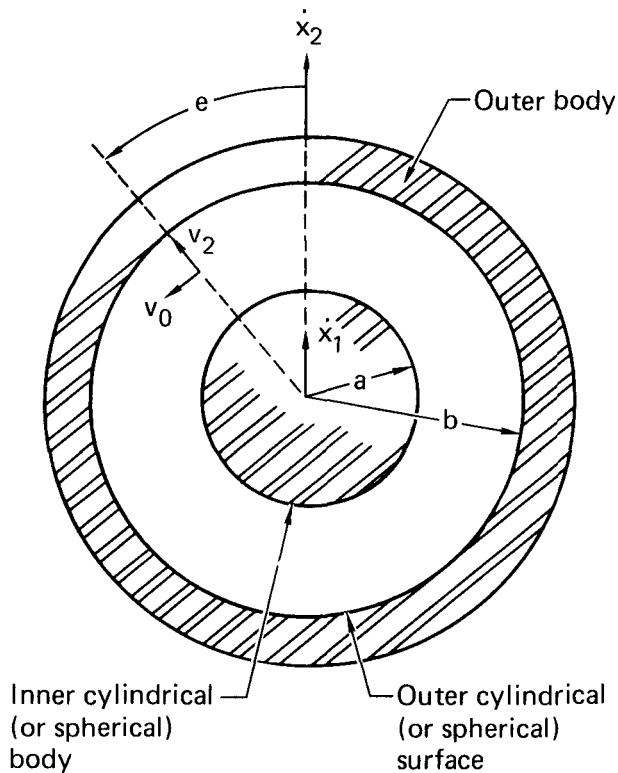


Fig. 36. Two-body motion with fluid coupling.⁷

fluid forces on the inner and outer cylinders are, respectively,⁷

$$F_{f_1} = -M_H \ddot{x}_1 + (M_1 + M_H) \ddot{x}_2, \quad (1)$$

$$F_{f_2} = (M_1 + M_H) \ddot{x}_1 - (M_1 + M_2 + M_H) \ddot{x}_2, \quad (2)$$

where,

$$M_1 = \pi a^2 L \rho = \text{mass of fluid displaced by the inner cylinder} \quad (3)$$

$$M_2 = \pi (b^2 - a^2) L \rho = \text{mass of fluid that could fill the outer cylindrical cavity in the absence of the inner cylinder} \quad (4)$$

$$M_H = M_1 \frac{b^2 + a^2}{b^2 - a^2} =$$

- mass term depending on the relative sizes of the inner and outer cylinders. (5)

L = length of the cylinders

ρ = mass density of the fluid.

Values for M_1 and M_2 can be determined experimentally or theoretically. Similar expressions are also presented in Ref. 30. These equations theoretically apply only to infinitely long cylinders; therefore, L should be significantly greater than the radii a and b. In addition, we expect that the solution's invalidity will diminish if the annular space is very small compared to radii a or b because the fluid would then be subjected to a significant amount of flow and shearing to accommodate the relative motions of the cylinders. The incompressible and inviscid assumptions would be less valid. Unfortunately, we have found no published indication of the range of applicability of the Eqs. (1) through (5) with respect to annulus size and motion amplitude.

Some comparison with experiments for five cases of two coaxial rigid cylinders are given in Table 9 taken from Ref. 7. The outer cylinder is fixed while the inner cylinder is vibrated. The added mass values on the inner cylinder, evaluated with Eq. (1), were compared with measured values. In the first four cases, the theoretical value was higher than the experimental by 21 to 36%, and, in the fifth case, it was lower by 33%. The comparison was fair.

The finite element technique developed in Refs. 21 and 42 compared very well with potential theory in terms of added mass coefficients for two coaxial rigid cylinders. (See Table 10 from Ref. 21). The basis of comparison was the M_1 , M_2 , and M_H of Eqs. (1) and (2). Therefore, the finite element technique is capable of duplicating the closed-form results very well. A comparison of the finite element technique with experimental results was presented in Ref. 42 for a 2 x 2 array of square cylinders surrounded by a circular cylinder, Fig. 37. Cylinder B is driven at a fixed displacement amplitude over the frequency range from 3 to 15 Hz, and the required force was monitored. The agreement between the finite-element and experimental results was reasonable.⁴²

A somewhat more sophisticated treatment of coaxial rigid cylinders is given in Refs. 27 and 45 using an incompressible viscous theory. The solution expressions are much more complex than those for potential theory and are contained in the references. A comparison with experiment was made for a fixed outer cylinder and oscillating inner cylinder. The outer cylinder diameter was varied from 0.625 in. to 2.5 in., while the inner cylinder diameter was kept at 0.5 in. The agreement between analysis and experiment was quite good, as shown in Fig. 38, and it is noticeably better than the comparisons discussed earlier for the potential theory. A possible conclusion is that viscous effects may be important and perhaps should be included when analyzing coaxial rigid cylinders. More experimental comparisons are needed to confirm this possibility.

Table 9. Added mass on coaxial rigid cylinders⁷

Annulus			Natural frequency, cpm	Calculated added mass, lbs	Experimental added mass, lbs	Difference, %
Radius, in.	Clearance, in.	Liquid				
4.0	0.16	Water	370	280	180	36
3.9	0.39	Water	520	100	75	27
4.0	0.25	Water	425	170	127	25
4.0	0.25	Glycerol solution	390	190	150	21
4.0	0.25	Oil	320	150	200	-33

Table 10. Comparing added mass coefficients between closed form and finite elements solutions for coaxial rigid cylinders.⁴²

	Closed form	Finite element
$M_H = \rho\pi a^2 \left(\frac{b^2 + a^2}{b^2 - a^2} \right)^*$	5.23ρ	5.169ρ
$M_1 + M_2 + M_H = \rho\pi b^2 \left(\frac{b^2 + a^2}{b^2 - a^2} \right)^*$	20.95ρ	20.792ρ
$M_1 + M_H = -2\rho\pi \left(\frac{a^2 b^2}{b^2 - a^2} \right)^*$	-8.38ρ	-8.29ρ

*a = radius of inner cylinder = 1 in.
 b = radius of outer cylinder = 2 in.

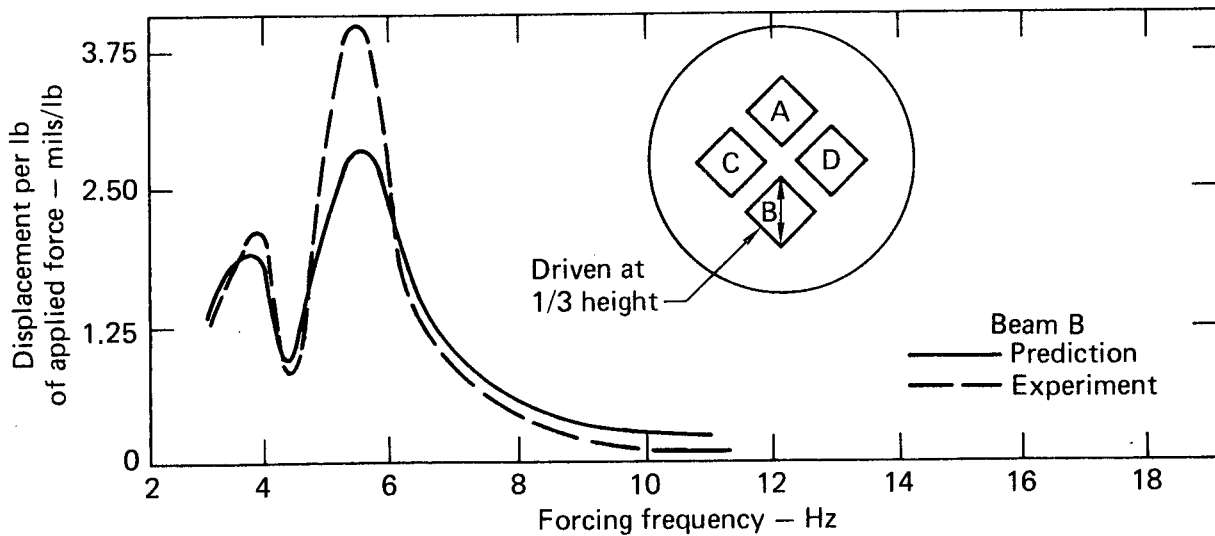


Fig. 37. Displacement response of a 2 × 2 square cylinder surrounded by a circular cylinder.⁴²

6.4 Hydrodynamic Coupling for Flexible Coaxial Cylinders

Coaxial cylinders with the inner cylinder analyzed as a flexible shell probably constitute a more realistic model of the internals of the reactor vessel than would coaxial rigid cylinders. Such a mathematical model was analyzed in Ref. 38 using an incompressible inviscid theory. The deformation of the inner cylinder is compared with experiment in Fig. 39 taken from Ref. 38, and the comparison is reasonable.

The case of three coaxial cylinders with the outer cylinder rigid and the inner cylinders flexible was analyzed in Ref. 46 using a compressible inviscid fluid theory. A simpler case involving only one inner cylinder was compared with experiment in terms of natural frequencies in Tables 11 and 12 taken from Ref. 46. The m and n quantities are, respectively, the axial and circumferential mode numbers of the inner cylinder. The agreement between theory and experiment is very good.

A finite element analysis using the code NASTRAN was applied to two coaxial cylinders, the outer one rigid and the inner flexible.⁴⁷ A compressible inviscid fluid theory was used. A comparison between analytical natural frequencies and experimental data is shown in Fig. 40 taken from Ref. 47. The comparison ranged from good to fair.

In general, based on the very limited amount of experimental comparison, the compressible inviscid fluid theory seems to do better than the incompressible inviscid potential theory. This indicates that fluid compressibility may be quite important to include when analyzing flexible members. Additional experimental confirmation is needed to fully establish this possibility.

6.5 Damping for Multiple Members

In Section 5.5 of this report we explained that for fully submerged structures in a finite size container, radiation damping can generally be ignored. The contributions to added damping that remain are fluid viscosity and component impact. Both theoretical and experimental values for fluid viscosity damping have been published, although no analytical treatment of impact damping has been found. For experiments involving both fluid viscosity and component impact, no separation of the measured total damping into these two contributions was made. Establishing a fixed value of damping for a general multiple member structure is very difficult, if not impossible, because damping can be significantly

influenced by member arrangement, spacing, and relative motions among the members.

Analyses were carried out for two coaxial cylinders using a viscous fluid theory.^{27,45} Three fluids were investigated in Ref. 27, and the theoretical damping was compared with the experimental as shown in Fig. 39 taken from Ref. 27. The agreement was quite good, indicating it is possible to obtain reliable damping values theoretically. Agreement was not as good in Ref. 45, where, by comparing the theoretical and experimental oscillatory motion amplitudes, it was determined that the theoretical damping underestimated the actual by a measureable amount.

The dependence of damping on the size of the annular space between two coaxial cylinders is clearly seen in Fig. 41. A sharp increase in damping is seen at a D/d ratio less than 1.75 to 2.75, depending on the fluid involved; the value of 1.75 applies to water. The quantities D and d are the diameters of the outer and inner cylinders, respectively. The diameter d was 0.5 in., and D varied from 0.625 in. to 2.5 in.

Experimental damping values for coaxial rigid cylinders submerged in three fluids are shown in Table 9 taken from Ref. 7. Adding the values for water to Fig. 41 indicates good agreement with the data from Ref. 27.

Experimentally determined damping from water viscosity are presented in Ref. 48 for a row of five cylinders (Fig. 22), a group of three cylinders (Fig. 23), a hexagonal array of seven cylinders (Fig. 24), a 2×2 array of cylinders (Fig. 25), a 2×2 array of cylinders near a wall (Fig. 42), and a 2×2 array of cylinders surrounded by a cylinder (Fig. 43). The results from Ref. 48 are reproduced in Tables 13 through 25. The tubes are all 0.5 in. diameter and 12.0 in. long. The damping values in these tables should be approximately the same as those in Fig. 41 because the inner cylinder used for Fig. 41 was also 0.5 in. diameter, and the space between cylinders reported in Tables 13 through 25 are generally within the gap size range covered in Fig. 41. In other words, space size-to-radius ratio values of 0.4 to 2.0 for Ref. 48 corresponds to D/d ratio values of 1.8 to 5.0 for Ref. 27. Comparing the damping values confirmed our speculation; i.e., the added damping values from Tables 13 through 25 ranged from 0.38 to 1.9%; this range compares very closely with the range 0.5 to 1.8% shown for water in Fig. 41 and corresponding to D/d ratios from 1.8 to 5.0.

Up to this point, all experimental data for damping are mutually supportive, and the damping for multiple members 0.5-in. in diameter is characterized to a usable degree. The next question is how can

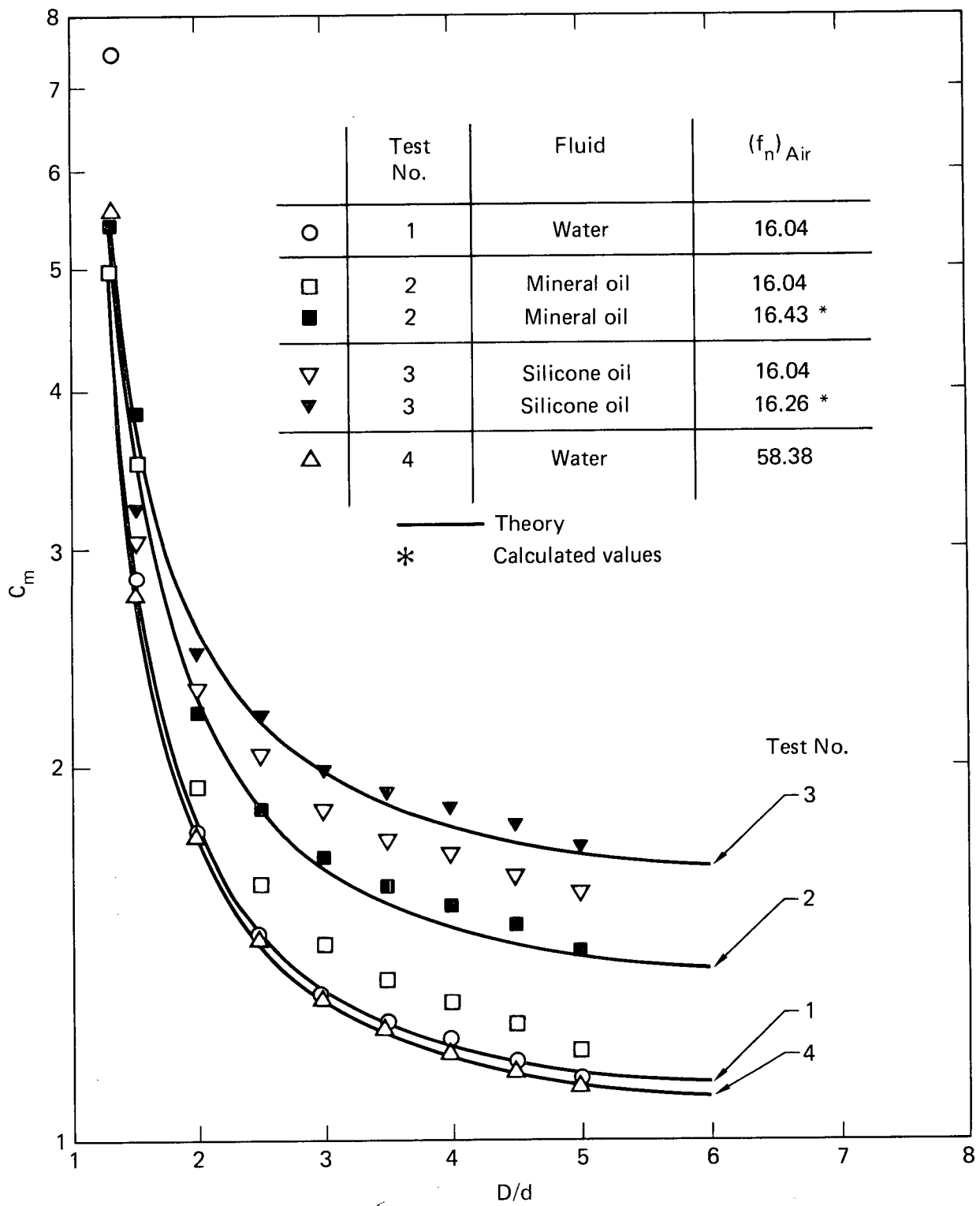
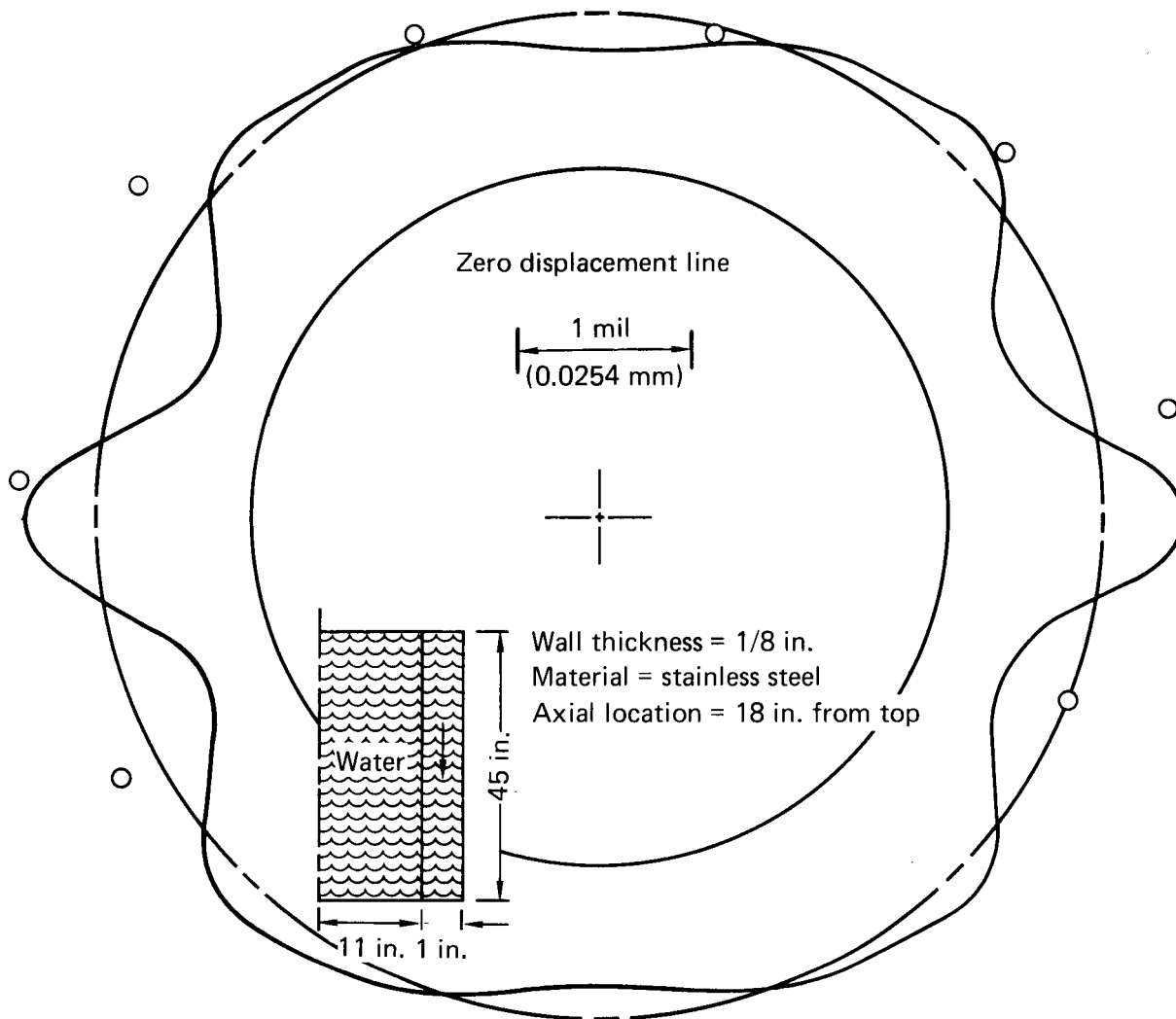


Fig. 38. Theoretical and experimental values of C_m as a function of D/d .²⁷



- Computed worst possible displacement (all ring modes in phase)
0.43–1.34 mils (0.0109 – 0.0340 mm)
- - - Computed most probable displacement (random phase between
ring modes) 0.94 mils (0.0239 mm)
- Measured displacement 0.90 – 1.26 mils (0.0229 – 0.0320 mm)

Fig. 39. Computed vs r.m.s. displacement of cylinder.³⁸

Table 11. Measured and computed natural frequencies for coaxial cylinders, inner cylinder flexible, inner cylinder filled with water only.⁴²

Mode (m, n)	Experimental frequency, Hz	Computed frequency, Hz	Discrepancies, % frequency
1, 3	103	90.6	12.0
1, 4	106	98.2	7.4
1, 5	145	144	0.7
1, 6	213	214	0.5
2, 5	219	203	7.3

Table 12. Measured and computed natural frequencies for coaxial cylinders, inner cylinder flexible, both inner and outer cylinders filled with water.⁴²

Mode (m, n)	Experimental frequency, Hz	Computed frequency, Hz	Discrepancies, % frequency
1, 2	64	62.4	2.5
1, 3	54	46.2	14.0
1, 4	60	55.9	6.8
1, 5	90	89.2	0.9
1, 6	139	140.9	1.4
1, 7	206	209.2	1.6
2, 5	136	127.4	6.3
2, 6	165	163.7	0.8

we extrapolate the results to structural sizes of concern. At this point, there is no established way. The extrapolation technique we developed for single isolated members, (Figs. 14 and 15) cannot be trusted to apply to multiple members in the absence of experimental evidence. A possible method is the analytical technique developed in Ref. 27 to form relationships that can relate the 0.5-in. specimens to structural sizes of concern. This might be a very useful area for future exploration because damping is a topic of high interest.

Some measurements of total damping in actual reactors and models of reactors are reported in Ref. 41. The values are 2 to 5% for core-barrel beam modes, 1 to 2% for core-barrel shell modes, 2 to 5% for guide tubes. These values are measured under low-displacement amplitudes on actual reactors. When the coolant is flowing, the damping increases with increasing flow rate, giving rise to core barrel damping ranging from 8.8 to 12%. In the opinion of the authors of Ref. 41, a significant contribution to

the total damping resulted from component impact, particularly while the coolant was flowing. Component impact was, therefore, very possibly responsible for a major part of the 8.8 to 12% damping measured. Unfortunately, no separation between fluid viscosity effects and component impact was made. Consequently, the usefulness of the damping values is limited for general application because the component impact contribution could vary from one reactor design to another.

Further evidence that component impact contributes significantly to the damping was found in Ref. 43. The effect of tube-support interaction on the dynamic response of heat-exchanger tubes was examined. The total damping measured was from 2 to 7.5%, whereas it was felt the combined structural damping and fluid viscosity damping should have been approximately 2%. Again, no separation between component impact and other contributions was made.

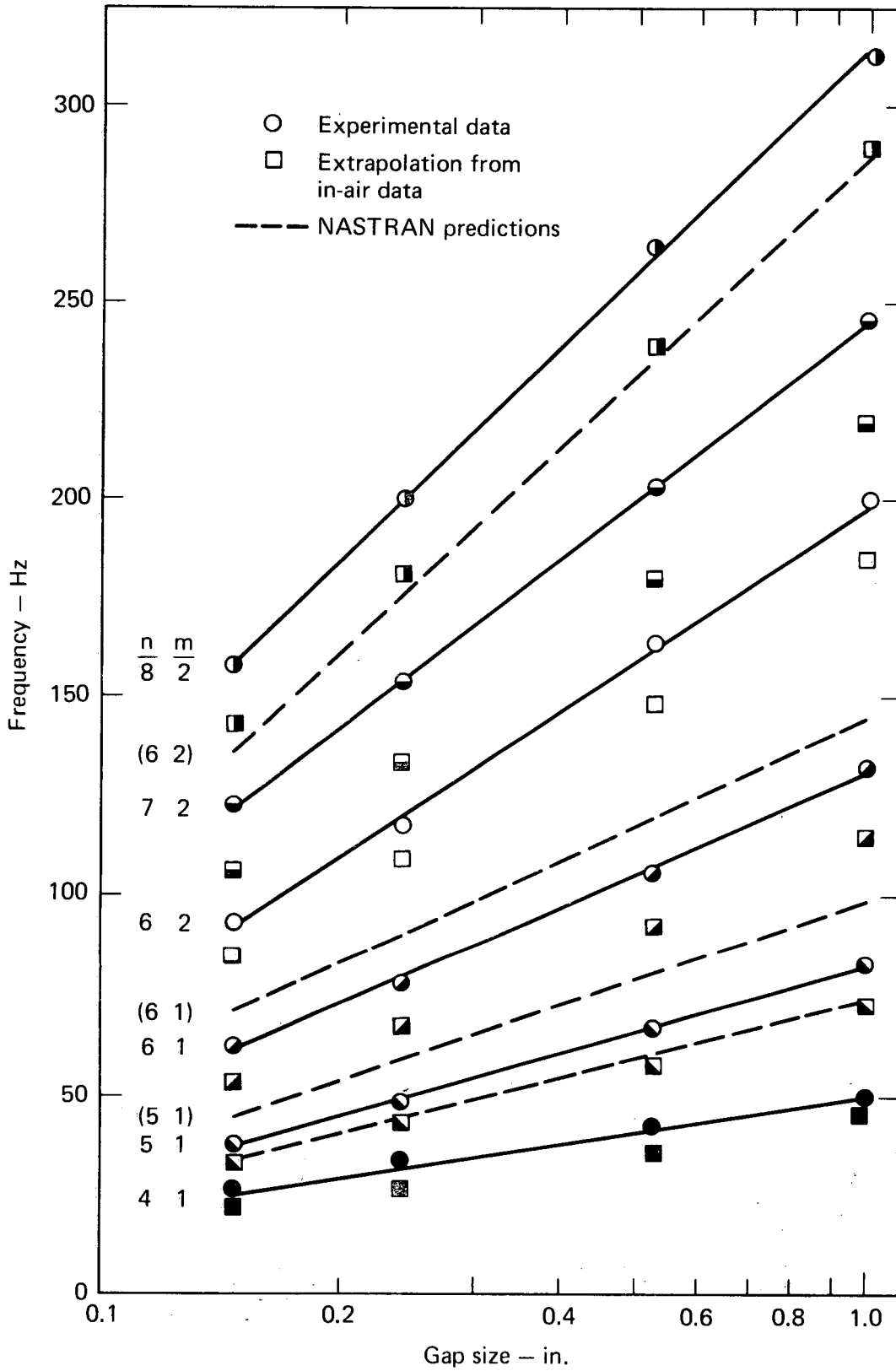


Fig. 40. Comparison of experimental and predicted vibration frequencies for the shell with a fluid filled gap.⁴⁷

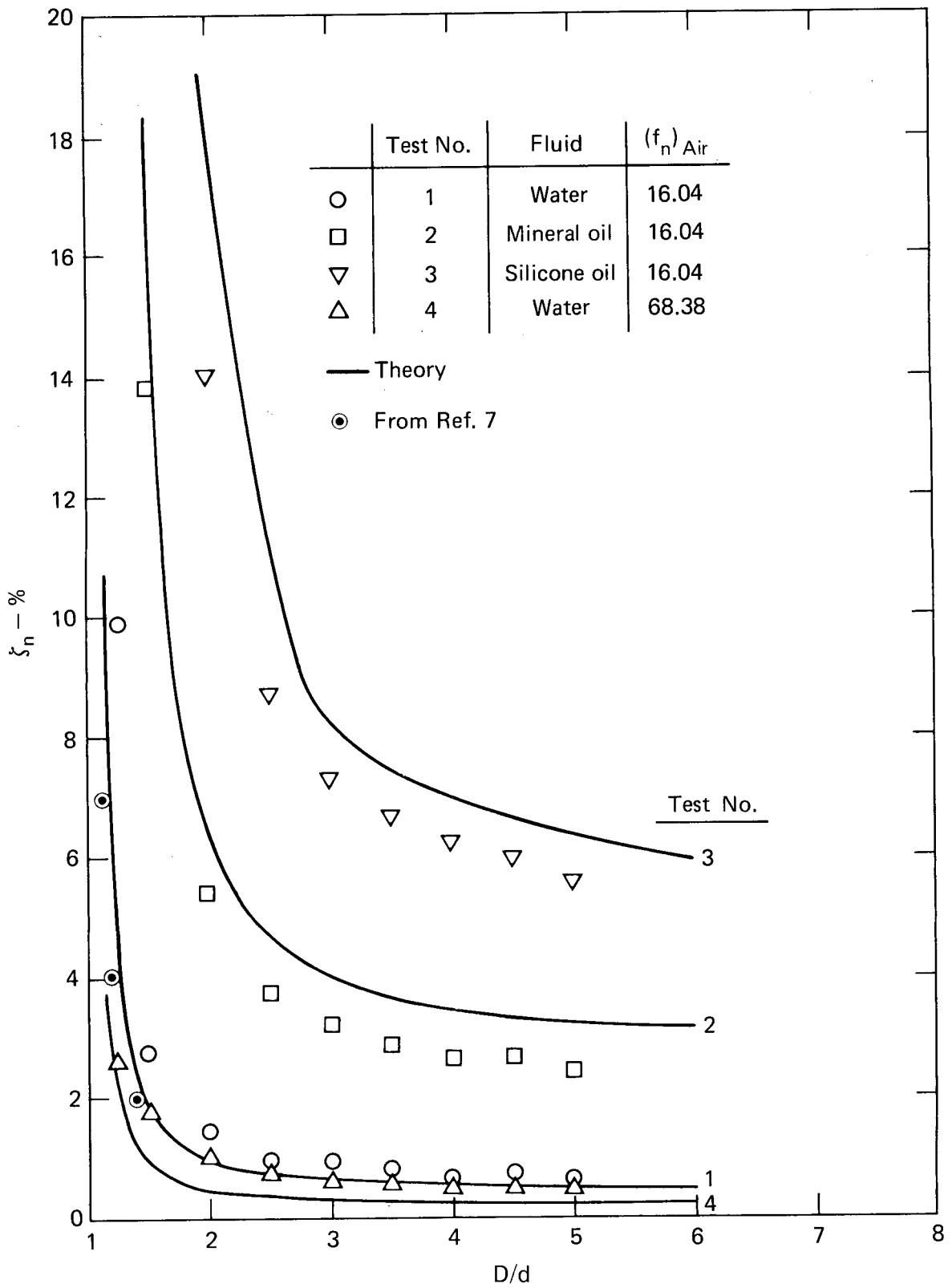


Fig. 41. Theoretical and experimental values of ζ_n as a function of D/d .²⁷

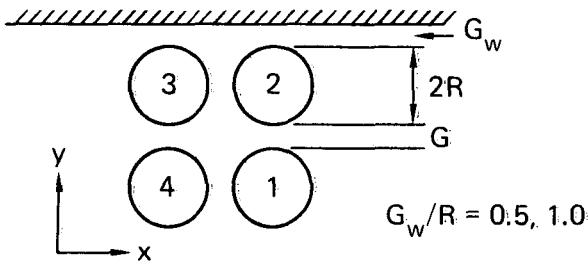


Fig. 42. A 2 × 2 array of cantilevered cylinders near a wall.⁴⁸

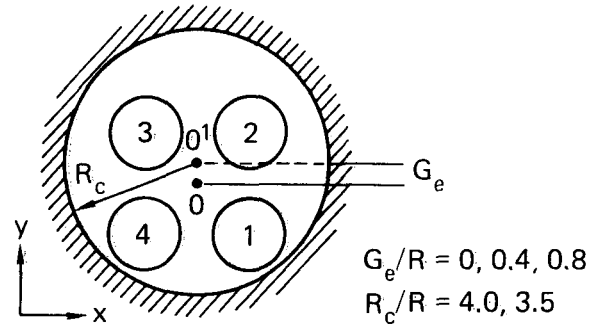


Fig. 43. A 2 × 2 array of cantilevered cylinders near a wall.⁴⁸

Table 13. Experimental and analytical results for uncoupled vibration of a row of five tubes.⁴⁸

Gap-to-radius ratio, C/R	Direction of motion	Tube number	Dimensionless spring constant, P_i	Measured uncoupled natural frequency, Hz		Measured damping ratio		Calculated uncoupled natural frequency in water, Hz
				In air	In water	In air	In water	
2.0 (1.988)	x	1	104.3	83.79	69.63	0.00118	0.0044	70.07
		2	99.0	84.67	70.41	0.00095	0.0049	70.58
		3	128.5	84.27	69.92	0.00031	0.0053	70.39
		4	155.2	84.38	70.21	0.00028	0.0045	70.57
		5	354.0	77.93	65.50	0.00062	0.0043	66.87
	y	1	129.0	84.08	70.02	0.00113	0.0042	70.31
		2	129.3	85.05	70.90	0.00032	0.0036	70.89
		3	242.6	84.86	70.51	0.00103	0.0044	70.86
		4	288.5	84.86	70.80	0.00078	0.0034	70.96
		5	354.0	77.93	66.70	0.00148	0.0042	66.87
1.0 (0.981)	x	1	105.1	83.40	69.24	0.00044	0.0063	69.54
		2	84.2	83.79	68.75	0.00052	0.0078	69.39
		3	98.3	83.69	68.85	0.00051	0.0088	69.43
		4	86.5	83.01	68.26	0.00063	0.0099	68.96
		5	186.6	77.05	64.94	0.00103	0.0047	65.93
	y	1	155.8	83.89	69.92	0.00032	0.0037	69.91
		2	114.1	84.28	69.53	0.00054	0.0043	69.72
		3	154.9	84.28	69.63	0.00073	0.0044	69.82
		4	127.4	83.59	69.04	0.00152	0.0051	69.37
		5	253.4	77.25	65.53	0.00092	0.0039	66.07
0.25 (0.248)	x	1	99.2	83.40	68.55	0.00093	0.0073	68.45
		2	85.2	83.50	66.99	0.00045	0.0124	67.08
		3	92.0	83.50	67.29	0.00146	0.0137	67.23
		4	97.2	83.40	67.38	0.00131	0.0190	67.28
		5	325.2	77.73	64.55	0.00108	0.0081	65.63
	y	1	131.5	83.79	69.24	0.00046	0.0062	68.52
		2	101.1	83.79	67.38	0.00055	0.0076	66.70
		3	97.2	83.59	66.80	0.00088	0.0070	66.53
		4	103.6	83.50	67.19	0.00069	0.0076	66.75
		5	930.5	78.02	65.42	0.00226	0.0046	65.66

Table 14. Experimental and analytical results for uncoupled vibration of a group of three tubes.⁴⁸

Gap-to-radius ratio, G/R	Direction of motion	Tube number	Dimensionless spring constant, p_i	Measured uncoupled natural frequency, Hz		Measured damping ratio		Calculated uncoupled natural frequency in water, Hz
				In air	In water	In air	In water	
2.0 (1.933)	x	1	53.2	82.03	68.35	0.00152	0.0038	68.53
		2	141.4	84.38	70.21	0.00090	0.0041	70.35
		3	386.0	77.24	65.82	0.00341	0.0041	66.22
	y	1	55.2	82.13	68.55	0.00103	0.0037	68.59
		2	79.1	83.50	69.53	0.00095	0.0045	69.63
		3	123.2	76.46	65.33	0.00217	0.0034	65.55
1.0 (0.983)	x	1	62.6	82.23	69.26	0.00072	0.0047	68.28
		2	79.5	83.50	69.14	0.00109	0.0087	69.08
		3	115.8	76.76	65.04	0.00073	0.0071	65.36
	y	1	71.1	82.52	68.36	0.00095	0.0042	68.37
		2	63.4	83.01	68.55	0.00174	0.0075	68.75
		3	77.4	76.17	64.55	0.00215	0.0063	64.91
0.5 (0.475)	x	1	58.5	82.42	67.58	0.00076	0.0044	67.62
		2	94.0	83.98	67.68	0.00183	0.0051	68.26
		3	82.9	76.07	63.09	0.00226	0.0052	63.76
	y	1	52.6	82.13	66.99	0.00125	0.0048	66.75
		2	59.2	83.01	67.77	0.00233	0.0053	67.79
		3	88.3	76.17	63.87	0.00119	0.0055	64.12

Table 15. Experimental and analytical results for uncoupled vibration of a group of seven tubes.⁴⁸

Gap-to-radius ratio, G/R	Direction of motion	Tube number	Dimensionless spring constant, P_i	Measured uncoupled natural frequency, Hz		Measured damping ratio		Calculated uncoupled natural frequency in water, Hz
				In air	In water	In air	In water	
1.5 (1.384)	x	1	52.2	82.42	67.91	0.00079	0.0049	68.29
		2	60.1	83.11	68.96	0.00044	0.0103	68.72
		3	73.6	83.06	68.75	0.00086	0.0043	69.94
		4	57.3	81.93	67.48	0.00050	0.0061	67.97
		5	55.9	81.98	68.02	0.00074	0.0054	68.03
		6	223.4	77.15	65.38	0.00052	0.0040	65.77
		7	47.4	81.78	67.19	0.00099	0.0047	67.29
	y	1	64.1	82.96	68.80	0.00107	0.0040	68.81
		2	79.5	83.74	69.17	0.00089	0.0045	69.32
		3	55.2	82.37	67.63	0.00140	0.0055	68.21
		4	72.0	82.47	68.46	0.00110	0.0033	68.49
		5	73.3	82.62	68.75	0.00054	0.0043	68.64
		6	106.4	76.46	64.45	0.00094	0.0039	65.05
		7	49.8	81.93	66.80	0.00109	0.0047	67.41
1.0 (0.867)	x	1	52.1	81.15	65.63	0.00104	0.0049	66.20
		2	54.7	81.84	66.21	0.00063	0.0040	66.61
		3	91.9	82.81	67.77	0.00083	0.0043	67.96
		4	75.7	82.62	67.19	0.00084	0.0040	67.48
		5	62.0	82.23	67.38	0.00085	0.0042	67.20
		6	88.3	75.49	63.39	0.00180	0.0043	63.68
		7	50.6	81.35	64.84	0.00092	0.0051	65.18
	y	1	71.5	81.93	67.19	0.00061	0.0044	67.09
		2	72.5	82.52	67.19	0.00063	0.0055	67.42
		3	61.2	81.98	66.60	0.00062	0.0049	66.75
		4	75.7	82.62	67.97	0.00084	0.0040	67.74
		5	63.2	82.28	68.16	0.00120	0.0041	67.49
		6	74.2	75.20	62.60	0.00134	0.0048	63.00
		7	48.9	81.25	64.84	0.00078	0.0055	65.10
0.4 (0.394)	x	1	66.2	82.62	67.20	0.00253	0.0072	64.11
		2	66.8	83.06	62.82	0.00263	0.0073	64.27
		3	61.1	82.62	65.14	0.00143	0.0056	65.72
		4	95.9	83.01	63.55	0.00121	0.0064	64.52
		5	91.2	82.81	61.91	0.00130	0.0010	64.40
		6	76.5	75.98	61.77	0.00048	0.0060	62.39
		7	48.8	81.64	59.13	0.00168	0.0103	60.13
	y	1	56.6	82.23	65.72	0.00250	0.0052	64.85
		2	53.2	82.62	66.11	0.00200	0.0050	64.99
		3	49.3	82.03	61.87	0.00082	0.0088	63.14
		4	77.1	82.62	69.77	0.00126	0.0050	65.26
		5	91.2	82.81	65.23	0.00118	0.0054	65.45
		6	62.6	75.59	59.52	0.00045	0.0066	60.28
		7	40.8	81.05	58.94	0.00062	0.0112	59.69

Table 16. Experimental and analytical results for uncoupled vibration of the four-tube array in unconfined water.⁴⁸

Gap-to-radius ratio, G/R	Direction of motion	Tube number	Dimensionless spring constant, ρ_1	Measured uncoupled natural frequency, Hz		Measured damping ratio		Calculated uncoupled natural frequency in water, Hz
				In air	In water	In air	In water	
0.5 (0.585)	x	1	98.1	83.79	68.65	0.00099	0.0079	68.57
		2	60.6	83.98	68.85	0.00169	0.0138	68.42
		3	78.1	83.59	68.55	0.00566	0.0125	68.41
		4	1030.0	77.83	65.33	0.00091	0.0080	65.55
	y	1	75.0	83.30	67.77	0.00131	0.0072	68.17
		2	74.9	84.28	68.95	0.00286	0.0147	68.82
		3	86.4	83.78	68.46	0.00290	0.0089	68.57
		4	228.1	77.34	64.16	0.00633	0.0117	65.13

Table 17. Experimental and analytical results for uncoupled vibration of the four-tube array near a flat wall.⁴⁸

Gap-to-radius ratio, G_w/R	Direction of motion	Tube number	Measured uncoupled natural frequency, Hz	Measured damping ratio	Calculated uncoupled natural frequency, Hz
1.0	x	1	68.46	0.0066	68.27
		2	67.24	0.0071	66.87
		3	66.75	0.0059	66.88
		4	65.14	0.0101	65.29
	y	1	67.58	0.0078	67.93
		2	67.04	0.0065	67.38
		3	66.55	0.0087	67.15
		4	64.06	0.0070	64.93
0.5	x	1	68.51	0.0059	68.14
		2	65.53	0.0138	65.31
		3	65.38	0.0143	65.31
		4	65.19	0.0094	65.18
	y	1	67.48	0.0038	67.85
		2	66.16	0.0087	66.15
		3	66.06	0.0096	65.91
		4	64.21	0.0103	64.86

Table 18. Experimental and analytical results for uncoupled vibration of the four-tube array contained in a cylinder.⁴⁸

Radius ratio, R_c/R	Eccentricity, G_c/R	Direction of motion	Tube number	Measured uncoupled natural frequency, Hz	Measured damping ratio	Calculated uncoupled natural frequency, Hz
4.0	0.0	x	1	65.33	0.0095	66.07
			2	65.77	0.0082	65.89
			3	65.92	0.0071	65.91
			4	62.26	0.0055	63.43
	0.4	y	1	64.70	0.0079	65.68
			2	65.53	0.0073	66.28
			3	65.87	0.0068	66.06
			4	62.26	0.0053	63.02
	0.8	x	1	65.48	0.0060	65.47
			2	65.14	0.0070	66.19
			3	65.38	0.0068	66.21
			4	62.60	0.0054	62.92
0.0	y	1	64.94	0.0069	65.07	
		2	65.33	0.0060	66.62	
		3	64.84	0.0106	66.40	
		4	62.55	0.0054	62.50	
3.5	0.0	x	1	65.33	0.0069	64.25
			2	62.84	0.0093	66.30
			3	63.82	0.0082	66.31
			4	62.79	0.0074	61.87
	0.4	y	1	65.82	0.0057	63.89
			2	64.21	0.0091	66.79
			3	62.94	0.0111	65.57
			4	62.45	0.0075	61.49
	0.8	x	1	63.67	0.0079	64.43
			2	64.31	0.0092	64.25
			3	64.75	0.0094	64.27
			4	60.84	0.0105	62.02
0.0	y	1	62.21	0.0101	64.05	
		2	64.50	0.0091	64.63	
		3	63.82	0.0100	64.42	
		4	59.91	0.0102	61.62	
0.4	x	1	64.65	0.0069	62.73	
		2	63.67	0.0085	64.94	
		3	63.92	0.0070	64.96	
		4	61.13	0.0128	50.56	
0.8	y	1	63.78	0.0085	62.36	
		2	62.45	0.0073	65.40	
		3	63.92	0.0090	65.19	
		4	61.67	0.0067	60.17	

Table 19. Experimental and analytical results for coupled vibration of five tubes.⁴⁸

Gap-to-radius ratio, G/R	Direction of motion	Mode number	Measured coupled natural frequencies, Hz	Calculated coupled natural frequencies, Hz	Damping ratio
2.0 (1.988)	x	1	66.16	66.45	0.0043
		2	68.12	68.50	0.0047
		3	69.34	69.46	0.0047
		4	71.12	71.15	0.0046
		5	73.29	73.28	0.0051
	y	1	66.08	66.18	0.0040
		2	68.64	68.44	0.0039
		3	70.21	70.54	0.1040
		4	71.80	72.08	0.0038
		5	72.68	73.04	0.0041
1.0 (0.981)	x	1	63.77	64.56	0.0061
		2	65.72	66.24	0.0072
		3	68.09	68.16	0.0075
		4	70.98	70.91	0.0080
		5	74.83	74.48	0.0088
	y	1	63.77	63.35	0.0040
		2	66.67	66.74	0.0039
		3	69.80	69.98	0.0043
		4	71.90	72.31	0.0046
		5	73.52	73.88	0.0046
0.25 (0.248)	x	1	59.96	61.02	0.0126
		2	62.50	62.92	0.0105
		3	66.29	66.59	0.0102
		4	71.53	71.55	0.0127
		5	77.64	77.19	0.0152
	y	1	57.33	56.45	0.0058
		2	64.67	64.56	0.0059
		3	69.14	69.67	0.0063
		4	72.95	73.39	0.0074
		5	75.39	75.65	0.0081

Table 20. Experimental and analytical results for coupled vibration of three tubes.⁴⁸

Gap-to-radius ratio, G/R	Mode number	Measured coupled natural frequencies, Hz	Calculated coupled natural frequencies, Hz	Damping ratio
2.0 (1.933)	1	64.02	64.61	0.0036
	2	65.20	65.23	0.0038
	3	67.65	67.76	0.0039
	4	69.04	69.10	0.0039
	5	71.28	71.10	0.0043
	6	71.52	71.61	0.0042
1.0 (0.983)	1	61.21	62.04	0.0061
	2	64.02	63.84	0.0063
	3	66.25	66.42	0.0060
	4	69.52	69.68	0.0065
	5	72.10	71.78	0.0069
	6	72.85	72.72	0.0070
0.5 (0.475)	1	57.42	58.15	0.0046
	2	62.29	62.32	0.0051
	3	64.76	64.86	0.0047
	4	70.24	70.14	0.0055
	5	72.88	72.66	0.0054
	6	74.47	74.32	0.0055

Table 21. Experimental and analytical results for coupled vibration of seven tubes.⁴⁸

Gap-to-radius ratio, G/R	Mode number	Measured natural frequencies, Hz	Calculated natural frequencies, Hz	Calculated damping ratio
1.5 (1.384)	1	60.25	61.18	0.0043
	2	61.91	62.66	0.0045
	3	62.70	62.76	0.0052
	4	64.65	64.74	0.0040
	5	66.06	66.33	0.0045
	6	66.46	66.94	0.0048
	7	67.53	68.31	0.0043
	8	68.99	68.79	0.0055
	9	69.87	70.22	0.0051
	10	70.75	71.07	0.0060
	11	71.58	72.03	0.0066
	12	72.41	73.13	0.0050
	13	73.44	73.32	0.0056
	14	74.36	74.47	0.0049
1.0 (0.867)	1	55.61	56.87	0.0041
	2	58.20	58.73	0.0044
	3	58.89	58.86	0.0042
	4	62.06	62.12	0.0041
	5	64.45	64.43	0.0043
	6	65.33	64.99	0.0042
	7	68.36	67.68	0.0050
	8	69.29	68.23	0.0044
	9	70.85	70.12	0.0049
	10	71.63	71.26	0.0047
	11	72.66	72.69	0.0048
	12	74.07	74.04	0.0052
	13	74.46	74.27	0.0056
	14	75.54	75.79	0.0050
0.4 (0.394)	1	48.39	49.69	0.0048
	2	50.96	51.35	0.0077
	3	51.41	51.70	0.0066
	4	59.47	59.30	0.0052
	5	60.99	61.35	0.0054
	6	62.40	62.09	0.0050
	7	68.41	67.99	0.0067
	8	69.14	68.30	0.0057
	9	70.80	70.74	0.0074
	10	72.46	72.09	0.0062
	11	74.46	74.22	0.0079
	12	76.07	76.02	0.0094
	13	76.46	76.09	0.0099
	14	78.56	78.28	0.0065

Table 22. Experimental and analytical results for coupled vibration of the four-tube array in unconfined water.⁴⁸

Gap-to-radius ratio, G/R	Mode number	Measured coupled natural frequencies, Hz	Calculated coupled natural frequencies, Hz	Damping ratio
0.5 (0.585)	1	56.79	57.90	0.0090
	2	62.79	62.99	0.0094
	3	66.26	66.73	0.0123
	4	67.38	67.87	0.0091
	5	69.53	69.66	0.0117
	6	71.88	71.38	0.0095
	7	74.32	74.19	0.0124
	8	76.95	76.39	0.0121

Table 23. Experimental and analytical results for coupled vibration of the four-tube array near a flat wall.⁴⁸

Gap-to-radius ratio, G_w/R	Mode number	Measured coupled natural frequency, Hz	Calculated coupled natural frequency, Hz	Damping ratio
1.0	1	56.69	57.78	0.0066
	2	61.87	62.08	0.0071
	3	64.84	64.75	0.0077
	4	66.94	66.69	0.0071
	5	69.04	68.95	0.0079
	6	71.19	70.32	0.0077
	7	73.54	73.35	0.0080
	8	76.81	76.35	0.0083
0.5	1	56.25	57.17	0.0094
	2	60.11	60.52	0.0093
	3	64.36	64.08	0.0098
	4	66.70	66.11	0.0091
	5	68.51	68.30	0.0097
	6	70.68	69.60	0.0112
	7	72.99	72.82	0.0084
	8	76.51	76.13	0.0115

Table 24. Experimental results for uncoupled vibration of the four-tube arrays in viscous fluids.⁴⁸

Conditions	Direction of motion	Tube number	Measured uncoupled natural frequency, Hz		Measured damping ratio	
			Water	Mineral oil	Water	Mineral oil
In unconfined fluid	x	1	68.65	68.31	0.0079	0.0262
		2	68.85	69.14	0.0138	0.0318
		3	68.55	68.41	0.0125	0.0285
		4	65.33	65.04	0.0080	0.0309
	y	1	67.77	67.48	0.0072	0.0284
		2	68.95	69.14	0.0147	0.0336
		3	68.46	68.56	0.0089	0.0285
		4	64.16	64.99	0.0117	0.0290
Near a flat wall ($G_w/R = 0.5$)	x	1	68.51	68.56	0.0059	0.0254
		2	65.53	66.31	0.0138	0.0311
		3	65.38	65.58	0.0143	0.0308
		4	65.19	64.70	0.0094	0.0375
	y	1	67.48	67.48	0.0038	0.0350
		2	66.16	65.82	0.0087	0.0268
		3	66.06	66.02	0.0006	0.0323
		4	64.21	64.84	0.0103	0.0243

7. CONSERVATIVE CHOICE FOR ADDED MASS

The calculation of added mass will generally involve varying degrees of engineering judgment regarding such considerations as the effects of finite length, neighboring members, irregularities in geometry, etc. Decisions on these factors can be significantly influenced by considering whether conservatism is increased by maximizing or minimizing the added mass. This generally varies from situation to situation, and for some cases, a preliminary analysis may be required to help make the decision. We will make some suggestions regarding the structures of concern subjected to seismic excitations prescribed by the response spectrum in R.G. 1.60⁵⁰ (shown in Fig. 1).

Let us assume that we are interested in the inertial forces; therefore, we will deal with the spectral accelerations. The maximum spectral acceleration occurs at a frequency of 2.5 Hz, as indicated in Fig. 1. Therefore, to help ensure conservative inertial forces at frequencies above 2.5 Hz, we would maximize the added mass to bring the calculated natural frequency into regions of higher spectral acceleration. Conversely, we would minimize the added mass at frequencies below 2.5 Hz to achieve the same objective.

Figure 1 shows the natural frequency ranges of the structures of concern listed in Table 3. The natural frequencies are for representative existing structures. According to the frequency values shown in Fig. 1, we should maximize the added mass for the reactor core barrel. For spent-fuel storage racks, the natural frequency can fall on either side of 2.5 Hz. Therefore, the natural frequency in air should be first determined to see whether the added mass should be maximized or minimized. The natural frequency of one fuel bundle we examined was close to 2.5 Hz. Other fuel bundles can presumably fall above or below 2.5 Hz. Therefore, again the natural frequency in air should be first evaluated to determine whether to maximize or minimize the added mass. The natural frequency of the main steam-relief valve line generally falls above 2.5 Hz; however, the upper limit is quite close to 2.5 Hz. Therefore, for cases suspected of having a high natural frequency, it would be best to check the natural frequency first. Otherwise, we would generally minimize the added mass for main steam-relief valve lines. This discussion applies in principle to all acceleration response spectrums; the frequency at which the maximum spectral acceleration occurs may differ from the 2.5 Hz applying to the spectrum of R.G. 1.60.

Table 25. Experimental and analytical results for coupled vibration of the four-tube array contained in a cylinder.⁴⁸

Radius ratio, R_c/R	Eccentricity, G_c/R	Mode number	Measured coupled natural frequency, Hz	Calculated coupled natural frequency, Hz	Damping ratio
4.0	0.0	1	56.15	57.86	0.0061
		2	59.52	59.98	0.0058
		3	62.21	62.11	0.0074
		4	62.25	62.37	0.0070
		5	67.53	68.31	0.0070
		6	69.43	69.27	0.0080
		7	72.27	72.22	0.0083
		8	76.66	76.43	0.0086
	0.4	1	56.25	57.81	0.0058
		2	59.40	59.12	0.0054
		3	61.67	61.96	0.0062
		4	62.26	62.80	0.0075
		5	67.68	68.06	0.0066
		6	69.43	69.15	0.0073
		7	72.11	72.34	0.0079
		8	76.61	76.43	0.0081
	0.8	1	55.86	57.29	0.0064
		2	58.11	57.63	0.0071
		3	60.74	61.25	0.0075
		4	62.65	63.14	0.0092
		5	67.29	67.33	0.0076
		6	68.60	68.79	0.0084
		7	71.53	72.34	0.0100
		8	76.32	76.35	0.0099
3.5	0.0	1	55.57	57.43	0.0091
		2	57.03	57.70	0.0090
		3	59.33	59.56	0.0085
		4	59.77	59.83	0.0087
		5	66.31	67.40	0.0105
		6	68.07	68.25	0.0100
		7	70.90	70.59	0.0102
		8	76.22	76.18	0.0113
	0.4	1	55.76	55.33	0.0076
		2	57.37	57.23	0.0084
		3	59.20	59.03	0.0078
		4	59.72	60.87	0.0076
		5	66.70	66.42	0.0088
		6	68.21	67.91	0.0087
		7	70.31	70.99	0.0089
		8	76.17	76.12	0.0099

8. COMPUTER CODES IN CURRENT USE

The computer codes used for various aspects of fluid-structure interaction analysis are listed in Table 26; this is not a complete list of such codes. The

attributes or capabilities of these codes were not explored for this study.

Table 26. Codes used in industry

Codes	Application	Firm
EDAC/MSAP4	Fluid motion in tanks	EDAC
ANSYS	Offshore reactor platform	Offshore Power Systems
SOLASURF	Incompressible fluid motions: waves	LASL
SOLAICE	Compressible fluid motions	LASL
SOLAFLEX	Internals of reactor vessel possible, said nus.	LASL
WECAN	Internals of reactor vessel	Westinghouse
NASTRAN	Booster tanks space shuttle tanks	Universal Analysis
MARC	General, including fluids	Marc Analysis Corp.
DYNA-3D	General, including fluids	LLL
PISCES	Fluid-structure interaction	Physics International
WATERHASS	Added mass	GE
MULTIFLEX	Internals of reactor vessel	Westinghouse
AMASS	Added mass	Argonne National Lab.
CESHOCK	Fluid-structure interaction	Combustion Engineering

9. CONCLUSIONS AND RECOMMENDATIONS

9.1 Idealized Single Isolated, and Multiple, Members

Hydrodynamic effects on submerged single isolated members are fairly well understood. The added mass and added damping concept is adequate under seismic and normal steam-relief excitations; however, it is probably inappropriate for blowdown accidents. The potential theory will accurately give the added mass values, and tabulated results are available in the literature for a wide variety of single member geometries (Table 6). A presentation of the potential theory can be found in standard textbooks on the mechanics of fluids, such as Ref. 16.

Values for added damping are generally determined experimentally, and values are published for single isolated specimens of small sizes; i.e., up to 3.0 in. in diameter. To project these values to structural sizes of concern, we devised an extrapolation technique based on the published data and established information for the damping of water sloshing in pools. This gave the damping values for the structures of concern shown in Table 7. We will emphasize that these values apply only to situations in which these structures can be considered single

isolated members. The damping values for multiple members can be very different.

For multiple rigid members under seismic and normal steam-relief excitations, the concept of added mass and added damping seems also to apply, although the experimental confirmation is far less extensive than for single isolated members. If we accept the concept's validity then the added mass effect can be calculated using potential theory. Analytical description of the added mass effect is more complex than for a single isolated member; it involves "self-added" and "added" mass coefficients. The first characterizes the force on a member from its own motion with other members stationary, while the second characterizes the force on a stationary member from the motion of other members. Some published values for these coefficients are available for certain simple multiple member arrangements (Refs. 10, 18, 19, 26, 27, 30, 31, 32, 34, 35, 36, and 42). An extensive compilation covering all configurations of interest would be a major analytical undertaking because the coefficient values are influenced by the member arrangement, the space between members, and the geometry of the individual members. Reference 26 has perhaps the most extensive compilation of values.

An approximation was suggested in Ref. 35 to help simplify the analysis of large arrays: i.e., only the hydrodynamic coupling between a member and its immediate neighbors needs to be considered. Coupling with members farther away may be ignored. This allows an array to be analyzed in subparts. The approximation was founded on theoretical results for the central member of hexagonal arrays; therefore, we are not certain how valid it would be for peripheral members. In particular, the corner members of an array receive the highest loads, and this technique may not apply. No experimental confirmation of the approximation was given.

An approximation that is even simpler was suggested in Ref. 10. The total interaction is considered to be the sum of interactions between two adjacent members. Therefore, the members of the array are analyzed two at a time and the results superimposed. The approximation was shown to be accurate to within 2 to 25% for a 4 x 4 array compared to a rigorous analysis. The accuracy varied, depending on the member of the array. Corner members can be analyzed.

As the gap between members of an array is increased beyond a certain point, the members respond as if single and isolated. For circular cylindrical members, when the gap reaches 1.5 times the member diameter, the members can be treated as if single and isolated. This 1.5 value was applicable to virtually all multiple member arrangements we found for circular cylindrical members.

In the case of coaxial rigid cylinders, the potential theory solution can be expressed very conveniently for design applications. The inertial forces are given in terms of the mass of the fluid displaced by the inner cylinder and the mass of fluid filling the interior of the outer cylinder in the absence of the inner cylinder. In a more sophisticated analysis, an incompressible viscous fluid theory was used instead of the potential theory. The results generally agreed better with experiments than did the potential theory. This indicates that viscosity effects may be important for coaxial cylinders; however, the analytical expressions are more complicated than those for potential theory. We would like to see further confirmation before recommending the more complex theory over the easy-to-apply potential theory.

Coaxial flexible cylinders probably provide a more accurate model for the reactor internals than do coaxial rigid cylinders. Analytical treatments generally involve a compressible inviscid fluid theory and are fairly complex. Much needs to be explored for this case before conclusions can be drawn

regarding design oriented methods. Interest in this area is currently high.

Damping for multiple members is presently a broad, imprecise topic, mainly because of its dependence on member arrangement, gap size between members, member geometry, and whether the member motions are in-phase or out-of-phase. If the gap size is not less than 0.4 times the member size, the damping is approximately that of a single isolated member. This convenient simplification may not always apply in practice, but when it does, it eliminates the dependence of damping on member arrangement and whether the members are moving in-phase or out-of-phase. It holds for coaxial cylinders as well as for arrays. Unfortunately, it is established for very small specimens (0.5-in. diameter) rather than for structural sizes of concern. However, we believe we can assume the 0.4 factor also applies to larger structures.

For gap sizes less than 0.4 times the member size, the damping increases rapidly with decreasing gap size when the members are moving out-of-phase with each other. On the other hand, if the members are moving in unison, the damping is very low, i.e., more in the range of damping values for single isolated members. Damping values for small gaps are available for small specimens, i.e., 0.5-in. diameter. At present, there is no established way to extrapolate these values to the structural sizes of concern. The analytical treatment presented in Ref. 27 fairly successfully predicted the damping for 0.5-in.-diameter specimens. The same procedure could be applied to large structures; however, the success of doing this would need to be explored.

9.2 Spent-Fuel Storage Racks

The fuel elements in a fuel bundle constitute an array of multiple members. The cans in a spent-fuel storage rack also form an array. The racks in a spent-fuel storage pool form yet another array. The added mass and added damping concept is applicable to these arrays under seismic excitation. The discussions we gave on this concept for single isolated members and arrays are directly applicable to these structures.

The racks are generally quite stiff so, more than likely, the entire rack will move in unison. If the rack is isolated, the added damping would be quite low, on the order of the values for fuel bundles shown in Table 7. Usually, however, the rack is next to other racks, or next to a wall. In this case, out-of-phase

motions between a rack and a neighboring structure could measurably increase the damping. Unfortunately, because of a lack of information, we are not in a position to recommend a damping value under this condition. On the other hand, in most cases, the racks are firmly anchored to the pool structure and to each other; consequently, out-of-phase motions would generally not occur. For this situation, the damping would be very low, on the order of the values for fuel bundles shown in Table 7.

Damping from component impact and the anchoring effect of water need to be addressed because they may be brought up as arguments against the use of such low damping values for racks. Component impact may occur between the fuel bundles and the cans, and, according to Refs. 41 and 43, component impact can contribute measurably to damping. However, without an indication of how much it contributes and how much it can vary from one rack design to another, we are not in a position to recommend a value for it. Because of the surrounding water, racks in a pool will tend to translate with the pool under seismic excitation. This is an anchoring effect, and it is a manifestation of inertial forces rather than damping. If the added mass effect is analyzed using the "self-added" and "added" mass coefficients described in Section 6.2 of this report, the anchoring effect of the water would be properly taken into account.

9.3 Main Steam-Relief Valve Line

The added mass and added damping concept can be applied to the main steam-relief valve line under seismic and normal steam-relief excitations. The line is submerged near the wall of the pressure suppression pool. If the gap between the line and pool wall is greater than 1.5 times the diameter of the line, the added mass can be evaluated as if the line is single and isolated. Otherwise, the presence of the wall needs to be taken into account, and the curve in Fig. 44 can provide the added mass coefficient for motions of the line in any direction.

If the gap is greater than 0.4 times the diameter of the line, the added damping can be assumed to be that of a single isolated member, and the values given in Table 7 apply. The damping will be greater if the gap is smaller. Unfortunately, without sufficient published information, we are not in a position to recommend damping values for this latter case.

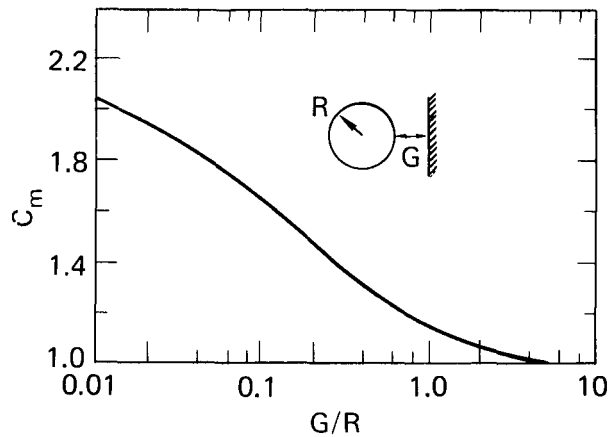


Fig. 44. Hydrodynamic mass coefficient for a cylinder vibrating near a wall.²⁶

9.4 Internals of the Reactor Vessel

Seismic excitation and blowdown accidents are two important concerns for the internals of the reactor vessel. The blowdown accident is at least an order of magnitude more complex than the other phenomena addressed in this project, and the analysis techniques required are significantly more complex and sophisticated than those required for the others. From the very beginning of the project, it was realized that an investigation of the accident problem would very likely be beyond the financial and time limitations of the project. However, NRC and we agreed to include it in the project to see what we could find out about it, and, if our findings were inconclusive, that would be totally acceptable to NRC. As it turns out, our findings are generally inconclusive.

It became increasingly clear to us as we neared the end of the project that, indeed, a meaningful investigation of the accident problem is beyond the financial and time resources of the project. Moreover, it was beyond the guidelines of the project in that the work required to address the accident problem is research rather than an evaluation of methods for design calculations. The project's guidelines⁵⁵ were, in essence, to investigate analytical techniques in current use or having a potential use for practical design calculations. Because we tailored our efforts to this guideline, we subsequently did not come across references which dealt in depth with the accident problem. Our findings are generally more applicable to seismic and normal operation excitations.

Analytical models commonly used for the internals of the reactor vessel include:

- (1) two coaxial rigid cylinders.
- (2) two coaxial cylinders with the inner cylinder flexible and the outer one rigid.
- (3) three coaxial cylinders with the two inner cylinders flexible and the outer one rigid.

Model (1) is generally used to approximate the first beam mode of the core barrel; models (2) and (3) are to approximate shell-bending modes. Model (3) models reactors with a thermal shield.

The added mass and added damping concept can be applied to model (1). The potential theory expressions for the added mass response are quite convenient for design applications and are characterized by fluid mass quantities that are simple to determine, as explained in Section 6.3 of this report. This technique is suitable for analysis of the first mode beam bending deformation of the core barrel under seismic or normal operation excitations. In a blowdown accident the hydrodynamic effects are most likely too severe for this treatment; however, the technique may provide a very rough estimate of the response. Because no experimental confirmation is available, we cannot make a more definite statement concerning blowdown accidents.

A more sophisticated analysis of model (1) using an incompressible viscous fluid theory is also available as explained in Section 6.3 of this report. The results seem to compare better with experimental results than did the added mass concept; however, the expressions are more complex. This is another technique suitable for analyzing the first mode beam-bending deformation of the reactor core barrel under seismic and normal-operation excitations. The same comments relating to the accident condition given in the preceding paragraph also apply here.

Models (2) and (3) are generally examined with a compressible inviscid theory as discussed in Section 6.4 of this report. These models are appropriate for shell bending modes of the core barrel and thermal shield under seismic or normal operation excitations. Again, the technique might be feasible for an approximate analysis of the shell-bending deformation under an accident, provided the fluid properties are properly adjusted.

Because the annular gap between the core barrel and the reactor vessel is small, less than 0.4 times the diameter of the core barrel, damping from water viscosity can be expected to be important. Total (structural plus added) damping measured on actual reactors revealed 2 to 5% for core barrel beam modes, and 1 to 2% for shell modes.⁴¹ These values are comparable with values in Fig. 41 for small D/d

ratios; i.e., for D/d less than 1.8, where D and d are the outer and inner diameters, respectively, of coaxial rigid cylinders. We are not implying that Fig. 41, which is for 0.5-in.-diameter specimens, necessarily applies to sizes of a core barrel; however, the core barrel values measured are at least not contradictory to those in Fig. 41. Other damping values given in Ref. 41 for reactors includes both the effects of fluid viscosity and component impact. These ranged from 8.8 to 12%, and no separation with respect to the two contributions was made. We believe the damping from component impact is bound to vary from one reactor design to another; therefore, no reliable value of damping can be assigned to it. In addition, component impact must be, at least in most cases, an undesirable phenomenon that is to be avoided if possible. Therefore, if the sought-after condition is such that component impact is virtually absent, the fluid viscosity would be the dominating cause of added damping. Consequently, we would recommend using a total (structural plus added) damping value of 2 to 5% for beam modes, and 1 to 2% for shell modes.

9.5 Methods for Current Design Analysis of Fuel Racks*

As mentioned in Section 4 of this report, the methods in current use for design analysis shown in Table 5 are based on engineering judgment together with analytical and/or experimental information available at the time. We will provide an assessment of validity of each method as compared with our suggested method based on the material presented earlier in this report. Because of the complexity of multiple structure-water interaction, an accurate assessment needs rigorous analyses of the types described in Section 6 of this report. However, because the methods listed in Table 5 are numerous, this is an effort beyond the scope of this project. Consequently, our assessment is based on observations only.

The methods described in Table 5 are formulated for low-amplitude dynamic phenomenon, such as seismic excitation. Our assessment focuses on fuel racks, for which many of the methods are formulated; however, our conclusions are not necessarily limited to fuel racks. Three types of racks of particular interest to NRC are:

Type 1: A regular array of 9 x 9 in. cans spaced 4 in. apart.

Type 2: A regular array of 6 x 6 in. cans spaced 1 in. apart.

* These methods are described in Table 5.

Type 3: A regular array of cans with no space between cans.

The effective mass of a submerged can is the sum of the mass of the can, the mass of the contained fuel rods, the mass of the water contained within the can, and the added mass from interaction with the surrounding water. The terms added mass and added damping, as commonly used, pertain only to the interaction with the surrounding water.

We will begin our discussion by first describing LLL's recommendations for fuel racks. This will be followed by our assessment of the methods in Table 5.

9.5.1 LLL Recommendations for Fuel Racks

If the fuel racks are arranged so that the predominate modes of vibration consist of the cans translating in unison, we recommend using the coefficients in Table 27 to evaluate the added mass per can. The added mass per can is the coefficient times the mass of the water displaced by the exterior volume of the can.

The basis for our recommendations, in the absence of a rigorous analysis, is that we believe the added mass per can in an array should be the smaller of either the added mass for the can if single and isolated or the mass of the water actually surrounding the can in the array. For the three rack types of interest, the coefficient values for these two

situations are shown in Table 28. Our recommendation is to use the coefficient values of the second situation.

For the three rack types, we are, in essence, saying the water between the cans translates directly with the cans. Accordingly, as far as the water-structure interaction of an entire rack module is concerned, the module interacts essentially as a solid structure. Therefore, in addition to the added mass for each can, the added mass effect on the module should be accounted for. For the three rack types of interest it should be evaluated assuming the module is a solid structure. To our knowledge, the space between rack modules is generally small compared to the module dimensions. Assuming the rack modules translate in unison, we would recommend adding the mass of the water between modules to the mass of the modules.

If the cans do not translate in unison, the situation becomes significantly more complex. The analytical method we recommended in Sections 9.1 and 9.2 of this report should then be used. The modules, however, can still be taken as solid structures for the three rack types of interest.

The added damping for fuel racks is a complex issue, and there is insufficient published technical information on which to base a sound recommendation. Further comments are given in Section 9.2 of this report. A major difficulty is the use of the simple added damping concept to approximate a phenomenon that is measurably more complex in the case of multiple members. Unfortunately, no better alternatives were found for a design-oriented approach. Therefore, we currently suggest using the added damping values given in Table 7; i.e., 0.6% for rack type 1, and 0.4% for rack type 2, and 0% for rack type 3, based on the type 3 rack module responding as a unit. We recommend that further studies on damping be carried out, particularly experimental studies.

Table 27. Added mass coefficients for evaluating added mass per can.

Rack type	Added mass coefficient
1	1.086
2	0.36
3	0

Table 28. The coefficient values for three rack types for (1) the added mass of a single isolated can and (2) the mass of water surrounding the can.

Rack type	Potential theory for situation 1	Actual surrounding water for situation 2*
1	1.186	1.086
2	1.186	0.36
3	1.186	0

* For 9 × 9 in. cans spaced 4 in. apart, $\frac{13 \times 13 - 9 \times 9}{9 \times 9} = 1.086$

For 6 × 6 in. cans spaced 1 in. apart, $\frac{7 \times 7 - 6 \times 6}{6 \times 6} = 0.36$

9.5.2 Methods No. 1 and No. 2

For single isolated members, potential theory will provide valid added mass values. Using the expressions tabulated in Table 6 is the same as applying potential theory.

Applying potential theory to evaluate the added mass for multiple members is likewise valid. However, the solution procedure is usually difficult, and approximate solutions are normally sought. The accuracy of the approximate analytical model may be of primary concern. Details on the approximations used, if any, and on the damping values used were not given by the firms using Methods No. 1 and No. 2.

9.5.3 Method No.3

For single isolated members, Method No. 3 gives the same results as the procedure recommended by Newmark and Rosenblueth (N&R).⁵ Therefore, as discussed in Sections 5.1 and 5.2 of this report, the added mass value would be two-thirds that given by potential theory for a square member. We would recommend using potential theory over Method No. 3 for greater accuracy, for essentially the same level of analytical complexity in the case of single isolated members.

For multiple members, Method No. 3 does not appear to be extracted from the references (Refs. 1, 3, and others) mentioned by the user. For the three rack types of interest the resulting coefficient values are shown in Table 29, in comparison with LLL's recommendations. It appears Method No. 3 will significantly underestimate the LLL recommendation for added mass for rack types 1 and 2.

Our objections to using a total damping of two times the structural damping was discussed in Section 4 of this report.

9.5.4. Method No. 4

Method No. 4 does not appear to be extracted from the references (Refs. 1, 3, 4, 7, and others) mentioned by the user. For single isolated square members, the added mass is approximately one-third that given by potential theory. For the rack types of interest the added mass per can is given by the coefficients values in Table 30, in comparison with LLL's recommendations. It appears Method No. 4 will significantly underestimate the LLL recommendation for added mass for rack type 1.

Based on the information available on added damping the use of zero added damping is certainly conservative.

9.5.5. Method No. 5

Potential theory will provide valid added mass values for single isolated members.

For multiple members, the user is addressing more general motions than unison translation. Fritz's method⁷ provides an approximation for a generic member surrounded by adjacent members. The procedure by which the user applied Fritz's method to an array was not totally clear to us. However, for unison motion, we speculated that recognition was probably given to the fact that a generic member plays two roles: as the central member and as part of the surrounding square cylinder for its adjacent members. Therefore, superimposing the forces given

Table 29. Coefficient values for three rack types comparing Method No. 3 of Table 5 with the LLL recommendation.

Rack type	Method No. 3 coefficients	LLL-recommended coefficients
1	0.44	1.086
2	0.17	0.36
3	0	0

Table 30. Coefficients for three rack types comparing Method No. 4 with the LLL recommendation.

Rack type	Method No. 4 coefficients	LLL-recommended coefficients
1	0.4	1.086
2	0.36	0.36
3	0	0

Table 31. Coefficients for three rack types comparing Method No. 5 with the LLL recommendation.

Rack type	Method No. 5 coefficients*	LLL-recommended coefficients
1	2.568	1.086
2	0.778	0.36
3	0	0

* For 9 × 9 in. cans spaced 4 in. apart, $\frac{17 \times 17 - 9 \times 9}{9 \times 9} = 2.568$

For 6 × 6 in. cans spaced 1 in. apart, $\frac{8 \times 8 - 6 \times 6}{6 \times 6} = 0.778$

in Fritz⁷ for the two roles played by a generic member lead us to conclude that the added mass for a given member is the mass of the water between the member and its surrounding square cylinder. This would result in the added mass coefficients for the rack types of interest shown in Table 31, in comparison with LLL's recommendations. Consequently, according to our speculation of how the user applied Fritz's method, Method No. 5 overestimates the LLL recommendation for added mass for rack types 1 and 2.

The added damping ranged from 0 to 3% as compared with our previously recommended value. Because of insufficient information on their use of added damping, we are in a poor position to assess the validity of these values.

9.5.6. Method No. 6

An added mass equal to the mass of water displaced by the exterior volume of a square can will be 0.843 times that given by potential theory, for single isolated square cans. We prefer using potential theory, for essentially the same analytical complexity.

For the three rack types of interest, the procedure for evaluating the natural frequency corresponds to LLL's recommendation. However, the procedure for evaluating inertial loads essentially ignores the added mass. Consequently, we consider Method No. 6 inappropriate (in comparison with LLL recommendations) for analyzing inertial effects for rack types 1 and 2.

An added damping of 2% does not correspond to the value we previously suggested.

9.5.7. Method No. 7

For single isolated members, the comments made for Method No. 6 also apply to Method No. 7. For multiple members translating in unison, Method No. 7 corresponds almost to LLL's recommendation. The only difference is LLL recommends using potential theory rather than the mass of the displaced water to evaluate the added mass for single isolated members. For the three rack types of interest, Method No. 7 and LLL's recommendations give the same values for the added mass.

We discourage the use of 2 to 2-½ times the structural damping as the total damping. An added damping of 2% does not correspond to the value we previously suggested.

9.5.8. Method No. 8

We consider Method No. 8 inappropriate (in comparison with LLL recommendations) for evaluating the added mass effect for rack types 1 and 2. We disagree with the use of two times the structural damping as the total damping for the reason discussed in Section 4 of this report.

9.5.9 Method No. 9

The user is apparently involved with only rack type 3, and Method No. 9 is appropriate for this configuration. The use of zero added damping could be appropriate and is certainly conservative.

10. ACKNOWLEDGMENTS

The author expresses his appreciation to G. A. Broadman, Leader, C. E. Walter, Deputy Leader, and F. J. Tokarz, Associate Leader, of the Nuclear Test Engineering Division, Mechanical Engineering Department, for their encouragement and support of this project. The project was initiated, sponsored,

and funded by the U.S. Nuclear Regulatory Commission. The attention and advice given by Dr. C. H. Hofmayer and Dr. K. S. Herring of the Division of Operating Reactors has been most helpful and appreciated.

11. REFERENCES

1. R. W. Clough, "Effects of Earthquakes on Underwater Structures," *Proc. of 2nd World Conference on Earthquake Engineering*, (Tokyo, 1960).
2. K. T. Patton, *Tables of Hydrodynamic Mass Factors for Translational Motion*, ASME Paper No. 65-WA/UNT-2.
3. A. R. Chandrasekaran, S. S. Saini, and M. M. Malhotra, "Virtual Mass of Submerged Structures," *Journal of the Hydraulics Div., Proc. of the ASCE*, (May, 1972).
4. T. E. Stelson and F. T. Mavis, *Virtual Mass and Acceleration In Fluids*, ASCE Trans. Paper No. 2870, Vol. 122, 1957.
5. N. M. Newmark and E. Rosenblueth, *Fundamentals of Earthquake Engineering*, (Prentice-Hall Inc., Englewood Cliffs, N. J. 1971), Chapter 6.
6. G. H. Keulegan, and L. H. Carpenter, "Forces on Cylinders and Plates in an Oscillating Fluid," *Journal of Research of the National Bureau of Standards*, 6 (5), (May, 1958).
7. R. J. Fritz, "The effects of Liquids on the Dynamic Motions of Immersed Solids," *Journal of Engineering for Industry, Trans. ASME* (Feb., 1972).
8. G. B. Wallis, *One-Dimensional Two-Phase Flow* (McGraw-Hill Book Co., New York, 1969), Chapter 8.
9. L. S. Jacobsen, "Impulsive Hydrodynamics of Fluid Inside a Cylindrical Tank and of Fluid Surrounding a Cylindrical Pin," *Bull. of the Seismological Society of America*, 39 (1949).
10. T. Yamamoto and J. H. Nath, "Hydrodynamic Forces on Groups of Cylinders," *Offshore Technology Conference, 1976 Proc., Vol. 1*, OTC 2449.
11. H. B. Amey, Jr., and G. Pomonik, "Added Mass & Damping of Submerged Bodies Oscillating Near the Surface," *Offshore Technology Conference, 1976 Proc., Vol. 1*, OTC 1557.
12. C. J. Garrison, and R. B. Berklite, "Hydrodynamic Loads Induced by Earthquakes," *Offshore Technology Conference, 1976 Proc., Vol. 1*, OTC 1554.
13. T. Sarpkaya, "Separated Flow About Lifting Bodies and Impulsive Flow About Cylinders," *AIAA Journal*, 4 (3), (March, 1966).
14. A. Selby and R. T. Severn, "An Experimental Assessment of the Added Mass of Some Plates Vibrating In Water," *Earthquake Engineering and Structural Dynamics*, 1 (1972).
15. H. Schlichting, *Boundary Layer Theory* (McGraw-Hill Book Co., New York, 1968).
16. J. H. Shames, *Mechanics of Fluids* (McGraw-Hill Book Co., New York, 1972).
17. A. R. Chandrasekaran and S. S. Saini, "Vibration of Submerged Structures," *Irrigation and Power* (July, 1971).
18. T. Yamamoto, "Hydrodynamic Forces on Multiple Circular Cylinders," *Journal of the Hydraulics Division, Proc. of the ASCE* (Sept., 1976).
19. C. Dalton and R. A. Helfinstine, "Potential Flow Past A Group of Circular Cylinders," *Journal of Basic Engineering, Trans. ASME* (Dec., 1971).
20. R. A. Skop, S. E. Ramberg, and K. M. Ferer, *Add Mass and Damping Forces on Circular Cylinders*, ASME Paper 76-Pet-3, 1976.
21. S. Levy, J. P. D. Wilkinson, "Calculation of Added Water Mass Effect for Reactor System Components," *Trans. of the 3rd Int. Conf. on Structural Mechanics in Reactor Tech.* (Sept., 1975).
22. J. G. Alibaud, (Abstract Only) "Virtual Mass Effect of Water on the Internals of Pressurized Water Reactors, Theory and Experimental Results," *Trans. of the 3rd Int. Conf. on Structural Mechanics In Reactor Tech.* (Sept., 1975).

23. R. Assedo, M. Dubourg, M. Livolant, A. Epstein, "Vibration Behavior of PWR Reactor Internals Model Experiments and Analysis," *Trans. of the 3rd Int. Conf. on Structural Mechanics in Reactor Tech.* Sept. 1975.
24. C. Carmignani, E. Manfredi, S. Reale, P. Cewetti, A. Fedevico, "Influence of the Assembly Configurations on the Flow Induced Vibrations of BWR Fuel Elements," *Trans. of the 3rd Intern. Conf. on Structural Mechanics In Reactor Technology* (Sept., 1975).
25. D. T. Ramani, "Stress and Deflection Analysis of Reactor Internals Due to Seismic & Maximum Hypothetical LOCA Loading Conditions," *Trans. of the 3rd Inter. Conf. On Structural Mechanics In Reactor Technology* (Sept., 1975).
26. S. S. Chen and H. Chung, *Design Guide for Calculating Hydrodynamic Mass, Part I: Circular Cylindrical Structures*, Argonne National Laboratory ANL-CT-76-45 (June, 1976).
27. S. S. Chen and M. W. Wambsganss, and J. A. Sendziejczyk, "Added Mass and Damping of a Vibrating Rod In Confined Viscous Fluids," *J. of Applied Mechanics*, **98** (2) (June, 1976).
28. M. Ohkusu, "Wave Action on Groups of Vertical Circular Cylinders," *Proc. of the Annual Spring Conf. of Japan Soc. of Naval Architects* (May, 1972).
29. T. Sarpkaya, "Forces on Cylinders and Spheres In A Sinusoidally Oscillating Fluid," *Trans. ASME, J. of Applied Mech.* (March, 1975).
30. P. M. Moretti, and R. L. Lowery, "Hydrodynamic Inertia Coefficients for a Tube Surrounded by Rigid Tubes," *Trans ASME J. of Pressure Vessel Technology* (August, 1976).
31. Y. S. Shin and M. W. Wambsganss, "Flow-Induced Vibration in LMFBR Steam Generators: A State-of-the-Art Review," *Nuclear Engineering and Design*, **40** (1977), pp. 235-284.
32. S. S. Chen, "Vibration of Nuclear Fuel Bundles," *Nuclear Engineering and Design*, **35** (1975), pp. 399-422.
33. L. W. Carpenter, "On the Motion of Two Cylinders in An Ideal Fluid," *Journal of Research of the National Bureau of Standards*, **61** (2) (August, 1958), Research Paper 2889, pp. 83-87.
34. H. Chung and S. S. Chen, *Vibration of a Group of Circular Cylinders in a Confined Fluid*, ASME Paper No. 77-APM-16 (1977), pp. 1-5.
35. S. S. Chen, *Dynamics of Heat Exchanger Tube Banks*, ASME Paper No. 76-WA/FE-28 (1976), pp. 1-7.
36. S. S. Chen, "Vibrations of a Group of Circular Cylindrical Structures in A Liquid," *Trans. of the 3rd International Conf. on Structural Mechanics in Reactor Technology, Vol. 1 Part D* (September, 1975), pp. 1-11.
37. M. Dubourg, R. Assedo, and C. Cauquelin, "Model Experimentation and Analysis of Flow-Induced Vibrations of PWR Internals," *Nuclear Engineering and Design*, **27** (1974), pp. 315-333.
38. M. K. Au-Yung, "Response of Reactor Internals to Fluctuating Pressure Forces," *Nuclear Engineering and Design*, **35** (1975), pp. 361-375.
39. D. T. Ramani, "Transient Dynamic Response and Stability Analysis of Reactor Core — Support Barrel Due to LOCA Pressure Pulse Loading," *Trans. 4th Int. Conf. on Structural Mechanics in Reactor Technology* (San Francisco, California, August, 1977) (Abstract available only).
40. R. Longo, F. W. Martsen, P. A. Perrotti, E. C. Bair, "Seismic Analysis of Spent Fuel Racks," *Trans. 4th Int. Conf. on Structural Mechanics in Reactor Technology* (San Francisco, California, August, 1977) (Abstract available only).
41. N. R. Singleton, and G. J. Bohm, "Damping of Reactor Internals," *Trans 4th Int. Conf. on Structural Mechanics in Reactor Technology* (San Francisco, California, August, 1977).
42. R. W. Wu, L. K. Liu, S. Levy, "Dynamic Analysis of Multibody System Immersed in a Fluid Medium," *Trans. 4th Int. Conf. on Structural Mechanics in Reactor Technology* (San Francisco, California, August, 1977).
43. Y. S. Shin, J. A. Jendrzejczyk, and M. W. Wambsganss, "The Effect of Tube-Support Interaction on the Dynamic Response of Heat Exchanger Tubes," *Trans. 4th Int. Conf. on Structural Mechanics in Reactor Technology* (San Francisco, California, August 1977).
44. J. J. Dubois, A. L. deRouvray, "Improved Coupled Euler-Lagrange Finite Element Analysis of the Fluid-Structure Dynamic Interaction Problem," *Trans. 4th Int. Conf. on Structural Mechanics in Reactor Technology* (San Francisco, California, August, 1977).
45. R. J. Fritz and E. Kiss, *The Vibration Response of a Cantilevered Cylinder Surrounded by An Annular Fluid*, KAPL-M-6539, General Electric Co., Schenectady, N.Y. (February, 1966).
46. M. K. Au-Yang, "Free Vibration of Fluid-Coupled Coaxial Cylindrical Shells of Different Length," *J. Of Appl. Mech.* **98** (3), (Sept., 1976).

47. T. M. Mulcahy, P. Turula, H. Chung and J. A. Jendrzejczyk, "Analytical and Experimental Study of Two Concentric Cylinders Coupled by a Fluid Gap," *Trans. 3rd Int. Conf. on Structural Mechanics in Reactor Technology* (London, Sept., 1975).
48. S. S. Chen, J. A. Jendrzejczyk, and M. W. Wambsganss, *Experiments on Fluid Elastic Vibrations of Tube Arrays*, ANL-CT-77-16, Argonne National Laboratory (April, 1977).
49. T. T. Yeh and S. S. Chen, *The Effect of Fluid Viscosity on Coupled Tube/ Fluid Vibrations*, ANL-CT-77-24, Argonne National Laboratory (April, 1977).
50. U.S. Nuclear Regulatory Commission, Regulatory Guide 1.60, *Design Response Spectra for Seismic Design of Nuclear Power Plants* (Dec., 1973).
51. H. N. Abramson, *The Dynamic Behavior of Liquids in Moving Containers*, National Aeronautics and Space Administration, Rept. NASA SP-106 (1966).
52. D. D. Kana, and F. T. Dodge, "Design Support Modeling of Liquid Slosh in Storage Tanks Subject to Seismic Excitation," *presented at Second ASCE Specialty Conf. on Structural Design of Nuclear Plant Facilities*, (New Orleans, LA., Dec., 1975).
53. D. G. Stephens, H. W. Leonard, and T. W. Perry, Jr., *Investigation of the Damping of Liquids in Right-Circular Cylindrical Tanks, Including the Effects of a Time-Variant Liquid Depth*, NASA TN D-1367 (July, 1962), Wash. D.C.
54. D. D. Kana, of the Southwest Research Institute, San Antonio, Texas, Personal communications, August 18, 1977, in San Francisco, California.
55. Project Proposal, *Effective Mass and Damping of Submerged Structure*, Contract No. B&R 20 19 04 02 FIN AO203, August 1976.